University of Arkansas, Fayetteville
ScholarWorks@UARK

12-2016

Influence of Concrete Compressive Strength on Transfer and Development Lengths of Prestressed Concrete

Alberto Teodoro Ramirez-Garcia
University of Arkansas, Fayetteville

Influence of Concrete Compressive Strength on Transfer and Development Lengths of Prestressed Concrete

A dissertation submitted in partial fulfillment
of the requirements for the degree of
Doctor of Philosophy in Civil Engineering

by

Alberto T. Ramirez-García
National University "Santiago Antúnez de Mayolo"
Bachelor of Science in Civil Engineering, 2001
University of Arkansas
Master of Science in Civil Engineering, 2012

December 2016
University of Arkansas

This dissertation is approved for recommendation to the Graduate Council.

_____

Dr. Micah Hale
Dissertation Director

_____   _____

Dr. Ernie Heymsfield   Dr. Douglas Spearot
Committee Member   Committee Member

_____

Dr. José R. Martí-Vargas
Committee Member

ABSTRACT

This research examines the relationship between concrete compressive strength and strand bond. The goal of this research was to develop an equation that relates strand bond to concrete compressive strength at strand release (approximately 1 day of age) and at 28 days of age, and those equations are presented in this investigation. Strand bond is assessed by measuring the transfer length and development length for prestressed beams cast in the laboratory. In the U.S., strand bond is predicted using transfer length and development length equations provided by the American Concrete Institute (ACI-318) Building Code and American Association of State and Highway Transportation Official (AASHTO) LRFD Bridge Design Specifications which were developed based on the 1950´s investigations. The equations provided by both ACI and AASHTO do not address concrete strength while equations, developed in this investigation, do account for the compressive strength of concrete at release and testing time. Although there has been much research conducted in this matter, this research provides a reliability data analysis relating to transfer and development lengths of prestressed concrete beams. Unlike many of the previous programs, this research includes strands of a known quality, the largest database of test specimens, and a variety of concrete mixtures and concrete strengths. This research concludes with the development of an analytical model to predict transfer length which includes concrete strength at release with fracture propagation around the strand.

ACKNOWLEDGMENTS

I thank God and my Lord and Savior Jesus Christ for giving me these abilities and strengths to reach this point in my life. I am extremely grateful to Dr. Micah Hale for providing me his guidance and his wisdom for the completion of this research. His inspiration and his knowledge in the concrete material fields of prestressed concrete are remarkable which I have achieved in order to aim my goals. It is extremely difficult to express all the gratitude which he deserves. He has changed my life forever.

I would like to thank my committee members: Dr. Ernie Heymsfield, Dr. Douglas Spearot, and Dr. José R. Martí-Vargas. Their contributions made this dissertation better than it should be.

I would like to thank my wife, Ketty, for her sincere gratitude and my kids: Ariadna, Cristopher, Daira, Emelyn, and Michael who day by day bring me their love and hopes selflessly. I would like to thank my Mom, brothers, and sisters for their supports and love. Despite hard times and issues along the way, they helped me get through some of the most difficult times.

This research cannot be completed without the assistance of a number of individuals at the Department of Civil Engineering. I would like to thank: Richard Deschenes Jr., Canh Dang, Cameron Murray, William Phillips, Doddridge Davis, Joseph Daniels III, and Ryan Hagedorn. They helped me cast and test all the beams during a hot summer in 2014. I also would like to thank David Peachee and Mark Kuss for their assistant in technical issues and the use of their equipment.

Finally, I would like to thank my friends who have spent their time with my family as well as a huge special gratitude to my American family: Michael and Diane Lawrence for their love and advice.

DEDICATION

I dedicate this dissertation to my family, who always encouraged me to complete my Ph.D.

study.

TABLE OF CONTENT

LIST OF FIGURES

LIST OF TABLES

NOTATIONS

A_s area of the prestressing strand (mm^2)

A_b nominal area of strand

A_g cross section area of concrete member

A_p total area of strand

A_c cross sectional area of concrete

c_y clear concrete cover

e_c eccentricity of the prestress force

E elastic modulus of element

E_c elastic modulus of concrete

E_p elastic modulus of strand

E_{pr} elastic modulus of strand in the transversal direction

d_b diameter of the strand (mm)

f'_{ci} concrete compressive strength at prestress release (MPa)

f'_c concrete compressive strength at 28-days or time of testing (MPa)

f_{si} initial prestress (MPa)

f_{se} effective prestress in strand after losses (MPa)

f_{ps} stress at nominal strength of the member (MPa)

f_t concrete's tensile strength

f_{cz} concrete compressive stress due to effective prestress

f_{pu} ultimate tensile strength

f_{py} yield strength

f_{pi} initial prestressing stress

L_t transfer length of prestressing steel in pretensioned concrete members

L_{fb} flexural bond length

L_e embedment length (mm)

L_d development length (mm)

k_e normalized embedment length factor

k_p normalized predicted development length factor

U'_t plastic transfer bond stress coefficient

U'_d plastic development bond stress coefficient

B bound modulus (MPa/mm)

I_g moment of inertia of concrete section

v Poisson's ratio of element

v_p Poisson's ratio of strand

v_c Poisson's ratio of concrete

$\eta = E_p / E_c$ Modular ratio

n integer number (2 for second-order equation and 3 for third-order equation)

λ_b bond factor

λ_{sp} strand perimeter factor (1 is for solid strand and 4/3 for strand seven wire)

λ_{uscE} factor of unit system conversion for elastic modulus

λ_{uscT} factor of unit system conversion for tensile strength

w unit weight of concrete

μ coefficient of friction between prestressing steel and concrete

σ_i interface pressure

σ_r radial stress at concrete and strand interface

σ_θ hoop stress

σ_z longitudinal stress

ε_r radial strain

ε_θ hoop strain

ε_z longitudinal strain

ε_{sh} drying shrinkage coefficient

K_f constant factor

k_t radial stress

k_{ii} constant factor (ii = 1,2,3,..,7)

k_{bi} bond surface stiffness

r_p nominal radius of strand

$r_{c,1}$ internal radius of concrete cylinder which equals to radius of strand after prestressing

$r_{c,2}$ external radius of concrete cylinder

r radius in the radial direction

R_1 inner radius

R_2 outer radius

R_{cr} crack radius

R_{fr} fracture radius

τ bond stress

(r, θ, z) polar coordinates stresses

(u, v, w) polar coordinates displacements

Δ_{fp}^{p} increase in radius of strand due to reduction in longitudinal stress from initial prestress f_{si}

   to effective prestress f_{se}

$\Delta_{\sigma i}^{p}$ reduction in radius of strand due to the uniform radial compression at interface σ_i

$\Delta_{\sigma i}^{c}$ increase in inner radius of the thick-walled concrete cylinder due to the interface pressure

σ_i

Δ_{fcz}^{c} increase in inner radius of the thick-walled concrete cylinder due to the longitudinal

compressive stress at the level of strand f_{cz}

Δ_{sh}^{c} reduction in inner radius of the thick-walled concrete cylinder due to drying shrinkage ε_{sh}

Δ_{cr}^{c} deformation of the real crack zone

Δ_{fr}^{c} deformation of the fracture zone

$u_{R_{fr}}^{c}$ radial displacement at $r = R_{fr}$

Δx incremental of transfer zone

Δf_{bi} bond force around the strand surface

Δf_{pxi} strand stress incremental

w_{cr} crack width at any point

w_a crack width

w_o initial crack width at the shear plane

A LIST OF PUBLISHED JOURNAL ARTICLES

Chapter 2: Ramirez-Garcia, A. T.; Floyd, R. W.; Micah Hale, W.; and Martí-Vargas, J. R., "Effect of concrete compressive strength on transfer length," Structures, V. 5. 2016, pp. 131-40.

Chapter 3: Ramirez-Garcia, A. T.; Floyd, R. W.; Micah Hale, W.; and Martí-Vargas, J. R., "Influence of Concrete Strength on Development Length of Prestressed Concrete Members," Journal of Building Engineering. V.6. 2016, pp. 173-83.

Chapter 4: Ramirez-Garcia, A. T.; Dang, C. N.; Micah Hale, W.; and Martí-Vargas, J. R., "A Higher-Order Equation for Modeling Strand Bond in Pretensioned Concrete Beams," Engineering Structures. 2016. (Submitted)

CHAPTER 1 : INTRODUCTION AND RESEARCH OBJECTIVES

1.1   INTRODUCTION

Transfer length is defined as the necessary length where the fully effective prestressing force, f_{se}, applied to the strand is transferred to the concrete. **Figure 1-1** illustrates how the prestressing force applied to the strand is transferred to the concrete. The cross-sectional area of the prestressing strand is reduced as a consequence of elongation from strand tensioning and tries to expand back to its original diameter when the tension is released. Since the prestress at the ends of the strand is zero, the variation of the diameter from the original value at the end to the reduced value after the transfer length creates a wedge effect in the concrete. This phenomenon helps to transfer the stress from the strand to the concrete and is known as Hoyer's effect [1-3].
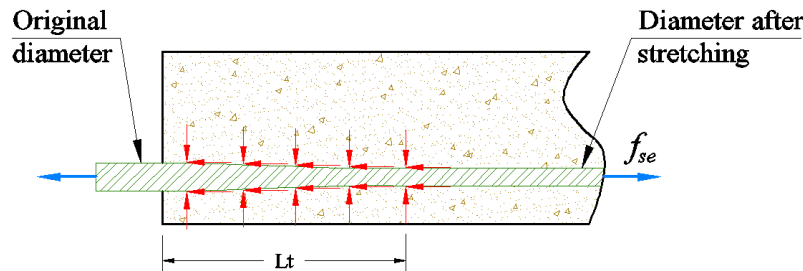
Figure 1-1. Hoyer's Effect - Transferring of prestress to the concrete

Development length, L_d, is defined as the essential length of strand required to develop the stress in the strand, f_{ps}, corresponding to the full flexural strength of the member. The flexural bond length is defined as the length of concrete beyond the transfer length required to develop the ultimate tensile strength of the prestressing strand. Therefore, development length is the sum of

1

the transfer length and the flexural bond length. **Figure 1-2** illustrates an idealization of strand stress versus length for the pretensioned strand.
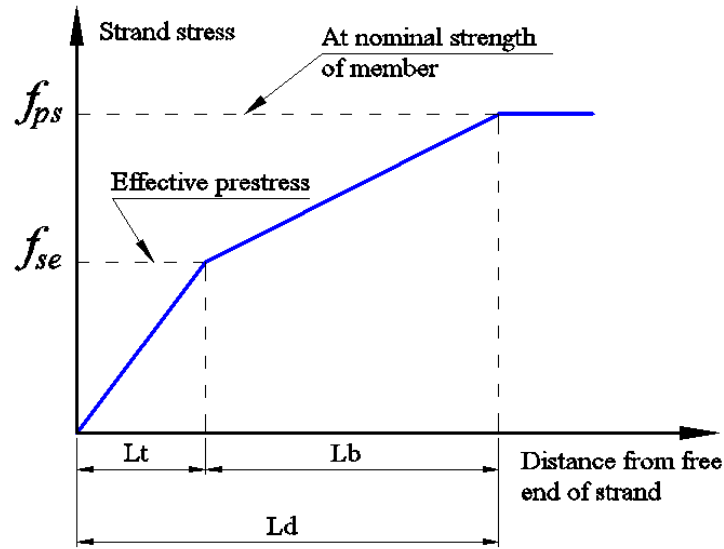
Figure 1-2. Strand stress vs. length

Investigations in transfer and development lengths began when Hanson and Kaar published their investigation in 1959 [4]. In 1963, the American Concrete Institute 318 Building Code (ACI 318-14) implemented these equations for predicting transfer and development lengths [5]. The equations were adopted in 1973 by the American Association of State and Highway Transportation Officials (AASHTO) Specifications [6-8]. The ACI and AASHTO equations for transfer length and development are shown below.

The equation for transfer length given by ACI 318-14 (Section 21.2.3) is written as follows

$$L_t = \frac{f_{se}}{20.7} d_b \tag{1}$$

where:

L_t = transfer length (mm)

2

f_{se} = effective prestressing stress after all losses (MPa)

d_b = strand diameter (mm)

In section 22.5.9.1, ACI 318-14 defines transfer length to be 50 strand diameter ($50d_b$), and the development length is a sum of the transfer length and the flexural bond length. The flexural bond is defined by

$$L_b = \frac{1}{6.9}(f_{ps} - f_{se})d_b \tag{2}$$

where:

L_b = flexural bond length (mm)

f_{se} = effective prestressing stress after all losses (MPa)

f_{ps} = strand stress at nominal strength of member (MPa)

d_b = strand diameter (mm)

Therefore, the development length, L_d, equation given by ACI 318-14 in its Section 25.4.8.1 is the following

$$L_d = \frac{f_{se}}{20.7}d_b + \frac{1}{6.9}(f_{ps} - f_{se})d_b = \frac{1}{6.9}\left(f_{ps} - \frac{2}{3}f_{se}\right)d_b \tag{3}$$

Although AASHTO LRFD adopted the same equations for transfer and development lengths given by ACI 318-14[5], AASHTO LRFD has specified that the transfer length can be taken as 60 strand diameters ($60d_b$) (Article 5.11.4.1) [6]. The development length, written in Eq. (4), must be taken as specified in its Article 5.11.4.2, and a k factor was added according to

3

recommendation of the 1988 FHWA memorandum mandated to the AASHTO Standard equation

which is the same equation given by ACI 318-14.

$$L_d = \frac{k}{6.9}\left(f_{ps} - \frac{2}{3}f_{se}\right)d_b \tag{4}$$

where:

L_d = development length (mm)

f_{se} = effective prestressing stress after all losses (MPa)

f_{ps} = strand stress at nominal strength of member (MPa)

d_b = strand diameter (mm)

k = 1.0 for pretensioned panels, piles, and other pretensioned members with a depth < 0.60 m.

k = 1.6 for pretensioned members with a depth ≥ 0.60 m.

k = 2.0 for debonded strand (Article 5.11.4.3)

These equations were based on early investigations which used stress-relieved Grade 1724

(Grade 250) strand with an ultimate strength, f_{pu}, of 1724 MPa (250 ksi) which was typically

tensioned to approximately 0.70f_{pu}. Currently, low relaxation, Grade 1862 (Grade 270) strand,

with f_{pu} of 1862 MPa (270 ksi), is used and is tensioned to stresses up to 0.80f_{pu} [8, 9]. In

addition to changes in strand properties, concrete properties have also changed since the

inception of these equations.

1.2   MOTIVATION

The transfer and development length equations presented in the ACI 318-14 and AASHTO

LRFD Codes are functions of the strand stress, including both the effective prestress in the strand

after all losses (*f_{se}*) and strand stress at nominal strength of member (*f_{ps}*), and the diameter of the

4

strand (d_b) [5, 6]. On the other hand, researchers have shown that variables such as initial prestress (f_{si}), concrete compressive strength at release time (f'_{ci}) and at 28-day (f'_c) affect both transfer and development lengths [9-13]. Research has shown that the equations, both transfer and development length, are conservative for high strength concrete (concrete with compressive strengths greater than 62 MPa (9000 psi) at 28 days). The conservativeness of the equations is due to the changes in material properties of both the strands and concrete since the 1950's. Such changes in material properties warrant a change in the prediction equations.

1.3   RESEARCH OBJECTIVES

The objectives of the research project are outlined below:

1.   Conduct a thorough review of literature pertaining to transfer and development length. The literature review will focus on experimental work and numerical analysis using finite element method. Emphasis will be placed on research that focuses on concrete compressive strength, initial prestress, and strand diameter.

2.   Collect data from early investigations on transfer and development lengths published by the University of Arkansas (UA) and other authors.

3.   Develop transfer and development length equations using experimental data. The development of these two equations will be the topic of the first and second journal articles (one article on transfer length and another on development length).

4.   Conduct an experimental measurement of the transfer and development lengths for 24 prestressed concrete beams which were cast at the UA. The beams were built as the same size as the earlier specimens [165 mm (6.5 in.) by 305 mm (12 in.) by 5.5 m (18 ft.)] cast at the UA. Preliminary research has shown that transfer lengths increased when the

5

compressive strength at release was less than 34.5 MPa (5000 psi). However, when the compressive strength at release was greater than 34.5 MPa (5000 psi), there was little difference in transfer length. Similar trends were apparent in the development length results. Therefore, the compressive strengths targets at release of the proposed beams were focused on a range from 21 MPa (3000 psi) to 55 MPa (8000 psi), but the compressive strengths at release measured in the field were in the range from 27 MPa (3860 psi) to 65 MPa (9390 psi). The majority of the beams were cast with compressive strengths at release less than 34.5 MPa (5000 psi).

5. Develop a numerical method to calculate the internal contact pressure between strand surface and concrete using the thick-walled cylinder theory, and develop a finite element model in one dimension to predict transfer length and compare the results with the experimental results reported in the literature. This is the subject of the third paper.

1.4   DISSERTATION ORGANIZATION

This dissertation is a compilation of three articles which were written to support the main idea of the research. This dissertation is organized in five chapters and two appendices. Chapter 1 describes the introduction and why this research is needed. Chapter 2 describes how a new transfer length equation was developed and examines the effect of concrete strength on the transfer length of the prestressing strand. Chapter 3 examines a wide range of concrete compressive strengths and their effects on the development length in prestressed concrete members and formulation of a new equation to predict this length. Chapter 4 describes a numerical method to calculate the contact pressure at the interface of strand and concrete which is implemented in a one dimensional, finite element analysis which measures the transfer length

6

in prestressed concrete by an iterative process. The results obtained through numerical analysis were compared and discussed with the experimental results reported by several authors. Finally, conclusions, contributions of the research, and recommendations for further research in this area are presented in Chapter 5. The appendices contain the codes of the programs written to achieve this research.

REFERENCES

[1] Mahmoud ZI, Rizkalla SH, Zaghloul E-ER. Transfer and development lengths of carbon fiber reinforced polymers prestressing reinforcement. ACI Structural Journal. 1999;96:594-602.

[2] Ruiz Coello ED. Prestress losses and development length in pretensioned ultra high performance concrete beams [Ph.D.]. United States - Arkansas: University of Arkansas; 2007.

[3] Staton BW. Transfer lengths for prestressed concrete beams cast with self-consolidating concrete mixtures [M.S.C.E.]. United States - Arkansas: University of Arkansas; 2006.

[4] Hanson NW, Kaar PH. Flexural bond tests of pretensioned prestressed beams. ACI Structural Journal. 1959;55:783-802.

[5] ACI-318-14. Building code requirements for structural concrete and commentary. Farmington Hills, MI: American Concrete Institute; 2014.

[6] AASHTO. AASHTO LRFD Bridge Design Specifications, Customary U.S. Units (6th ed.). Washington, D.C.: American Association of State and Highway Transportation Officials 2012.

[7] Lane SN. A new development length equation for pretensioned strands in bridge beams and piles. Turner-Fairbank Highway Research Center, 6300 Georgetown Pike, McLean, VA 22101 USA: Federal Highway Administration; 1998.

[8] Buckner CD. A review of strand development length for pretensioned concrete members. PCI Journal. March-April 1995;40:84-105.

[9] Mitchell D, Cook WD, Khan AA, Tham T. Influence of high strength concrete on transfer and development length of pretensioning strand. PCI Journal. May-June 1993;38:52-66.

[10] Cousins TE, Johnston DW, Zia P. Transfer and development length of epoxy coated and uncoated prestressing strand. PCI Journal. July-August 1990;35:92-103.

[11] Ramirez JA, Russell BW. Transfer, Development, and Splice Length for Strand/Reinforcement in High-Strength Concrete. Washington, D.C.: Transportation Research Board, National Research Council (NCHRP-603); 2008.

8

[12] Zia P, Mostafa T. Development length of prestressing strands. PCI Journal. September-October 1977;22:54-65.

[13] Martí-Vargas JR, Serna P, Navarro-Gregori J, Bonet JL. Effects of concrete composition on transmission length of prestressing strands. Construction and Building Materials. 2012;27:350-6.

9

CHAPTER 2 : EFFECT OF CONCRETE COMPRESSIVE STRENGTH ON TRANSFER LENGTH

Alberto T. Ramirez-Garcia [a], RoyceW. Floyd [b],W. Micah Hale [a], J.R.Martí-Vargas [c]

[a] Department of Civil Engineering, 4190 Bell, University of Arkansas, Fayetteville, AR 72701, United States

[b] School of Civil Engineering and Environmental Science, 202 W. Boyd St. Room 334, Norman, OK 73019, United States

[c] Universitat Politècnica de València (UPV), València, Spain

Abstract:

This paper examines the effect of concrete compressive strength on the transfer length of prestressing strands. The paper includes the results from several research projects conducted at the University of Arkansas (UA) and from testing reported in the literature. At the UA, 57 prestressed, precast beams have been cast since 2005. The beams were cast with selfconsolidating concrete (SCC), high strength concrete (HSC), lightweight self-consolidating concrete (LWSCC), and ultra-high performance concrete (UHPC). Using data from the UA and from the literature, an equation to estimate transfer length was developed and presented. The results were also compared with the American Concrete Institute (ACI 318) and the American Association of State Highway and Transportation Officials (AASHTO) prediction equations for transfer length, which were designed for conventional concrete. The results also showed that there was little change in transfer length when the compressive strength at release was greater than 34.5 MPa.

Keywords: Pretensioned concrete, Transfer length, Bond

2.1   INTRODUCTION

Prestressed concrete has been used extensively since the 1950's. Many buildings and bridge
structures utilize its principles, especially pre-cast structures. In the design of pretensioned
members, there is a particular focus on the length a strand must be embedded in the concrete in
order to develop its bond strength. Transfer length refers to the strand length required to transfer
the initial prestress in the strand to the concrete.

The ACI 318 Building Code and Commentary (hereafter referred to as ACI 318-14) [1] and the
AASHTO Load and Resistance Factor Design (LRFD) [2] Specifications (hereafter referred to as
AASHTO) provide equations to estimate transfer length. The equation is a function of the
effective prestress (f_{se}) and the strand diameter (d_b) [1-3]. Investigators have shown that initial
prestress (f_{si}), and concrete compressive strength both at prestress release (f'_{ci}) and at 28-days
(f'_c), contribute to transfer length [3-8].

With the changes occurring regarding concrete mixture proportioning and properties, researchers
have and are questioning the accuracy of the ACI 318-14 and AASHTO equations. In these
design codes, concrete compressive strength is not a variable in the transfer length equations
even though it has been shown to affect bond [8-10]. For example, the transfer length for high
strength concrete members is less than that predicted by ACI 318-14 and AASHTO [5, 6, 11].
Transfer length is an important parameter in shear design and in determining allowable stresses.
An incorrect estimation of this length can affect the shear capacity of a member and may result
in serviceability issues that occur in the end zones at strand release [10, 12]. Therefore, there is a
need to better estimate transfer length and this can be accomplished by incorporating concrete
compressive strength in the transfer length equation.

11

2.2 BACKGROUND

Research on the transfer length in prestressed concrete members began when Hanson and Kaar published their findings on the flexural bond behavior of prestressing strand in 1959 [13]. In 1963, the ACI Building Code implemented equations for these lengths [1]. The ACI formulas were adopted in 1973 by AASHTO [2, 14, 15]. The equation for transfer length given by ACI 318-14 section R21.2.3 [1, 3] is written as follows:

$$L_t = \frac{f_{se}}{20.7} d_b \tag{1}$$

where:

L_t = transfer length (mm)

f_{se} = effective prestress after all losses (MPa)

d_b = strand diameter (mm)

ACI 318 also states that transfer length can be estimated as 50 strand diameters ($50d_b$) [1, 3] and AASHTO uses $60d_b$ (Article 5.11.4.1) [2].

The early transfer length research used stress-relieved Grade 1724 strand with an ultimate strength, f_{pu}, of 1724 MPa, and were typically pretensioned to approximately $0.70f_{pu}$. In current practice, low-relaxation Grade 1862 strand (f_{pu} of 1862 MPa) is used, and is pretensioned up to $0.80f_{pu}$ [2, 5, 15]. However these changes are not reflected in the code equations.

In 1977, Zia and Mostafa proposed a formula to calculate the transfer length of prestressing strands [7]. Their equation accounted for the effects of strand size, initial prestress, effective prestress, ultimate strength of the prestressing strand, and concrete compressive strength at prestress release (ranging from 14 to 55 MPa). Their research showed that the equations were more conservative (predicted larger values) than the ACI Code when the concrete strength at release is low (14 MPa $\leq f'_{ci} \leq$ 28 MPa).

12

In 1990, Cousins, Johnson, and Zia developed analytical equations for transfer length that included plastic and elastic behavior. In these equations new variables were introduced such as the plastic transfer bond stress coefficient (U'_t), the bond modulus (B), and the prestressing strand area (A_s). Even though Cousins et al. expressed that the ACI 318 Code and AASHTO provisions were inadequate and should be revised, the equations remained unchanged [4].

In 1993, Mitchell et al. studied the influence of concrete strength on transfer length. Their reported concrete strengths at prestress release varied from 21 to 50 MPa and from 31 to 89 MPa at the time of testing. Mitchell et al. developed and proposed an equation for transfer length which predicted shorter values than ACI 318-14 for higher strength concretes [5]. Their findings indicated a reduction in transfer length with increasing concrete compressive strength.

In 1994, Deatherage, Burdette, and Chew cast twenty full scale AASHTO Type I beams with different strand diameters to investigate the transfer length. This work came after the Federal Highway Administration (FHWA) enforced restrictions on the use of Grade 1862 low relaxation seven wire prestressing strand in prestressed concrete girders in October 1988 [16]. Deatherage, Burdette, and Chew considered different strand stresses to formulate an equation for transfer length. The proposed equation resembles the ACI 318-14 and AASHTO equations, but the transfer length is governed by the initial prestress (f_{si}) instead the effective prestress (f_{se}) [1-3]. Although Deatherage, Burdette, and Chew made suggestions on the transfer length equation, no changes were made because the suggestions were more conservative.

In 1996, Russell and Burns investigated the transfer length for 12.7 mm and 15.2 mm diameter strands. They examined several variables such as strand spacing, strand debonding, reinforcement confinement, number of strands per specimen, and size and shape of the cross section [17]. The results showed that the transfer lengths, measured using the "95 Percent

13

Average Maximum Strain" method (95% AMS), for both 12.7 and 15.2 mm strands, were very similar and were larger than ACI 318 and AASHTO standard provisions. Consequently, a new equation for transfer length was proposed by the expression $f_{se}d_b/13.8$; where f_{se} (MPa) and d_b (mm).

In 2006, Marti-Vargas et al. showed that for concretes with compressive strengths in the range of 21 MPa to 55 MPa, the transfer lengths were about 50% to 80% of those calculated by ACI 318-11 [18]. Later, Marti-Vargas et al. investigated the relationship between the average bond stress for the transfer length as a function of the concrete compressive strength [19]. The transfer length decreased as the concrete compressive strength at prestress release increased [8, 20, 21], and the transfer length depended on the cement content, water content, and bond stress.

In 2008, Ramirez and Russell published a report based on an investigation sponsored by the National Cooperative Highway Research Program (NCHRP-603) [6]. In this project the transfer length was measured in concrete specimens cast with normal-weight and high-strength concrete at compressive strengths up to 103 MPa. The research showed that increasing concrete strength correlated clearly with the shortening of transfer length. As a result, a new equation was recommended for the AASHTO specifications. In particular, this new equation included the concrete compressive strength at release (f'_{ci}). In addition, for concrete compressive strengths at release of 28 MPa, the transfer length was recommended to be $60d_b$, which was the same value provided by AASHTO. On the other hand, for concrete strengths at release greater than 62 MPa, 40 strand diameters ($40d_b$) was the recommended transfer length. Although new equations were proposed to AASHTO, these equations for transfer length were not added to the specifications. Shown in **Table 2-1** are several equations that were developed for predicting transfer length [4, 6, 7, 14-16, 22].

Table 2-1 - Proposed equations for predicting transfer length (MPa and mm).

Source	Transfer Length, Lt
ACI-318 / AASHTO LRFD [1]	$L_t = \dfrac{f_{se}}{20.7} d_b$
Zia and Mostafa, 1977 [7]	$L_t = 1.5 \dfrac{f_{si}}{f_{ci}^{'}} d_b - 117$
Cousins et al., 1990 [4]	$L_t = \dfrac{U_t^{'}\sqrt{f_{ci}^{'}}}{2B} + \dfrac{f_{se}A_s}{\pi d_b U_t^{'}\sqrt{f_{ci}^{'}}}$
Mitchell et al., 1993 [5]	$L_t = \dfrac{f_{si}}{20.7} d_b \sqrt{\dfrac{20.7}{f_{ci}^{'}}}$
Deatherage et al., 1994 [16]	$L_t = \dfrac{f_{si}}{20.7} d_b$
Buckner, 1995 [15]	$L_t = \dfrac{f_{si}}{20.7} d_b$
Lane, 1998 [14]	$L_t = 4 \dfrac{f_{si}}{f_c^{'}} d_b - 127$
Kose and Burkett, 2005 [22]	$L_t = 0.045 \dfrac{f_{si}}{\sqrt{f_c^{'}}} \left(25.4 - d_b\right)^2$
Ramirez and Russell, 2008 [6]	$L_t = \dfrac{315}{\sqrt{f_{ci}^{'}}} d_b \geq 40 d_b$

Since 2005, Hale et al have conducted a significant amount of research on transfer length [11, 23-29]. These investigations focused on different types of concrete ranging from normal strength to ultra-high performance concrete. This paper summarizes the findings of the research and those from the literature and proposes an equation that was based on research encompassing many concrete types with different compressive strengths.

2.3   RESEARCH SIGNIFICANCE

The research project included transfer lengths measured at the University of Arkansas (UA) and from results published in the literature. At the UA, the transfer length was measured for 57 beam specimens. The specimens were cast with a variety of concrete types at a wide range of compressive strengths. In addition, measured transfer lengths data were collected from the literature.   This research focuses on the effect of concrete compressive strength (at release and 28-days or time of testing) on transfer lengths. With the data, an equation was developed that encompasses a wide range of concrete types and concrete compressive strengths.

2.4   EXPERIMENTAL PROGRAM

2.4.1   Concrete mixtures

For the specimens cast at the UA, 11 different mixture proportions were developed. These 11 mixtures are shown in **Table 2-2**. For the first six mixtures listed in **Table 2-2**, the first two letters represent the compressive strength. "NS" refers to normal strength concrete mixtures and "HS" refers to high strength concrete mixtures. The last two letters represent the type of coarse aggregate used in the mixtures. The aggregate type included shale (SH), clay (CL), and limestone (LS). The mixtures containing shale or clay are also lightweight mixtures with a unit weight of approximately 1922 kg/m^3. These first six mixtures were also self-consolidating. The next two mixtures, SCC-I and SCC-III, were normal weight SCC mixtures cast with either Type I or Type III cement. These mixtures were also normal weight (approximately 2323 kg/m^3). Mixture "HSC" was a high strength concrete mixture. Mixture "UHPC" was a commercially available ultra-high performance concrete mixture. The final mixture "LWSCC" was a lightweight SCC mixture proportion that was developed by prestressed concrete beam fabricator.

16

The mixture proportions were discussed in greater details in earlier publications by the authors [11, 23-30].

The number of beams cast from each mixture and the number of transfer length tests performed on beams cast with that particular mixture are also presented in **Table 2-2**. Fifty-one beams were cast with 15.2 mm diameter [24, 26, 29] strands, and six beams were cast with 12.7 mm diameter strands [27].

Also shown in **Table 2-2** is the mean compressive strength at release and at 28 days for each mixture. The compressive strengths at release using 15.2 mm strand ranged from 23 MPa to 155 MPa, and the 28 day strengths ranged from 34.5 MPa to 199 MPa. Furthermore, for 12.7 mm diameter strand the compressive strengths at release ranged from 24 MPa to 37 MPa, and the 28 day strengths ranged from 41 MPa to 52 MPa.

Table 2-2 - Mixture identifications, number of tests, and compressive strength.

Concrete Mixtures	Number of Trial Beams	Number of L_t tests	f'_{ci} Mean, MPa	f'_c Mean, MPa
NSSH: Normal strength shale	5	10	28	42
NSCL: Normal strength clay	4	8	31	39
NSLS: Normal strength limestone	4	8	33	52
HSSH: High strength shale	4	8	42	48
HSCL: High strength clay	4	8	43	49
HSLS : High strength limestone	4	8	48	64
SCC-III : Self-consolidating concrete Type III	5	10	51	76
SCC-I : Self-consolidating concrete Type I	8	16	54	84
HSC : High strength concrete	6	12	64	85
UHPC : Ultra high performance concrete	7	14	124	182
LWSCC * : Lightweight self-consolidating concrete	6	12	31	46

(*) 12.7 mm diameter strand

2.4.2 Beam fabrication

At the UA, 57 fully bonded, prestressed, precast beams have been cast since 2005. Each beam had a rectangular cross-section of 165 mm by 305 mm and was 5.5 m length. The beams contained two, low relaxation wire Gr. 1862 prestressing strands located a distance of 254 mm, measured from the top (compression fiber) of the beam to the centroid of the strand as shown in **Figure 2-1**. Strand diameters of 12.7 mm and 15.2 mm were included in the study. Two No. 19, Gr. 414 reinforcing bars were located near to 51 mm from the top of each beam. The beams were reinforced with No 6 smooth bars spaced at 150 mm. The beams were cast with mixtures shown in **Table 2-2** [24, 26, 27, 29]. Two beams were cast simultaneously on a 15.2 m prestressing bed. The strands were tensioned to 75% f_{pu}, 1397 MPa.
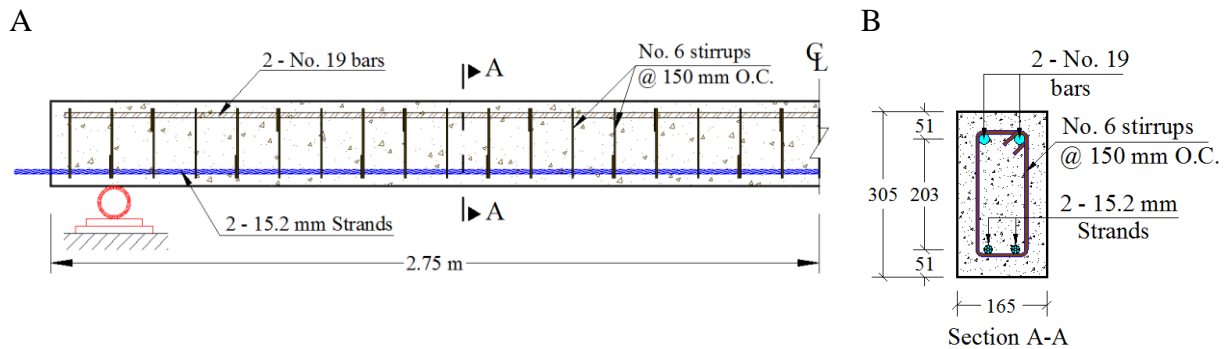
Figure 2-1. Beam section and reinforcement detail

2.4.3 Bond quality assessment

The Standard Test for Strand Bond (STSB) was used to assess the quality of the strands used in the UA study. The force required to induce 2.54 mm of free end slip for each specimen exceeded the 4899 kg minimum required for individual specimens. For the three sources of strands used in the study, the average pull out values of 8700, 10083, and 9339 kg exceeded the

18

minimum requirement of 5715 kg. Thus, the results showed that the strands were of good
quality.

2.4.4   Instrumentation

Before prestress release, detachable mechanical (DEMEC) strain gauge targets were attached to
the beam at the level of the prestressing strand (**Figure 2-2**). These targets were placed at both
ends of the beam on both faces [7, 17, 31-34]. The first target was approximately placed at 25.4
mm from the beam end, and the other DEMEC points were placed at 100 mm intervals. The
prestress was gradually released approximately 24 hours after casting. This was accomplished
by releasing the pressure in the hydraulic strand tensioning system. Each beam specimen was
labeled based on the concrete type along with a beam number. For instance, the first beam cast
using SCC with Type I cement was labeled SCCI-1 [11, 23, 25, 28]. Surface strains were
assessed using a digital DEMEC strain gauge with 200 mm gauge length. Strain readings were
taken immediately before and after prestress release and at 3, 5, 7, 14, and 28 days (**Figure 2-3**).
Transfer lengths were determined using the 95% Average Maximum Strain method (AMS) [17].
Transfer length was measured for both beam ends which results in 114 total tests as is shown in
Table 2-2.

www.manaraa.com

Figure 2-2. Placement of DEMEC points (Photo by author).

Figure 2-3. DEMEC measurements (Photo by author).

20

2.5   TRANSFER LENGTH ANALYSIS

2.5.1   Measured transfer length data

The measured minimum, average, and maximum transfer lengths at release and at 28-days are presented in **Table 2-3**. Additionally, the average concrete compressive strengths at release (f'_{ci}) and at 28-days (f'_c), the average of the effective strand stress after all losses (f_{se}), and the predicted transfer lengths using ACI 318-14 & AASHTO are presented.

As shown in **Table 2-3**, the maximum measured transfer length for all beams was 1090 mm. This occurred in the NSSH series which also had the lowest concrete compressive strength at release. This value was greater than the predicted value of 792 mm by approximately 37.5%. The average transfer length for all NSSH beam was 733 mm at release which was 92.4% of the predicted value.

Table 2-3 - Measured transfer lengths and predicted lengths.

Series	f'_{ci}, MPa	f'_c, MPa	f_{se}, MPa	Reported Transfer Lengths (mm): Release			Reported Transfer Lengths (mm): 28 days			ACI / AASHTO
				Min.	Avg.	Max.	Min.	Avg.	Max.	Predicted
NSSH	28	42	1076	505	733	1090	559	681	970	792
NSCL	31	39	1069	495	597	815	424	635	841	787
NSLS	33	52	1166	450	557	991	470	609	1031	858
HSSH	42	48	1146	409	520	681	361	426	521	843
HSCL	43	49	1154	361	486	780	399	487	610	850
HSLS	48	64	1215	460	503	551	490	531	640	895
SCC-III	51	76	1216	381	457	584	368	483	610	895
SCC-I	54	84	1244	394	507	635	343	512	673	916
HSC	64	85	1256	394	506	635	432	579	724	925
UHPC	124	182	1297	267	358	432	279	361	457	955
LWSCC (*)	31	46	1186	381	525	838	330	510	686	873

(*): Strand 12.7 mm diameter was used in this case

21

At the other extreme, the predicted transfer length for the UHPC series was over 250% greater than the average measured transfer length. The UHPC series possessed the highest compressive strength at release and at 28 days of age. **Table 2-3** shows that once the compressive strength at release achieved 42 MPa or greater, all measured transfer lengths were less than the values predicted by ACI 318-14 and AASHTO.

The data was analyzed using a power regression which is shown in **Figure 2-4**. The measured transfer lengths are plotted versus the concrete compressive strength. The measured transfer length at both beam ends is plotted (L = live end and D = dead end) along with the compressive strength at release and at 28-days. The data in **Figure 2-4** confirms that the measured transfer lengths decreased as the concrete strengths increased [6, 35]. Based on the data shown in **Figure 2-4**, concrete compressive strength should be included in the transfer length equations [8, 20, 22, 35].
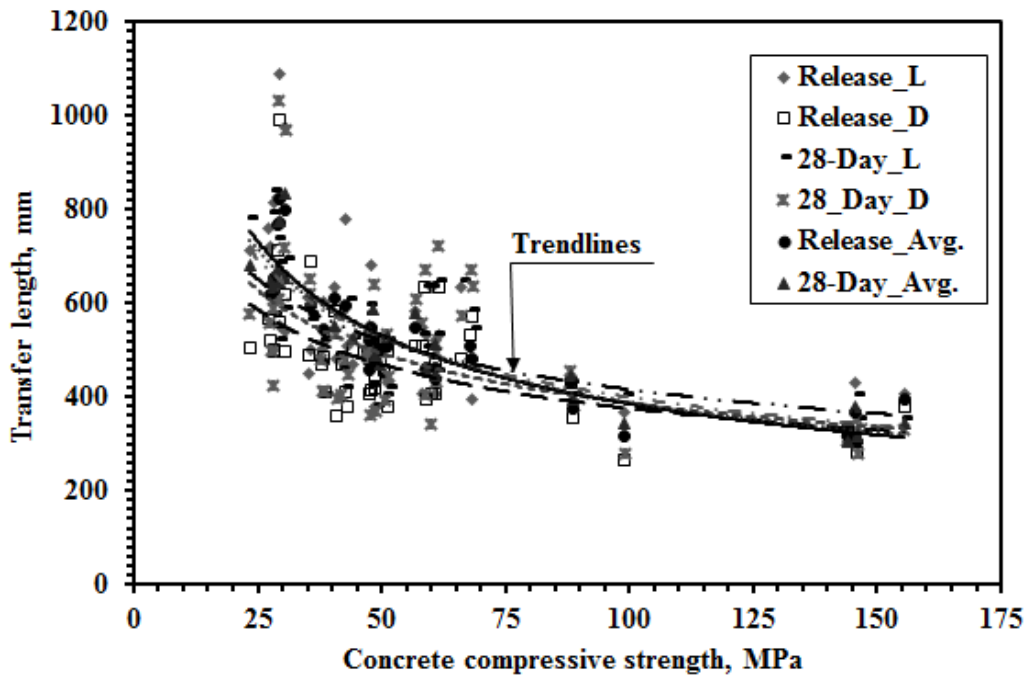
Figure 2-4. Transfer length analysis – power regression.

22

Several researchers have examined the influence of other variables on transfer length [4, 7, 8, 19, 20, 22, 31, 36]. Based on this previous research, two variable sets were included in this study. For the first set, concrete compressive strength at release (f'_{ci}), initial prestress (f_{si}) (75 % f_{pu} = 1397 MPa), and strand diameter (d_b) were examined. The variables for the second set were concrete compressive strength at release (f'_{ci}), effective strand stress after all losses (f_{se}), and strand diameter (d_b). Statistical analysis was conducted for the two variable sets, and from this analysis the first set of variables (f'_{ci}, f_{si}, and d_b) were chosen because these variables had a greater affect transfer length at release [5, 7]. Consequently, an equation for transfer length (**Eq. 2**) was derived and is shown below:

$$L_t = 25.7 \left(\frac{f_{si}}{f'_{ci}} d_b \right)^{0.55}$$

(2)

where:

f_{si} = initial prestress (MPa)

f'_{ci} = concrete strength at prestress release (MPa)

d_b = nominal strand diameter (mm)

Figure 2-5 shows the ratio between predicted and measured transfer length for the ACI/AASHTO, NCHRP-603, and the proposed equation (**Eq. 2**). The ratio due to the proposed equation and NCHRP-603 are similar when the concrete strength at release is less than 62 MPa. The ratio is almost equal to one when the concrete strength at release is equal to 62 MPa. At compressive strengths greater than 62 MPa, the proposed equation provides a better estimate than the NCHRP-603 equation. At compressive strengths less than 41 MPa, the ACI 318-14 and AASHTO equations are more accurate than the proposed and NCHRP-603 equations. In

23

addition, the ratio of the ACI 318-14 and AASHTO equations increases suddenly for higher compressive strength ($f'_{ci} \geq 62$ MPa) while the ratio due to the proposed equation remains closer to one.
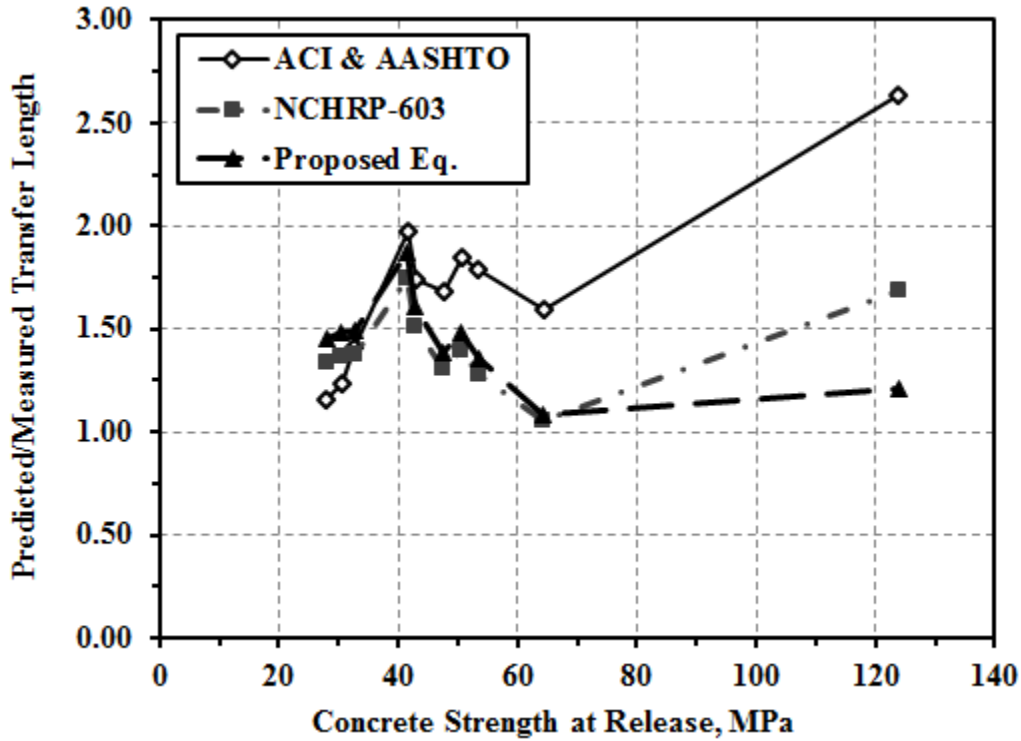
Figure 2-5. Ratio of predicted to measured transfer length.

2.5.2   Transfer length data from the literature

Transfer length data [4-6, 16, 17, 19, 33, 34, 37-41] were collected from the literature in order to examine the accuracy of the proposed equation. For 12.7 mm strands, 293 transfer length tests were identified in the literature, and this number was reduced to 180 data points (**Table 2-4).** Many researchers reported transfer lengths for the dead ends, live ends, or the average of both ends. Therefore, the 180 data points represent the total number of transfer length analyzed, and each transfer length was the average transfer length of both ends of a beam. For 15.2 mm

strands, 345 transfer length measurements were identified in the literature and then reduced to

139 data points (**Table 2-5**). This number represents the average transfer length for 139 beam

ends.

Table 2-4 - Transfer lengths from the literature for 12.7 mm strand.

Literature Source	Number of Tests	Data Analyzed	Reported Transfer Length, mm			Average f'_{ci}, MPa
			Min.	Avg.	Max.	
Cousins et al., 1990	20	20	813	1262	1880	35
Mitchell et al., 1993	14	8	367	513	711	40
Deatherage et al., 1994	16	16	457	602	914	33
Russell and Burns, 1996	34	17	432	748	978	30
Rose and Russell, 1997	30	15	300	392	587	29
Russell and Burns, 1997	12	6	661	1050	1461	25
Mahmoud et al., 1999	8	8	350	469	600	41
Oh and Kim, 2000	36	18	463	606	826	40
Hodges, 2006	6	3	343	474	699	36
NCHRP-603, 2008 (A/B)	30	15	311	412	554	52
NCHRP-603, 2008 (D)	31	16	391	597	937	53
Bhoem et al., 2010	12	6	343	411	465	47
Marti-Vargas et al., 2012	12	12	400	533	650	39
Myers et al, 2012	8	8	351	460	630	39
UA (release)	12	6	406	525	686	31
UA (28-day)	12	6	394	510	610	46
Total Number of Tests	293	180				

Note: Ramirez and Russell, 2008 (NCHRP R-603)

Table 2-5 - Transfer lengths from the literature for 15.2 mm strand.

Literature Source	Number of tests	Data Analyzed	Reported transfer length, mm			Average $f'ci$, MPa
			Min.	Avg.	Max.	
Cousins et al., 1990	10	10	1118	1435	1727	33
Mitchell et al., 1993 (*)	12	6	305	545	803	40
Deatherage et al., 1994	8	8	889	1032	1270	33
Russell and Burns, 1996	40	20	711	1016	1264	31
Russell and Burns, 1997	13	8	762	1043	1245	28
Oh and Kim, 2000	36	18	539	758	1022	40
NCHRP-603, 2008 (A6)	22	11	475	667	785	51
UA (release)	102	30	305	524	824	64
UA (28-day)	102	28	305	532	833	89
Total Number of Tests	345	139				

(*) strand 15.75 mm; UA: University of Arkansas

The measured transfer lengths from the data set were plotted against the concrete compressive strength at release (f'_{ci}) which ranged from 19 MPa to 155 MPa as shown in **Figure 2-6** and **Figure 2-7**. For most of the data collected from the literature, the concrete compressive strengths at release ranged from 19 MPa and 69 MPa. However, there is a limited amount of data that includes concrete compressive strengths at release over 69 MPa [25]. Both figures show the decrease in transfer length as concrete compressive strength at release increases. The figures also show the range of transfer lengths at lower concrete compressive strengths. For 12.7 mm strands, the transfer lengths ranged from approximately 250 mm to 1900 mm at 28 MPa. The highest transfer lengths were reported by Cousins et al. (1990). These values may have been caused by unreported factors such as poor strand surface condition [4]. The data also show the lack of change in transfer length at high release strengths.
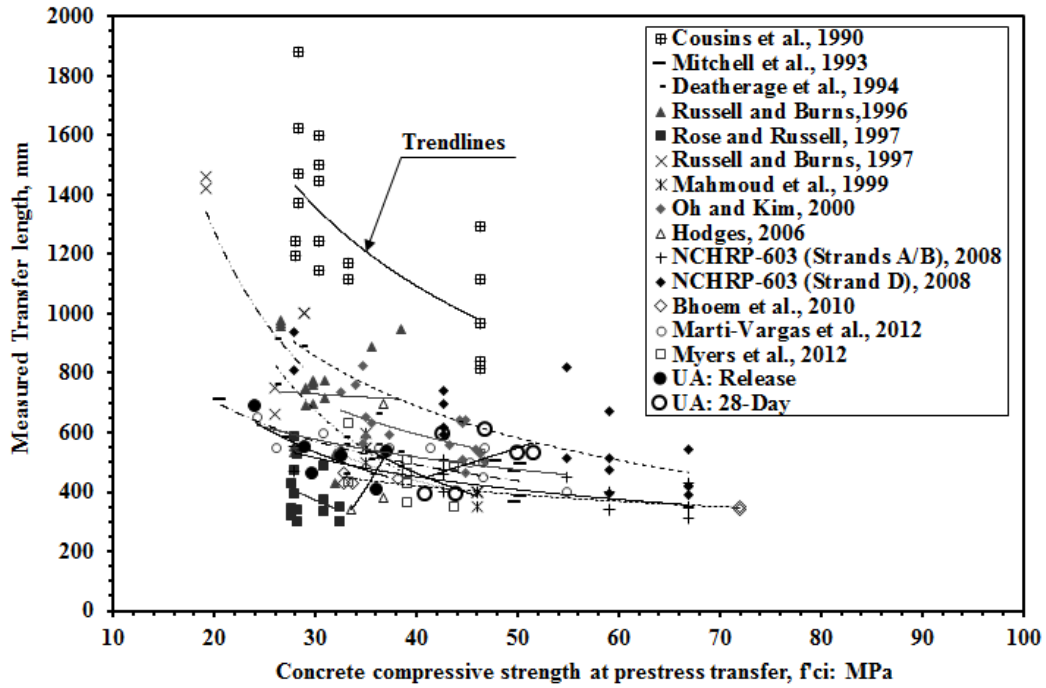
Figure 2-6. Transfer length of 12.7 mm strand from the literature.
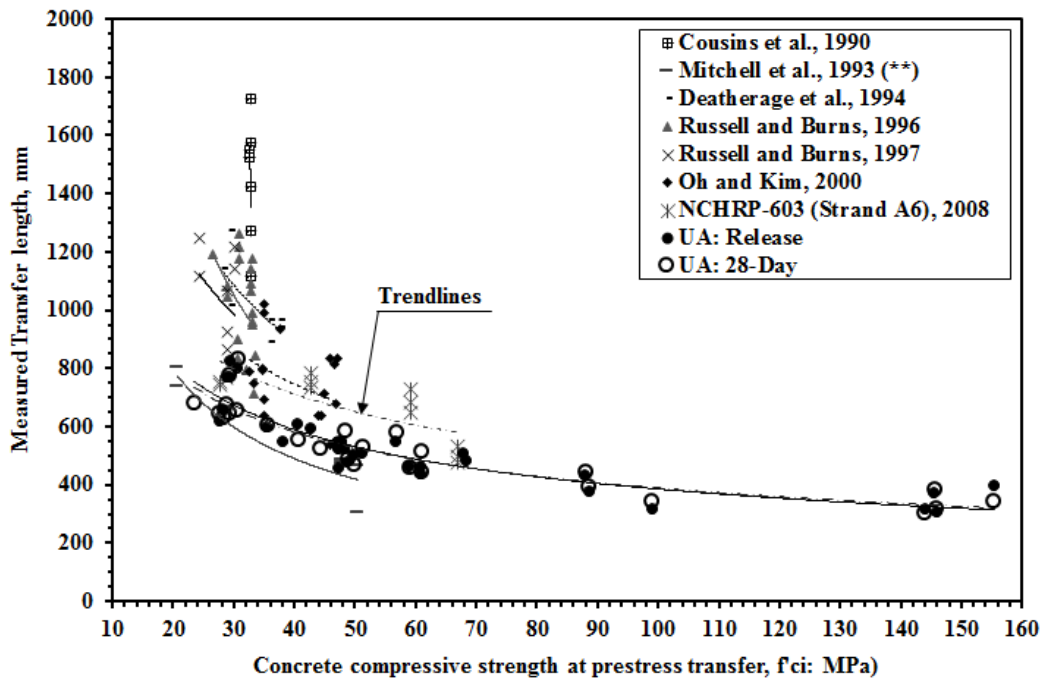
Figure 2-7. Transfer length of 15.2 mm strand from literature (** = 15.75 mm).

2.5.3 Data reduction

To determine the accuracy of the proposed equation, outliers in the data set were removed. Outliers were determined based on the average transfer length ratio and standard deviation. The transfer length ratio was calculated by dividing the predicted transfer length by the measured transfer length. Predicted transfer lengths were calculated using the ACI 318-14 equation and **Eq. 2**. Some assumptions were made in order to use these equations. These assumptions included a low relaxation wire, Grade 1862 strand (12.7 mm and 15.2 mm diameter) with an ultimate strength, f_{pu}, of 1862 MPa, an initial prestress of 1397 MPa ($f_{si} = 0.75f_{pu}$), and an effective prestress after all losses of 1117 MPa ($f_{se} = 0.60f_{pu}$) [20]. Using these values, the predicted transfer lengths obtained using ACI 318-14 were 686 mm and 823 mm for 12.7 mm and 15.2 mm strand, respectively.

Figure 2-8 and **Figure 2-9** show the transfer length ratios (predicted/measured) versus the measured transfer lengths. The transfer length ratios were calculated using the data set and the values using the ACI 318-14 equation. These figures also show the average transfer length value (AV), the standard deviation (SD), the underestimated values (UV), and the overestimated values (OV), and the upper bound (AV + SD) and lower bound (AV – SD). For the 12.7 mm strand, the average transfer length ratio was 1.32 with a standard deviation of ±0.35. Furthermore, since the predicted transfer length using the ACI 318-14 equation was constant for both strand sizes (686 mm and 823 mm), the plotted ratios follow the same power trend line as shown in **Figure 2-8** and **Figure 2-9**. **Figure 2-10** and **Figure 2-11** show the values predicted using **Eq. 2**. Since the predicted transfer length values using **Eq. 2** are dependent on the concrete strength at release (f'_{ci}), the predicted transfer length is not constant unlike the values determined using ACI 318-14. This is reflected in the plot of the data in **Figure 2-10** and **Figure 2-11**.

28
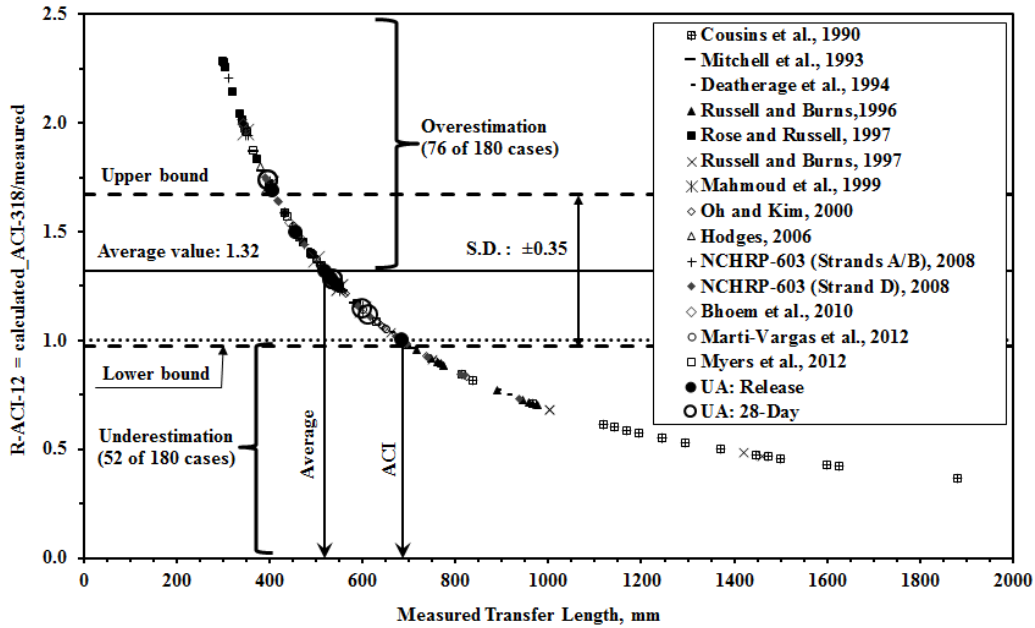
Figure 2-8. Transfer length ratio using ACI 318-14 for 12.7 mm strand.
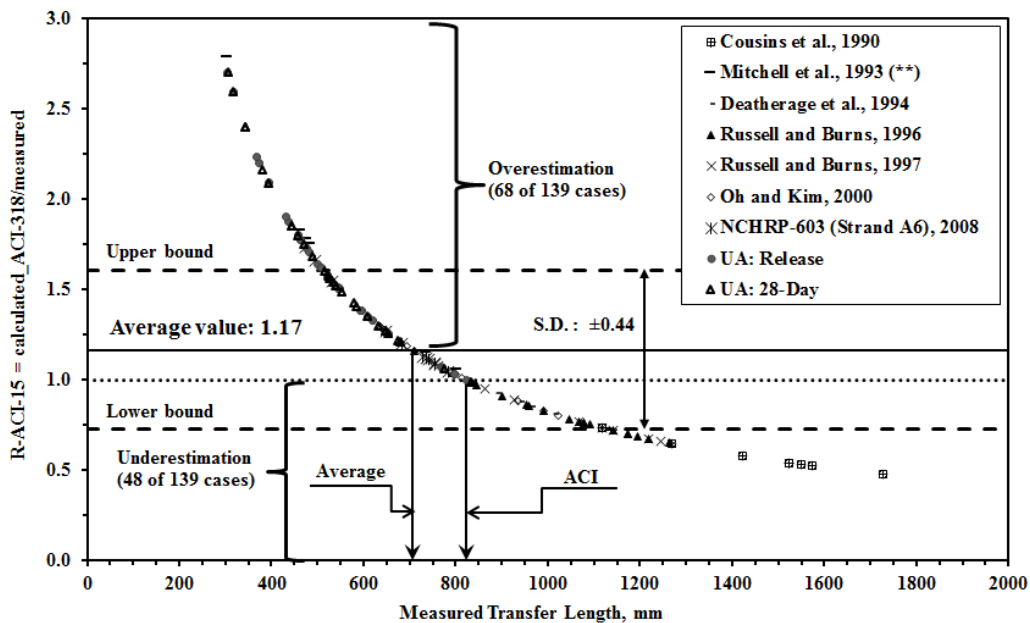
Figure 2-9. Transfer length ratio using ACI 318-14 for 15.2 mm strand.

29
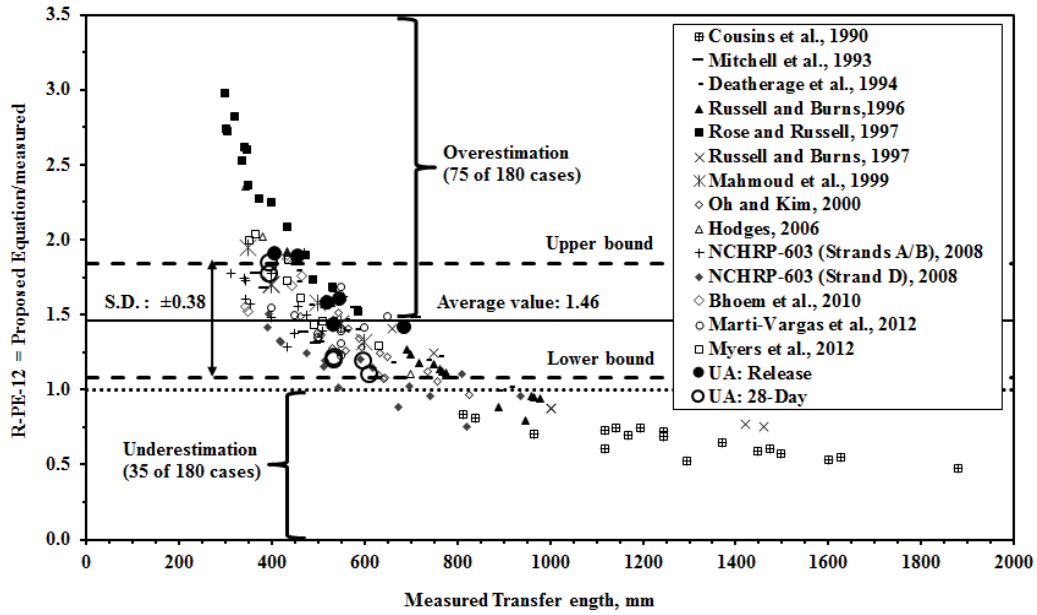
Figure 2-10. Transfer length ratio using Eq. 2 for 12.7 mm strand.
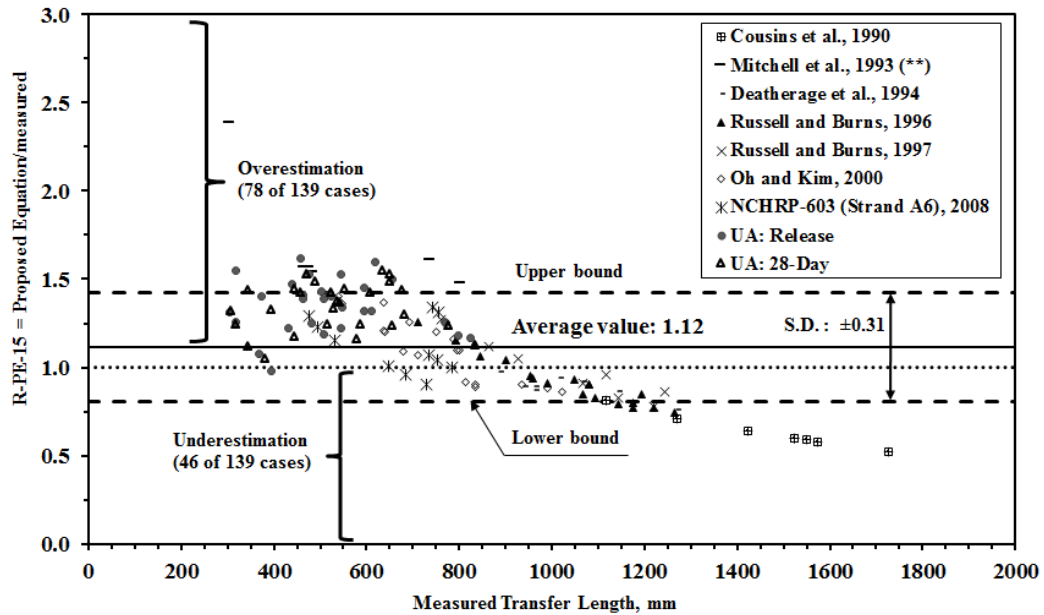
Figure 2-11. Transfer length ratio using Eq. 2 for 15.2 mm strand.

The following conclusions can be determined from **Figure 2-8** and **Figure 2-10** (12.7 mm

diameter strand). The average transfer length ratio using ACI 318-14 was 1.32, and its SD was

±0.35 while the average transfer length ratio using **Eq. 2** was 1.46 and its SD was ±0.38.

Therefore, the ACI 318-14 equation overestimates transfer length by 32% while the proposed

equation, **Eq. 2**, overestimates by 46%. Although **Eq. 2** had a greater standard deviation than

ACI 318-14 (0.38 vs 0.35), the total number of measured transfer lengths between UV and OV

lines represents 39% of the data set analyzed. This represents 10% more than the ACI 318-14

equation. The percentage of excluded data for the ACI 318-14 equation is 71% which represents

10% more than the proposed equation, **Eq. 2**. Therefore, more data are represented between the

lower and upper bounds for **Eq. 2** which means **Eq. 2** better represents the measured transfer

length values obtained from the literature than the ACI 318-14 equation.

The same analysis was performed using the data set of 15.2 mm diameter strand. The average

transfer length ratio using ACI 318-14 was 1.17 with a SD of ±0.44. The average transfer length

ratio was 1.12 using **Eq. 2** and had a SD of ±0.31. For the 15.2 mm strands, **Eq. 2** overestimated

transfer length by 12% compared to 17% for ACI 318-14. The total measured transfer lengths

between the lower and upper bounds for **Eq. 2** represents 72% of the data which is 9 percent

more than that represented by ACI 318-14.

2.5.4 Influence of compressive strength on transfer length

To determine the accuracy of **Eq. 2**, its predicted values were compared to those from other

proposed equations. The other proposed equations include those listed in **Table 2-1** with the

exception of the Buckner equation. This equation was not included in the study because of its

similarity to the Deatherage equation which was included. In order to use some of the equations

31

shown in **Table 2-1**, additional inputs were necessary. Values for f_{pu}, f_{si}, f_{se} were assumed in the previous task, but additional values were needed for the Cousins et al. equation. Those values included the plastic transfer bond stress coefficient ($U'_t = 0.556$), the bond modulus ($B = 0.0815$ MPa/mm.), and the area of the prestressing strand ($A_s = 140 \text{ mm}^2$) for 15.2 mm diameter strand. Using these values, the transfer lengths were calculated, normalized with respect to the nominal strand diameter, and plotted as shown in **Figure 2-12**.
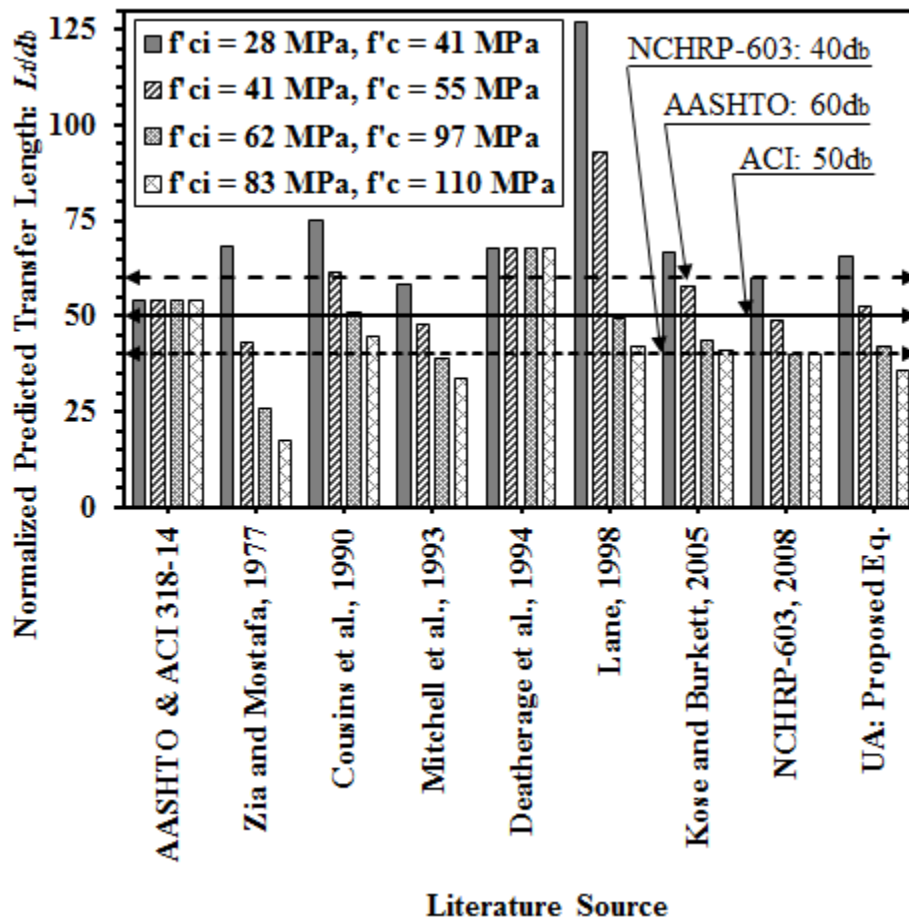
Figure 2-12. Comparison of normalized transfer lengths.

For this analysis, the concrete compressive strength at release was varied from 28 MPa to 83 MPa while the 28 day concrete strength ranged from 41 MPa to 110 MPa.   As shown in the **Figure 2-12**, the ACI 318-14, AASHTO, and Deatherage et al. equations are not dependent on concrete strength and therefore their predicted transfer length values are constant for all strengths.

When the concrete strength at release and at 28-days were 28 MPa and 41 MPa respectively, all predicted transfer length values using the equations in **Table 2-1** were greater than the predicted value using ACI 318-14. On the contrary, when concrete strength at release is 62 MPa or more, all equations except for the Deatherage et al. equation predict a transfer length that is less than that predicted by ACI 318-14. The UA equation, **Eq. 2**, predicts values that follow similar trends as the other equations (excluding ACI 318-14, AASHTO, and Deatherage et al.). **Eq. 2** predicts values which are slightly different than those of the NCHRP-603 equation. For instance, **Eq. 2** predicts larger transfer length values at lower compressive strengths and shorter values at higher compressive strengths.

It should be noted that Zia and Mostafa's equation for transfer length [7] was not recommended for compressive strengths over 55 MPa. For release strengths of 62 MPa and 83 MPa, their equation predicts transfer lengths that are approximately 40 to 50% less than the minimum limit recommended by NCHRP-603 ($40d_b$). In addition, **Figure 2-12** shows two important conclusions which are:

1. When the concrete strength at release and 28-days increases, the normalized transfer length decreases for all estimated values except those predicted using the ACI 318-14 (R21.2.3) and Deatherage et al. equations. Value predicted using these two equations

are constant due to the fact that the transfer length does not depend on concrete compressive strength.

2. For compressive strength at release of 83 MPa, the transfer lengths for 5 of the 7 proposed equations which are function of concrete compressive strength predict values that are lower or equal values than the minimum transfer length ($40d_b$) [6]. The exceptions are the Kose and Burkett's equation and Lane's equation. However, at a concrete strength (f'_c) greater than 117 MPa, both equations predict transfer lengths less than $40d_b$.

2.6   SUMMARY AND CONCLUSIONS

The research project examined the measured transfer lengths of 57 prestressed concrete beams cast with a variety of different concrete types. The concrete types included normal strength (NS), high strength (HS), self-consolidating concrete (SCC), ultra-high performance (UHP), and light weight (LW) concrete. Fifty one beams were fabricated with 15.2 mm, Grade 270, seven wire low relaxation prestressing strand. The concrete compressive strengths at release for those 51 beams ranged from 23 MPa to 155 MPa. Six beams were fabricated using 12.7 mm diameter strands with concrete compressive strengths at release between 24 MPa and 31 MPa. Measured transfer lengths were determined using concrete surface strains along with the AMS method. The UA data was analyzed using the power regression in order to develop a new transfer length equation. A power regression was chosen to develop this new equation because this repression provided a better fit than the linear regression. This was due to the influence of concrete compressive strength on the transfer length. In addition, measured transfer lengths from the literature were collected and analyzed and compared with ACI 318-14, ACI ($50d_b$), AASHTO

($60d_b$), NCHRP-603 ($40d_b$), equations from the literature, and the proposed equation, **Eq. 2**. Based on the investigation, the followings conclusions were made:

1. Transfer length in prestressed concrete members decreases as concrete compressive strength increases. Research results also show that the ACI 318-14 and AASHTO equations overestimate transfer lengths in members containing concrete with high compressive strengths. Therefore, concrete compressive strength should be a factor in predicting transfer length.

2. Based on the results of the study, **Eq. 2** and the ACI 318-14 equation are recommended when the concrete compressive strength at release is less than 34.5 MPa. Based on the UA experimental data, $40d_b$ should be used as minimum transfer length for members containing concrete with compressive strengths at release greater than 34.5 MPa but less than 55 MPa. When the concrete compressive strength at release is greater than 55 MPa, transfer length can be taken as $33d_b$. There is little change in transfer length as concrete compressive strength at release increases beyond 55 MPa.

3. The proposed UA equation, **Eq. 2**, is based on experimental data with good strand bond (STSB values of 117 MPa or more). For strands with poor surface quality, further investigation is needed in order to determine the applicability of the UA equation.

4. Measured transfer length values collected from the literature were compared to values predicted using the ACI 318-14, AASHTO, and NCHRP-603 equations. The predicted values were greater than the mean experimental values for approximately 18% of the beams containing 12.7 mm diameter strand and 40% for beams containing 15.2 mm diameter strand.

5. The total data between the lower and upper bounds, [AV±SD], was 53 % for the measured transfer length ratios using ACI 318-14 and 64% for the same ratio using **Eq. 2** for 12.7 mm diameter strand. For 15.2 mm strands, the total data within this range was 63% when ACI 318-14 was used and 72% when **Eq. 2** was used. Therefore, the proposed question, **Eq. 2** better represents the experimental data than the ACI 318-14 equation.

6. Current equations do not adequately estimate transfer length for higher strength concretes. Since the 1970's, many researchers have recommended including concrete strength in the equation for transfer length. The proposed equation, **Eq. 2**, does include concrete strength and more accurately estimates transfer length for beams containing high strength concrete.

REFERENCES

[1] ACI-318-14. Building code requirements for structural concrete and commentary. Farmington Hills, MI: American Concrete Institute; 2014.

[2] AASHTO. AASHTO LRFD Bridge Design Specifications, Customary U.S. Units. 6th ed. Washington, D.C.: American Association of State Highway and Transportation Officials (AASHTO); 2012.

[3] ACI-318-11. Building code requirements for structural concrete and commentary. Farmington Hills, MI: American Concrete Institute; 2011.

[4] Cousins TE, Johnston DW, Zia P. Transfer and development length of epoxy coated and uncoated prestressing strand. PCI Journal. 1990;35:92-103.

[5] Mitchell D, Cook WD, Khan AA, Tham T. Influence of high strength concrete on transfer and development length of pretensioning strand. PCI Journal. 1993;38:52-66.

[6] Ramirez JA, Russell BW. Transfer, Development, and Splice Length for Strand/Reinforcement in High-Strength Concrete. Washington, D.C.: Transportation Research Board, National Research Council (NCHRP-603); 2008.

[7] Zia P, Mostafa T. Development length of prestressing strands. PCI Journal. 1977;22:54-65.

[8] Martí-Vargas JR, Serna P, Navarro-Gregori J, Bonet JL. Effects of concrete composition on transmission length of prestressing strands. Construction and Building Materials. 2012;27:350-6.

[9] Kose MM. Prediction of Transfer Length of Prestressing Strands Using Neural Networks. ACI Structural Journal. 2007;104:162-9.

[10] Barnes RW, Grove JW, Burns NH. Experimental Assessment of Factors Affecting Transfer Length. ACI Structural Journal. 2003;100:740-8.

[11] Floyd RW, Ruiz E, D., Do NH, Staton BW, Hale WM. Development lengths of high-strength self-consolidating concrete beams. PCI Journal. 2011;56:36-53.

[12] Carroll JC, Cousins TE, Roberts-Wallmann CL. A practical approach for finite-element modeling of transfer length in pretensioned, prestressed concrete members using end-slip methodology. PCI Journal. 2014;59:110-29.

[13] Hanson NW, Kaar PH. Flexural bond tests of pretensioned prestressed beams. ACI Structural Journal. 1959;55:783-802.

[14] Lane SN. A new development length equation for pretensioned strands in bridge beams and piles. Turner-Fairbank Highway Research Center, 6300 Georgetown Pike, McLean, VA 22101 USA: Federal Highway Administration; 1998.

[15] Buckner CD. A review of strand development length for pretensioned concrete members. PCI Journal. 1995;40:84-105.

[16] Deatherage JH, Burdette EG, Chew CK. Development length and lateral spacing requirements of prestressing strands for prestressed concrete bridge girders. PCI Journal. 1994;39:70-83.

[17] Russell BW, Burns NH. Measured transfer lengths of 0.5 and 0.6 in. strands in pretensioned concrete. PCI Journal. 1996;41:44-65.

[18] Martí-Vargas JR, Arbelaez CA, Serna-Ros P, Fernandez-Prada MA, Miguel-Sosa PF. Transfer and development lengths of concentrically prestressed concrete. PCI Journal. 2006;51:74-85.

[19] Martí-Vargas JR, Serna P, Navarro-Gregori J, Pallarés L. Bond of 13 mm prestressing steel strands in pretensioned concrete members. Engineering Structures. 2012;41:403-12.

[20] Martí-Vargas J, Hale W. Predicting Strand Transfer Length in Pretensioned Concrete: Eurocode Versus North American Practice. Journal of Bridge Engineering. 2013.

[21] Martí-Vargas JR, Arbelaez CA, Serna-Ros P, Navarro-Gregori J, Pallares-Rubio L. Analytical model for transfer length prediction of 13 mm prestressing strand. Structural Engineering and Mechanics. 2007;26:211-29.

[22] Kose MM, Burkett WR. Formulation of new development length equation for 0.6 in. prestressing strand. PCI Journal. 2005;50:96-105.

[23] Floyd RW, Howland MB, Micah Hale W. Evaluation of strand bond equations for prestressed members cast with self-consolidating concrete. Engineering Structures. 2011;33:2879-87.

[24] Floyd RW. Investigating the bond of prestressing strands in lightweight self-consolidating concrete. United States - Arkansas: University of Arkansas; 2012.

[25] John EE, Ruiz ED, Floyd RW, Hale WM. Transfer and Development Lengths and Prestress Losses in Ultra-High-Performance Concrete Beams. Transportation Research Record: Journal of the Transportation Research Board. 2011;2251:76-81.

[26] Ruiz Coello ED. Prestress losses and development length in pretensioned ultra high performance concrete beams [Ph.D.]. United States - Arkansas: University of Arkansas; 2007.

[27] Ward D. Performance of prestressed double-tee beams cast with lightweight self-consolidating concrete [M.S.C.E.]. United States - Arkansas: University of Arkansas; 2010.

[28] Staton BW, Do NH, Ruiz ED, Hale WM. Transfer lengths of prestressed bemas cast with self-consolidating concrete. PCI Journal. 2009;54:64-83.

[29] Staton BW. Transfer lengths for prestressed concrete beams cast with self-consolidating concrete mixtures [M.S.C.E.]. United States - Arkansas: University of Arkansas; 2006.

[30] Do NH, Staton BW, Hale WM. Development of high strength self-consolidating concrete mixtures for use in prestressed bridge girders. The PCI National Bridge Conference. Grapevine, Texas: CD-ROM; 2006.

[31] Cousins TE, Nassar A. Investigation of transfer length, flexural strength, and prestress losses in lightweight prestressed concrete girders Charlottesville, VA: Virginia Department of Transportation; 2003.

[32] Girgis AFM, Tuan CY. Bond strength and transfer length of pretensioned bridge girders cast with self-consolidating concrete. PCI Journal. 2005;50:72-87.

[33] Oh BH, Kim ES. Realistic Evaluation of Transfer Lenghs in Pretensioned, Prestressed Concrete Members. ACI Structural Journal. 2000;97:821-30.

[34] Russell BW, Burns NH. Measured of transfer lengths of pretensioned concrete elements. Journal of Structural Engineering. 1997;123:541-9.

[35] Ramirez-Garcia AT, Floyd RW, Hale M, Martí-Vargas JR. Effect of concrete compressive strength on transfer length and development length. PCI-2013 Convention and National Bridge Conference: Discover High Performance Precast. Gaylord Texan Resort-Grapevine, Texas: PCI Journal; 2013.

[36] Martí-Vargas JR, Serna P, Hale WM. Strand bond performance in prestressed concrete accounting for bond slip. Engineering Structures. 2013;51:236-44.

[37] Rose DR, Russell BW. Investigation of standardized tests to measure the bond performance of prestressing strand. PCI Journal. 1997;42:56-80.

[38] Mahmoud ZI, Rizkalla SH, Zaghoul E-ER. Transfer and Development Lengths of Carbon Fiber Reinforced Polymers Prestressing Reinforcement. Structural Journal. 1999;96:594-602.

[39] Hodges HT. Top Strand Effect and Evaluation of Effective Prestress in Prestressed Concrete Beams [Research]. Blacksburg, VA: Virginia Polytechnic Institute and State University; 2006.

[40] Bhoem KM, Barnes RW, Schindler AK. Performance of self-consolidating concrete In prestressed girders Highway Research Center, Harbert Engineering Center Auburn University, AL 36830: The Alabama Department of Transportation; 2010.

[41] Myers JJ, Volz JS, Sells E, Porterfield K, Looney T, Tucker B et al. Self-Consolidating Concrete (SCC) for Infrastructure Elements: Report B-Bond, Transfer Length, and Development Length of Prestressing Strand. Rolla, Missouri, MO: Missouri University of Science and Technology; 2012.

40

CHAPTER 3 : INFLUENCE OF CONCRETE STRENGTH ON DEVELOPMENT LENGTH OF PRESTRESSED CONCRETE MEMBERS

Alberto T. Ramirez-Garcia [a], Royce W. Floyd [b], W. Micah Hale [c], J.R. Martí-Vargas [d]

[a] Tatum-Smith Engineering, Inc, Rogers, AR, 72757, USA

[b] University of Oklahoma, School of Civil Engineering and Environmental Science, 202 W. Boyd St., Norman, OK 73019, USA

[c] University of Arkansas, Department of Civil Engineering, 4190 Bell Engineering Center Fayetteville, AR 72701, USA

[d] Institute of Concrete Science and Technology (ICITECH), Universitat Politècnica de València, 4G, Camino de Vera s/n, 46022 Valencia, Spain

Abstract:

Fifty seven prestressed concrete beams were fabricated at the University of Arkansas (UA) to determine the influence of concrete strength on the development length of seven wire prestressing strand. The variables considered in the investigation were the concrete compressive strength (f'_c), which ranged from 34.5 MPa to 199 MPa, and the strand diameter, which included 12.7 mm and 15.2 mm. The beams were cast with concrete types which included self-consolidating concrete, high strength concrete, lightweight concrete, and ultra-high performance concrete. Development length was determined through flexural testing. The research project also summarized the findings of several studies from the literature. The measured development lengths were compared to those calculated using the American Concrete Institute (ACI 318-14) prediction equation for development length. The results showed that compressive strength affects the development length and the ACI 318 equation overestimates development length. Also, a development length equation was developed and presented in the paper.

Keywords: Prestressed concrete, strand bond, development length

3.1   INTRODUCTION AND BACKGROUND

When designing prestressed concrete members, engineers must determine the development length of the prestressing strands. The development length is the sum of the transfer length and the flexural bond length. The transfer length is the distance from the free end of the prestressing strand necessary to fully bond the strand to the concrete. The flexural bond length, L_b, is the length required, beginning at the end of the transfer length, to fully develop the strength of the strand. Therefore the development length, L_d, is the distance from the free end of the strand to the section where the nominal moment can be resisted [1]. The transfer length, flexural bond length, and development length are shown in **Figure 3-1**. The ACI 318-14 (**Equation 1.a**) and AASHTO (**Equation 1.b**) equations for estimating development length are shown below.

$$L_d = \frac{f_{se}}{20.7} d_b + \frac{1}{6.9}(f_{ps} - f_{se})d_b \tag{1.a}$$

$$L_d = \frac{\kappa}{6.9}\left(f_{ps} - \frac{2}{3}f_{se}\right)d_b \tag{1.b}$$

The AASHTO equation is similar to the ACI 318-14 equation for development length, except the development length has been modified by a k factor (**Eq. 1.b**) as recommended by the 1988 Federal Highway Administration (FHWA) memorandum [2-4]. The k factor amplifies the development length calculated by the ACI 318-14 equation. For pretensioned members (panels, piles, etc) with a depth less than 0.60 m, $k = 1.0$ and for other pretensioned members with a depth greater than 0.60 m, $k = 1.6$. For debonded strands, k = 2.0.

42
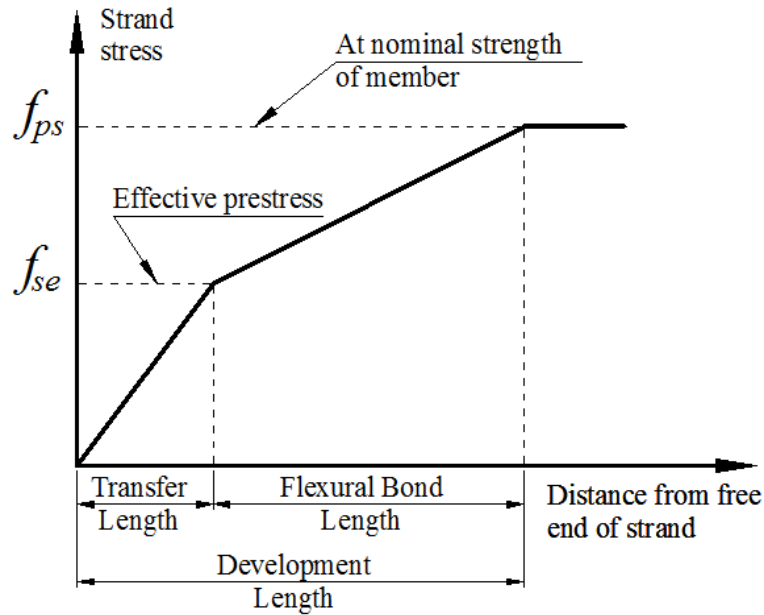
Figure 3-1. Strand stress vs. length, ACI 318-11 (R12.9) and AASHTO LRFD (C5.11.4.2-1).

The ACI 318-14 equation was implemented in 1963 based on investigations conducted in the 1950's [1, 5], and later the ACI 318-14 equation was adopted by AASHTO LRFD Bridge Design Specifications (hereafter referred to as AASHTO) in 1973 [2, 3, 6]. Concrete technology has advanced since the equations were adopted, but the equations have remained unchanged. For example, the compressive strength of the concrete used in the seminal strand bond research by Hanson and Kaar ranged from 26 to 54 MPa for the development length tests [5]. The use of high strength concrete has become common in prestressed concrete bridge girders. Higher concrete compressive strengths can increase span length, decrease girder height, and eliminate the total number of girders in a bridge when compared to bridge girders cast with normal strength concrete [7]. Since the original equations were based on lower strength concrete and the compressive strength being used in current prestressed concrete applications is increasing, it is necessary to determine the applicability of the development equations given by the ACI318-14 and AASHTO.

43

Since the inception of prestressed concrete research, researchers have investigated the bond between the concrete and prestressing steel. The current equations provided by ACI 318-14 and AASHTO are a function of the effective prestress (f_{se}), stress at nominal strength of the member (f_{ps}), and the diameter of the strand (d_b) [1, 6]. Updated equations have been published to amend the current equations, but most have not been implemented by ACI 318-14 or AASHTO. Current investigations have shown that the initial prestress (f_{si}) and concrete compressive strength, both at prestress release (f'_{ci}) and at 28-days (f'_c), affect both transfer and development lengths [8-12]. Researchers have also shown the measured transfer and development lengths for high strength concrete members are less than those values predicted using ACI 318-14 and AASHTO equations [9, 10, 13]. As such, the question has risen as to whether concrete compressive strength should be included as a principal variable in development length equations. Several variables have been investigated in order to improve the accuracy of the development length equation. These variables include the concrete compressive strength at prestress release (f'_{ci}) and at the time of testing (f'_c), the initial prestress in the strand (f_{si}), the effective prestress in the strand after all losses (f_{se}), the stress in the strand at nominal strength (f_{ps}), and the nominal strand diameter (d_b). Although these variables are essential for development length, other variables can be considered, such as friction between the strand and concrete, type of strand release, strand surface condition, confining reinforcement around the strand, and type of loading [5, 8, 10, 11, 14, 15]. **Table 3-1** contains several equations for transfer lengths and flexural bond lengths.

Some of the proposed equations in **Table 3-1** were developed for concrete with compressive strength at prestress release between 14 MPa to 55 MPa [11]. Other investigators have studied

44

the transfer and development lengths of prestressed concrete containing high-strength and normal-weight concrete which included compressive strengths up to 103 MPa [10] and 199 MPa [13, 16, 17]. These investigations focused on a wide range of concrete including conventional concrete and ultra-high performance concrete. The research showed that increasing concrete strength correlated clearly with shortening of the transfer and development lengths.

Some flexural bond length equations [3, 4, 11] use the same equation given by ACI-318-14 [1], but includes a modification factor, λ, which varies from 0.145 to 0.290 (1 to 2 for f_{pu} and f_{se} in ksi, and d_b in inches) [3]. For example, some researchers [11] recommend a modification factor of 0.181 (1.25 is for f_{pu} and f_{se} in ksi, and d_b in inches) while others [4] suggest 0.218 (1.5 is for f_{ps} and f_{se} in ksi, and d_b in inches). Some of the analytical equations for transfer length and flexural bond length which are shown in **Table 3-1** include the plastic and elastic behavior [8]. Through these studies, new variables were introduced which included the plastic transfer bond stress coefficient (U'_t), the plastic bond stress coefficient for development (U'_d), the bound modulus (B), and the area of the prestressing strand (A_s).

Researchers at the University of Arkansas (UA) have examined the transfer length and flexural bond length of members cast with a variety of compressive strength [13, 16, 18-23]. These investigations focused on a wide range of concrete mixtures including conventional concrete and ultra-high performance concrete. The research showed that increasing concrete strength correlated clearly with shortening of the transfer and development lengths.

The types of concrete and the properties of concrete have changed since Hanson and Kaar's seminal research on strand bond. However, the equations to predict transfer and development have not changed. This paper examined the development length of concrete with a wide range of compressive strengths in order to develop an updated equation for estimating the development

45

length of prestressing steel. Once the equation was developed, data sets were collected from the

literature to determine its accuracy when compared to the ACI 318-14 equation.

Table 3-1 – Proposed equations for predicting development length ($L_d = Lt + L_{fb}$) from the literature (in MPa and mm).

Source	Transfer Length, L_t	Flexural bond length, L_{fb}
ACI-318 / AASHTO LRFD [1]	$L_t = \dfrac{f_{se}}{20.7}d_b$	$L_{fb} = 0.145\left(f_{ps} - f_{se}\right)d_b$
Zia and Mostafa, 1977 [11]	$L_t = 1.5\dfrac{f_{si}}{f_{ci}^{'}}d_b - 117$	$L_{fb} = 0.181\left(f_{pu} - f_{se}\right)d_b$
Cousins et al., 1990 [8]	$L_t = \dfrac{U_t^{'}\sqrt{f_{ci}^{'}}}{2B} + \dfrac{f_{se}A_s}{\pi d_b U_t^{'}\sqrt{f_{ci}^{'}}}$	$L_{fb} = \left(f_{ps} - f_{se}\right)\left(\dfrac{A_s}{\pi d_b U_d^{'}\sqrt{f_c^{'}}}\right)$
Mitchell et al., 1993 [9]	$L_t = \dfrac{f_{si}}{20.7}d_b\sqrt{\dfrac{20.7}{f_{ci}^{'}}}$	$L_{fb} = 0.145\left(f_{ps} - f_{se}\right)d_b\sqrt{\dfrac{31}{f_c^{'}}}$
Deatherage et al., 1994 [4]	$L_t = \dfrac{f_{si}}{20.7}d_b$	$L_{fb} = 0.218\left(f_{ps} - f_{se}\right)d_b$
Buckner, 1995 [3]	$L_t = \dfrac{f_{si}}{20.7}d_b$	$L_{fb} = 0.145\lambda\left(f_{ps} - f_{se}\right)d_b$ $1 \le \lambda \le 2$
Lane, 1998 [2]	$L_t = 4\dfrac{f_{si}}{f_c^{'}}d_b - 127$	$L_{fb} = \dfrac{6.4\left(f_{pu} - f_{se}\right)}{f_c^{'}}d_b + 381$
Kose and Burkett, 2005 [25]	$L_t = 0.045\dfrac{f_{si}}{\sqrt{f_c^{'}}}\left(25.4 - d_b\right)^2$	$L_{fb} = 203.2 + 0.19\dfrac{\left(f_{pu} - f_{si}\right)}{\sqrt{f_c^{'}}}\left(25.4 - d_b\right)^2$
Ramirez and Russell, 2008 [10]	$L_t = \dfrac{315}{\sqrt{f_{ci}^{'}}}d_b \ge 40d_b$	$L_{fb} = \dfrac{591}{\sqrt{f_c^{'}}}d_b \ge 60d_b$

3.2 EXPERIMENTAL PROGRAM

3.2.1 Concrete Mixtures

For the specimens cast at the UA, 11 different mixture proportions were developed. The beams were cast with normal strength concrete (NSC), self-consolidating concrete (SCC), high strength concrete (HSC), lightweight self-consolidating concrete (LWSCC), and ultra-high performance concrete (UHPC) [18, 20-22]. In addition, NSC and HSC included subgroups with different coarse aggregates: Clay (CL), Shale (SH), and Limestone (LS). For instance, NSCL represents a concrete mixture with normal compressive strength and contains clay coarse aggregate. The clay and shale were lightweight aggregates, and the resulting concrete mixtures were also lightweight. The development of these concrete mixtures and their properties (fresh and hardened) has been discussed in detail in earlier publications by the authors [13, 16, 18-24].

The number of beams cast from each mixture and the number of flexure tests performed are presented in **Table 3-2**. The mean compressive strength at release and at 28 days for each mixture is also provided in **Table 3-2**. Fifty-one beams were cast with 15.2 mm diameter strands [18, 20, 22] and six beams were cast with 12.7 mm diameter strands [21]. The compressive strengths at release using 15.2 mm strand ranged from 23 MPa to 155 MPa, and the 28 day strengths ranged from 34.5 MPa to 199 MPa. Furthermore, for beams containing 12.7 mm diameter strands, the compressive strengths at release ranged from 24 MPa to 37 MPa, and the 28 day strengths were between 41 MPa to 52 MPa.

Table 3-2 – Number of trial beams, tests performed for transfer lengths, and concrete strength mean for release and time of testing.

Concrete Series	Number of Trial Beams	Number of L_d tests	f'_{ci} Mean, MPa	f'_c Mean, MPa
NSCL: Normal strength clay	4	8	31	39
NSSH: Normal strength shale	5	10	28	42
NSLS: Normal strength limestone	4	8	33	52
HSCL: High strength clay	4	8	43	49
HSSH: High strength shale	4	8	42	48
HSLS : High strength limestone	4	8	48	64
SCC-I : Self-consolidating concrete Type I	8	8	54	84
SCC-III : Self-consolidating concrete Type III	5	5	51	76
HSC : High strength concrete	6	6	64	85
UHPC : Ultra high performance concrete	7	7	124	182
LWSCC * : Lightweight self-consolidating concrete	6	6	31	46

(*) 12.7 mm diameter strand

3.2.2 Beam Fabrication

At the UA, 57 fully bonded, prestressed, precast beams have been cast. Each beam had a rectangular cross-section of 165 mm by 305 mm and was 5.5 m in length. The beams contained two, low relaxation, Gr. 1862 prestressing strands, located a distance of 254 mm, measured from the top (compression fiber) of the beam to the centroid of the strand. Strand diameters of 12.7 mm and 15.2 mm were included in the study. Two No. 19, Gr. 414 reinforcing bars were located 51 mm from the top of each beam. The shear reinforcement consisted of No 6 smooth bars spaced at 150 mm as shown in **Figure 3-2**. Two beams were cast simultaneously on a 15.2 m prestressing bed. The strands were tensioned to 75% f_{pu}, 1397 MPa.

48
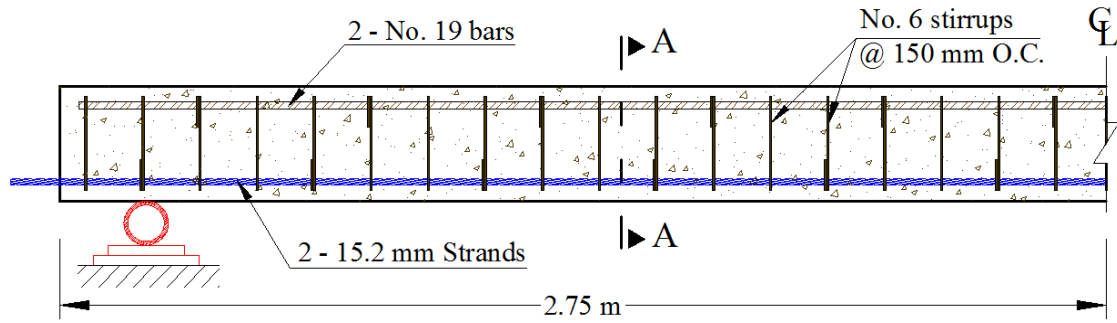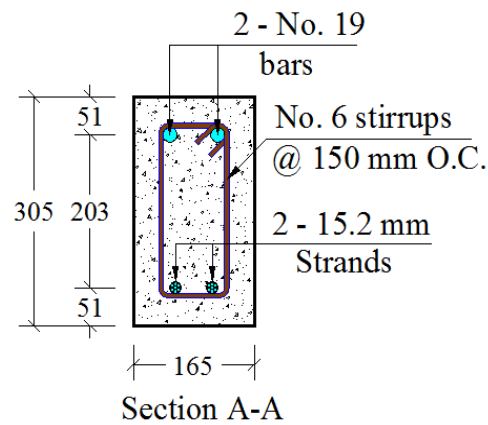
Figure 3-2. Reinforcement details of a prestressed concrete beam.

3.2.3 Instrumentation and Testing

Fifty-one prestressed concrete beams, using 15.2 mm strand, were tested in flexure resulting in 76 embedment lengths (L_e). The remaining 6 embedment lengths were obtained from the six prestressed concrete beams containing 12.7 mm strand. Twenty five of the fifty seven prestressed concrete beams were tested at both ends while the remaining beams were tested at only one end.

Each beam was loaded with a single concentrated load at a pre-determined distance. Determination of the development length was an iterative process using different embedment lengths. Before the start of each test, the first embedment length was assumed or was determined

49

using the value obtained from the ACI 318-14 equation. The beams were tested to failure, and the failure mechanism was then determined. The typical failure modes observed were flexure (FL), flexure/end slip (FL/SL), shear/flexure (SH/FL), shear/end-slip (SH/SL), flexural/end-slip/shear (FL/SL/SH), bond (BD), shear/bond (SH/BD), or flexural/shear (FL/SH).

The applied load was measured using a pressure transducer connected to the hydraulic actuator system. The load was continuously monitored using a data acquisition system (DAS). Linear variable differential transformers (LVDT) were attached to each strand at the end of the beam being tested. Readings from the LVDTs were continuously recorded and monitored using a DAS in order to pinpoint the beginning of any strand slip [13, 16, 19]. If the beam did not exhibit strand slip at failure, and the beam failed in flexure with crushing in the compression fiber, a pure flexural failure was recorded. This indicated that the development length was shorter than what was assumed. A shorter embedment length was used for the next test. However, if strand slip was observed before the nominal moment capacity was achieved and a bond failure occurred, a longer embedment length was used for the next test. The development length was considered to occur at the embedment length where the bond failure and flexural failure occurred at the same time while achieving the nominal moment capacity for the specimen. This method for determining the development length has been employed by other researchers [2, 4, 5, 10, 14, 25, 26].

In addition, beam deflection was recorded and monitored using a linear cable encoder placed between the hydraulic actuator and the top plate of the loading steel roller. In general, for flexural failures, the measured moment capacity was greater than the nominal capacity, and the beam experienced large deformations prior to failure. The beams experiencing a pure flexural failure experienced no strand end slip. Shown in **Figure 3-3** is a shear/end slip failure. This

50

failure was characterized by noticeable shear cracks and end slip due to a partial loss of bond between the strands and concrete. A flexural/end slip failure is characterized by typical flexural behavior with cracks occurring directly beneath and near the applied load. There is also significant deflection after achieving the maximum load and corresponding moment. Strand slip occurred generally prior to or immediately after achieving the nominal moment capacity.

Figure 3-3. Shear/End-Slip failure of NSLS-3D (Photo by author).

3.3   DEVELOPMENT LENGTH ANALYSIS

3.3.1   Measured Development Length Data from UA

Eighty-two development length tests were conducted, and the results are summarized in **Tables 3- 3**, **3-4**, and **3-5**. Shown in **Tables 3-3** and **3-4** is information from the development length test for the normal (26 tests) and high strength concrete members (24 tests). These beams were

51

subjected to flexural tests at both ends. Likewise, data from the development length tests for

self-consolidating concrete, high strength, ultra-high performance concrete, and light weight self-

consolidating concrete members are shown in **Table 3-5**. The embedment length, L_e is shown in

each table. This was the location of the point load for the flexural test.

Table 3-3 – Development length test results of the NSCL, NSSH, and NSLS beams tested at both ends.

Test No.	Specimen	L_e, mm	f'_c, MPa	f_{se}, MPa	f_{ps}, MPa	L_d, mm	M_n, kN-m	M_{max}, kN-m	Failure Type
1	NSCL-1D	1270	35	1057	1792	2402	105	106	FL
2	NSCL-1L	1143						79	SH/SL
3	NSCL-2D	1270	46	1105	1809	2367	111	121	FL
4	NSCL-2L	1397						124	FL/SH
5	NSCL-3D	1321	36	1048	1789	2407	106	109	SH/SL
6	NSCL-3L	1219						96	SH/SL
7	NSCL-4D	1219	40	1068	1802	2406	108	116	FL/SL/SH
8	NSCL-4L	1524						123	FL
9	NSSH-1D	1143	34	1041	1790	2420	105	115	FL/SL
10	NSSH-1L	1270						114	FL/SL
11	NSSH-2D	1245	42	1085	1805	2388	109	112	FL
12	NSSH-2L	1016						108	SH/SL
13	NSSH-3D	1016	43	1090	1804	2379	109	94	SH/SL
14	NSSH-3L	1143						116	FL
15	NSSH-4D	1207	46	1088	1806	2387	110	113	FL
16	NSSH-4L	1143						114	SH/SL
17	NSSH-5D	1143	45	1077	1805	2400	109	116	FL
18	NSSH-5L	1016						94	SH/SL
19	NSLS-1D	940	46	1172	1808	2267	110	107	SH/SL
20	NSLS-1L	1003						121	FL/SL
21	NSLS-2D	1016	55	1186	1813	2257	112	133	FL
22	NSLS-2L	1092						127	FL
23	NSLS-3D	1016	54	1148	1812	2310	112	123	SH/SL
24	NSLS-3L	864						115	FL/SL
25	NSLS-4D	1422	54	1159	1814	2298	113	93	SH/SL
26	NSLS-4L	1194						129	FL

52

Table 3-4 – Development length test results of HSCL, HSSH, and HSLS beams (tested at both ends).

Test No.	Specimen	L_e, mm	f'_c, MPa	f_{se}, MPa	f_{ps}, MPa	L_d, mm	M_n, kN-m	M_{max}, kN-m	Failure Type
27	HSCL-1D	1016	49	1154	1811	2299	111	114	FL/SL
28	HSCL-1L	1270						124	FL
29	HSCL-2D	1124	52	1150	1812	2308	112	116	FL
30	HSCL-2L	1143						116	FL/SH/SL
31	HSCL-3D	1080	46	1158	1810	2292	110	104	SH/SL
32	HSCL-3L	1143						117	SH/SL
33	HSCL-4D	953	49	1154	1811	2299	111	110	SH/SL
34	HSCL-4L	1207						117	FL
35	HSSH-1D	1016	45	1148	1809	2304	110	108	SH/SL
36	HSSH-1L	1270						122	FL
37	HSSH-2D	1080	44	1134	1808	2320	109	124	FL
38	HSSH-2L	1143						121	FL
39	HSSH-3D	889	56	1126	1812	2343	113	104	BD
40	HSSH-3L	1016						108	FL
41	HSSH-4D	1016	48	1174	1812	2272	111	118	FL
42	HSSH-4L	953						106	BD
43	HSLS-1D	1016	61	1214	1819	2229	114	123	BD
44	HSLS-1L	1270						131	FL
45	HSLS-2D	1207	63	1217	1821	2228	115	119	FL/SL
46	HSLS-2L	1143						129	FL/SL
47	HSLS-3D	1080	64	1216	1821	2229	115	118	FL
48	HSLS-3L	1207						118	FL
49	HSLS-4D	889	67	1215	1822	2233	116	107	BD
50	HSLS-4L	1016						119	FL/SL

The concrete compressive strength, f'_c, at the time of the flexural test, the effective strand stress, f_{se}, and the stress in the strand at nominal strength, f_{ps}, are shown in the tables. The calculated development length, L_d, using ACI 318-14 is shown in the tables along with the calculated nominal moment capacity, M_n, and the maximum measured moment, M_{max}, for all beams. Finally, the failure type for all beam tests is shown.

Table 3-5 – Development length test results of SCC, LWSCC, HSC, & UHPC beams tested at only one end.

Test No.	Specimen	L_e, mm	f'_c, MPa	f_{se}, MPa	f_{ps}, MPa	L_d, mm	M_n, kN-m	M_{max}, kN-m	Failure Type
51	SCC-I-1	953	96	1216	1837	2266	122	135	FL/SL
52	SCC-I-2	953	99	1209	1839	2280	123	144	FL/SL
53	SCC-I-3	1016	78	1272	1834	2176	120	144	FL
54	SCC-I-4	889	84	1241	1833	2219	119	143	SH/FL
55	SCC-I-5	762	79	1266	1834	2185	120	139	FL/SL
56	SCC-I-6	1016	81	1261	1835	2193	120	147	FL
57	SCC-I-7	1143	76	1239	1832	2220	119	135	FL
58	SCC-I-8	889	83	1252	1836	2209	121	140	FL
59	SCC-III-1	826	75	1221	1833	2250	120	147	SH/FL
60	SCC-III-2	889	71	1219	1833	2252	120	153	FL
61	SCC-III-3	826	71	1211	1833	2263	120	125	FL/SL
62	SCC-III-4	889	75	1214	1834	2262	120	145	FL
63	SCC-III-5	762	89	1216	1832	2254	119	115	SH/FL
64	HSC-1	889	87	1264	1837	2194	122	149	FL
65	HSC-2	762	88	1263	1835	2191	121	154	FL
66	HSC-3	889	86	1261	1833	2190	120	138	SH/FL
67	HSC-4	1016	87	1254	1832	2197	119	143	FL
68	HSC-5	762	74	1250	1834	2209	120	137	FL/SL
69	HSC-6	1194	90	1244	1835	2220	121	151	FL
70	UHPC-1	635	193	1278	1846	2194	180	227	FL/SL
71	UHPC-2	508	199	1277	1846	2196	186	*	FL
72	UHPC-3	635	119	1300	1847	2163	111	193	FL/SL
73	UHPC-4	635	186	1307	1846	2151	173	226	FL
74	UHPC-5	889	195	1310	1847	2150	182	197	FL/SL
75	UHPC-6	1143	191	1305	1846	2154	178	174	FL
76	UHPC-7	1524	192	1304	1846	2155	180	175	FL
77	LWSCC-1	1143	47	1181	1829	1921	85	104	FL
78	LWSCC-2	889	41	1155	1829	1952	84	102	SH/BD
79	LWSCC-3	762	50	1187	1829	1914	85	96	FL
80	LWSCC-4	699	43	1174	1829	1930	85	94	FL
81	LWSCC-5	635	44	1214	1830	1881	85	83	FL/SL
82	LWSCC-6	699	52	1205	1830	1893	86	97	FL

(*) exceeded capacity of load actuator

12.7 mm strand was used in specimens LWSCC

54

Figure 3-4 shows the normalized embedment length factor (k_e) for all the tests. k_e is the ratio between the measured embedment length and strand diameter (L_e/d_b). Also, the normalized predicted development length factor (k_p) is the ratio of the predicted development length from the ACI 318-14 equation and the strand diameter (L_d/d_b). This is also shown in **Figure 3-4**. Those values were normalized in order to compare the development lengths of the two strand diameters (12.7 mm and 15.2 mm) that were examined in this investigation. As shown in **Figure 3-4**, the predominant failure mode was pure flexural failures (FL), which represented 47.6% of the results. This was followed by flexural/end-slip failures (FL/SL) with 20.7%.
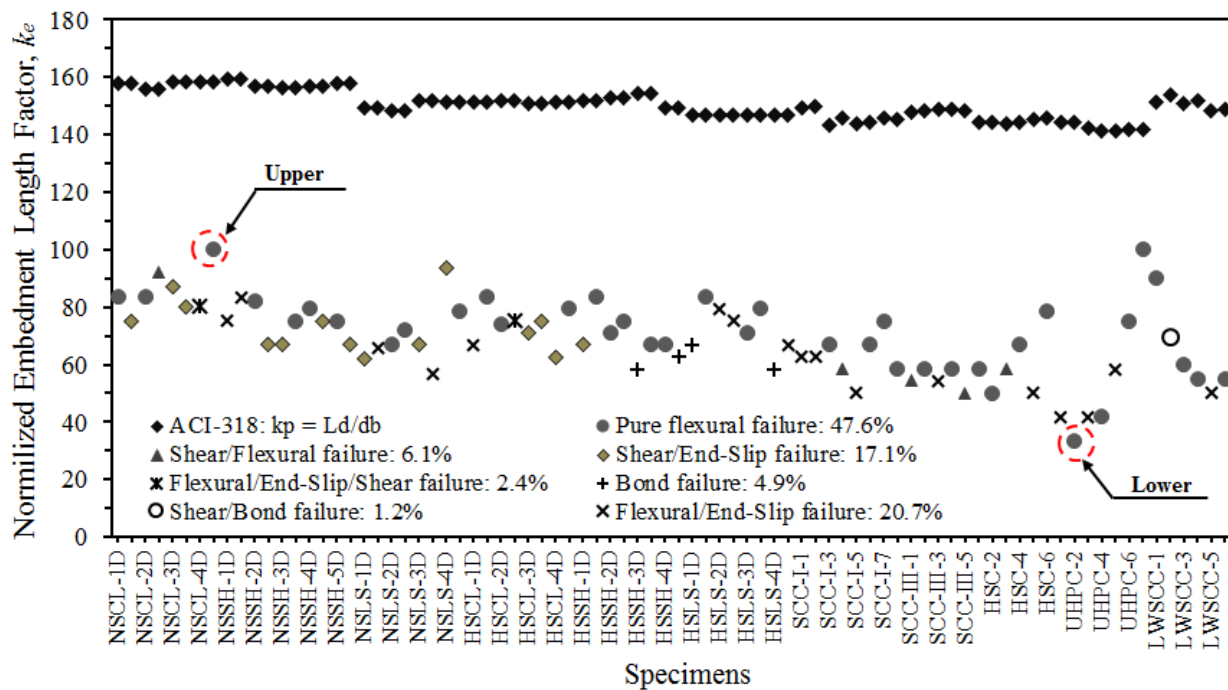
Figure 3-4. Development length test results for each case of failures.

The lower and upper values of the k_e are 33 and 100 are also shown in **Figure 3-4**. These values were found in the ultra-high performance concrete types and in the normal strength concrete types, respectively. Beams with the greatest compressive strength had the lowest k_e, and k_e

generally increased as compressive strength decreased. The shortest embedment length tested

was $33d_b$ which was in the UHPC specimens, and the longest embedment length tested was

$100d_b$ which was for the normal strength specimens. When using ACI 318-14 to predict

development length, the k_p values range from 141 to 159 as shown in **Figure 3-4**. According to

these values, the predicted development length is conservative. This is evident in the difference

between the largest k_e of 100 using the measured values and the smallest value of 141 using the

development length predicted from ACI 318-14.

3.3.2   Equation development

The results of development length tests for each series are summarized in **Table 3-6**. In each set

of tests, at least one beam exhibited strand slip before the nominal moment capacity (M_n) was

achieved, and at least one failed without strand slip occurring. When the moment causing strand

slip (M_{slip}) and the nominal moment capacity (M_n) occurred at the same time, that particular

embedment length was taken as the development length. Although shear failures at short

embedment lengths made determination of the development length difficult at times, comparing

the M_{slip} to M_n allowed the researchers to determine the development length [13, 16, 19].

As previously mentioned, the development length is the sum of the transfer length and flexural

bond length. In order to develop a new equation for development length, the flexure bond length

must first be determined [5, 27]. Flexural bond length analyses are complicated because not all

embedment length data can be considered in the statistical analysis. As explained previously, the

embedment length can only be taken as the development length when the failure occurs in both

bond and flexure simultaneously while reaching the nominal moment capacity (M_n).

56

Table 3-6 – Reduction of the UA data set of embedment length.

Beam Series	Specimens	L_e, mm	f'_c, MPa	f_{se}, MPa	f_{ps}, MPa	M_n, kN-m	M_{max}, kN-m	M_{slip}, kN-m
NSCL	4	1295	39	1069	1798	108	109	93
NSSH	5	1134	42	1076	1802	109	110	103
NSLS	4	1068	52	1166	1812	112	119	90
HSCL	4	1117	49	1154	1811	111	115	103
HSSH	4	1048	48	1146	1810	111	114	98
HSLS	4	1103	64	1215	1821	115	120	111
SCC-I	5	953	84	1244	1835	121	141	117
SCC-III	8	838	76	1216	1833	120	137	125
HSC	6	919	85	1256	1834	120	146	123
UHPC	7	853	182	1297	1846	170	199	198
LWSCC*	6	804	46	1186	1829	85	96	83

*: strand 12.7 mm

A flexural bond length equation was obtained using a power regression analysis and is shown in

Figure 3-5. In this figure, the flexural bond length is plotted versus values of "x". The flexural

bond length was taken as the difference between embedment length and measured transfer length

at testing time or 28 days, and these values were plotted against values of factor "x", defined as

$$\frac{f'_c}{\left(f_{ps} - f_{se}\right)d_b}.$$

A linear and power regression analysis was performed in order to calculate an appropriate

flexural bond length. The exponent value, however, was modified from -0.40 to -0.55 in order to

use the same value as previously proposed for transfer length [17]. Finally, the flexural bond

length equation is given by:

$$L_b = 66.5 \left(\frac{f_{ps} - f_{se}}{f'_c} d_b \right)^{0.55} \tag{2}$$

57
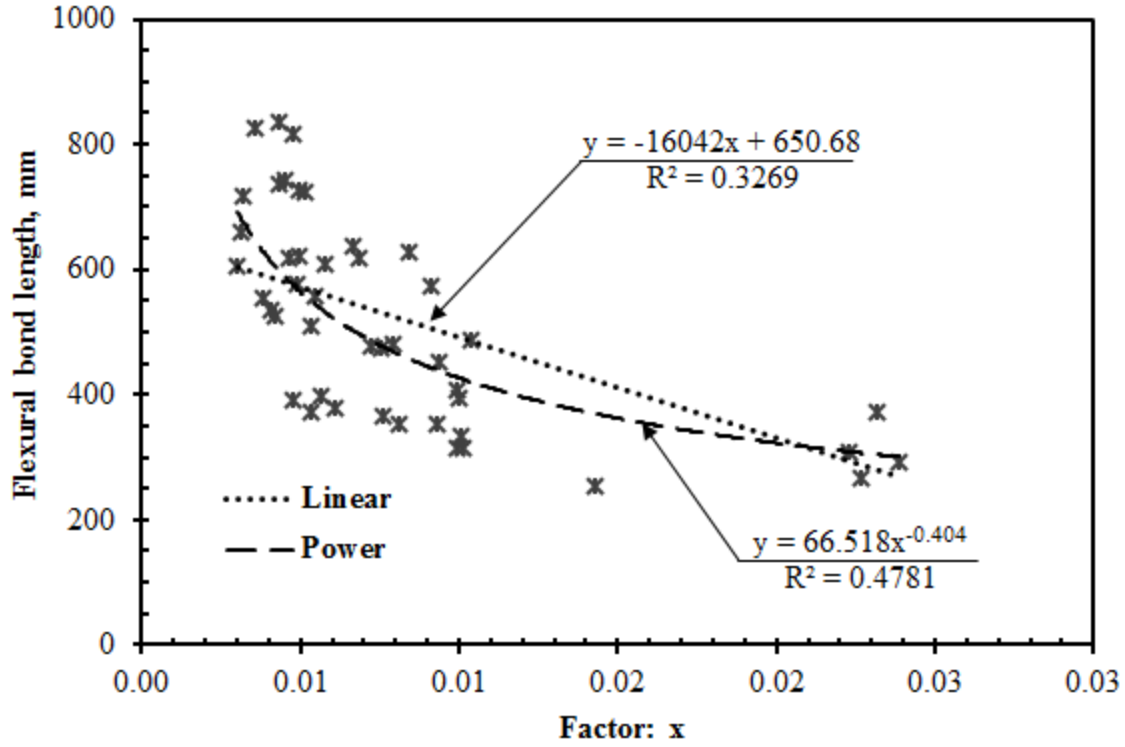
Figure 3-5. Flexural bond length analysis.

The proposed transfer length equation developed in a previous study is shown below in **Eq. (3)** [17, 28]. Therefore, the development length equation (UAPE) is then given by **Eq. (4)**.

$$L_t = 25.7 \left(\frac{f_{si}}{f'_{ci}} d_b \right)^{0.55} \tag{3}$$

$$L_d = 25.7 \left(\frac{f_{si}}{f'_{ci}} d_b \right)^{0.55} + 66.5 \left(\frac{f_{ps} - f_{se}}{f'_c} d_b \right)^{0.55} \tag{4}$$

3.3.3 Development Length Data from Literature

A data set of embedment lengths (L_e) has been collected from the literature [4, 9, 10, 12, 27, 29-31]. This data set is shown in **Table 3-7** and includes the results of 188 specimens. This data set is comprised of 103 specimens cast with 12.7 mm strand and 85 specimens cast with 15.2 mm

58

strand. As shown in **Table 3-7**, some researchers reported only the average value of the embedment length, not a specific development length. In order to analyze all the data in the same conditions, the UA data set was reduced from 82 to 57 specimens. **Table 3-7** shows the lower and upper values for embedment length and concrete strength at the time of testing. The embedment lengths range from a low of 508 mm reported by the UA and to a high of 2946 mm reported by Deatherage et al. The concrete strength at the time of testing ranged from 31 MPa, reported by Mitchell et al., to 199 MPa reported by the UA.

Table 3-7 – Data set from the literature.

| Source | Strand size, mm | Specimens | Reported Results from the Experimental Procedure | | | | | |
| | | | Embedment Length (L_e), mm | | | Concrete strength at testing time (f'_c), MPa | | |
			Lower	Avg.	Upper	Lower	Avg.	Upper
Mitchell et al., 1993 [9]	12.7	12	650	1021	1600	31	59	89
Deatherage et al., 1994 [4]	12.7	16	1768	1962	2337	37	42	52
Mahmoud et al., 1999 [27]	12.7	8	750	775	800	35	48	63
Hodges, 2006 [30]	12.7	6	1524	1676	1981	44	45	45
Ramirez and Russell, 2008 [10] (A/B)	12.7	16	1168	1492	1854	49	71	100
Ramirez and Russell, 2008 [10] (D)	12.7	19	1168	1561	1854	49	76	100
Marti-Vargas et al., 2012 [12]	12.7	12	600	688	850	43	64	75
Myers et al., 2012 [29]	12.7	8	1473	1664	1854	40	52	64
University of Arkansas	12.7	6	635	804	1143	41	46	52
Mitchell et al., 1993 [9]	15.75	12	676	1154	1864	31	58	89
Deatherage et al., 1994 [4]	15.2	8	1890	2255	2946	35	45	55
Ramirez and Russell, 2008 [10] (A6)	15.2	14	1473	1876	2235	49	63	101
University of Arkansas	15.2	51	508	1010	1524	34	80	199

Note: Ramirez and Russell [10] (NCHRP R-603)

59

The distribution of the k_e values for the data set are plotted in **Figure 3-6a**. As previously discussed, k_e is the ratio between the measured embedment length and strand diameter (L_e/d_b). For the measured data, the mean k_e was 97 with a standard deviation of 38. Approximately 68 percent of the data set from the literature falls between -1.0 and +1.0 standard deviation from the mean. Notice also that 11 percent of the data set falls between -1.0 and -1.7 and another 15 percent between +1.0 and +2.6. Approximately 6 percent of data set falls outside the standard normal curve. According to this analysis, the most probable development length is found between $59d_b$ and $135d_b$ (which is 97 ± 38).

(a) Dataset (μ= 97 and σ = 38)
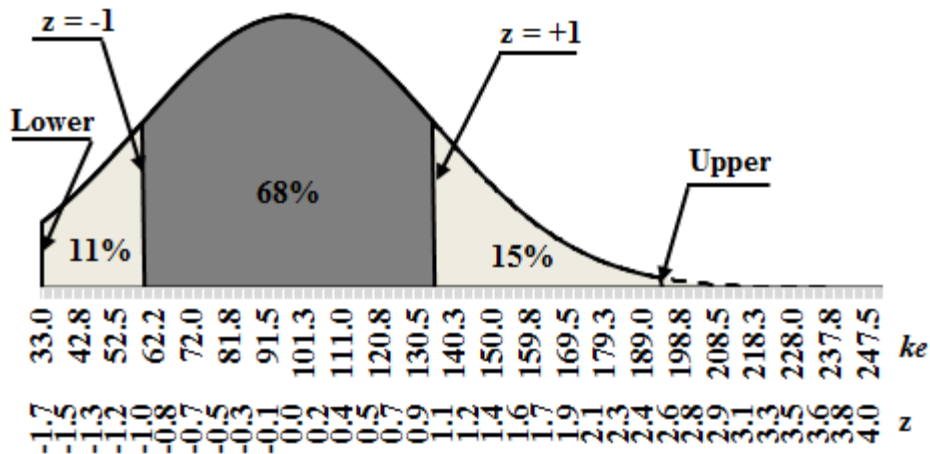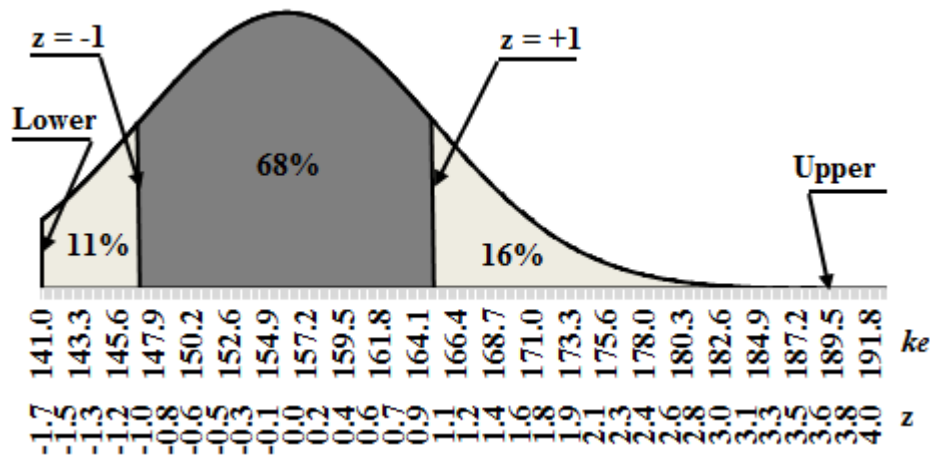
(b) ACI-318 (μ = 156 and σ = 9)
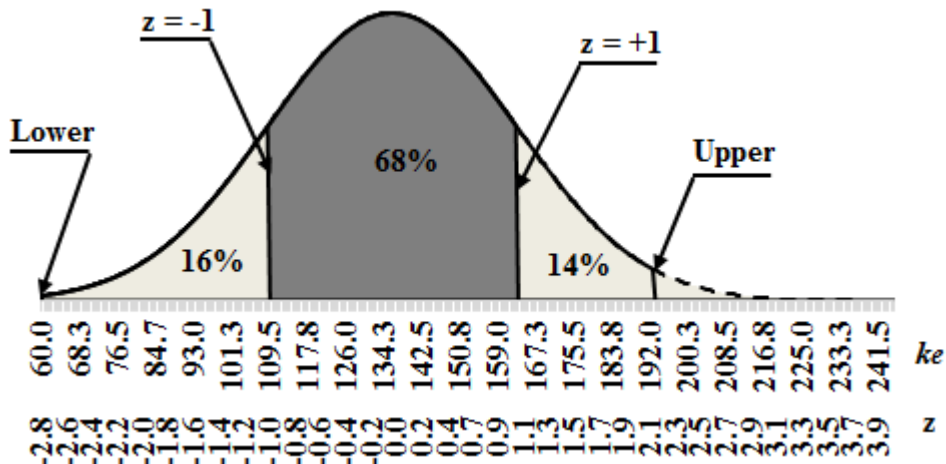
(c) UA proposed equation (μ = 136 and σ = 27)

Figure 3-6. Standard normal distribution with z-scores of -1 and +1 indicated.

61

3.3.4 Development Length Comparison of Measured and Predicted Lengths

The data set obtained from the literature and shown in **Table 3-7** was used to compare the accuracy of the UAPE to the ACI 318-14 equation. Using the ACI 318-14 equation to predict development length, the k_p values were plotted in **Figure 3-6b**. As previously mentioned, k_p represents that ratio of predicted development length to strand diameter. For some cases, values for f_{ps} and f_{se} were not reported and were assumed to be f_{ps} = 1862 MPa and f_{se} =1117 MPa, respectively. As shown in **Figure 3-6b**, the mean k_p was 156 with a standard deviation of 9. Approximately 68 percent of the data set from the literature falls between -1.0 and +1.0 standard deviation from the mean. Notice also that 11 percent of the data set falls between -1.0 and -1.7 and another 16 percent between +1.0 and +3.6. Approximately 5 percent of data set falls outside the standard normal curve. According to this analysis, the most probable development length is between $147d_b$ and $165d_b$,

A similar analysis was performed using the data set shown in Table 7 and the UAPE. The k_p values using the UAPE are shown in **Figure 3-6c**. The mean k_p was 136 with a standard deviation of 27. Approximately 68 percent of the data set from the literature falls between -1.0 and +1.0 standard deviation from the mean. Also, 14 percent of the data set falls between -1.0 and -2.8 and another 16 percent between +1.0 and +2.1. Approximately 2 percent of data set falls outside the standard normal curve. According to this analysis, the most probable development length is between $109d_b$ and $163d_b$,

There are differences between predicted values of the two equations when using the data set. The mean development length using the ACI 318-14 equation was $156d_b$, and for the UAPE, the mean value was $136d_b$. Both mean values are greater than the actual mean of the data set which was $97d_b$. When comparing the two equations, the mean value predicted using the UAPE was

closer to the measured mean than the values predicted using ACI 318-14. This analysis also indicates that the standard normal deviation generated by UAPE is more accurate than the ACI 318-14 equation. For the UAPE, only 2 percent of data are outside of the normal curve, compared to 5 percent for the ACI-318 equation.

Another analysis was performed using the data shown in **Figure 3-6**. In **Figure 3-7**, the three normal distributions were superimposed so that the intersection points between the three curves could be determined. The area between the intersection points represents an area where the development length can be found with a 41 percent probability. This area bridges the gap that exists between the experimental results and the results from ACI 318-14. These points represent a development length of $111d_b$ to $143d_b$.
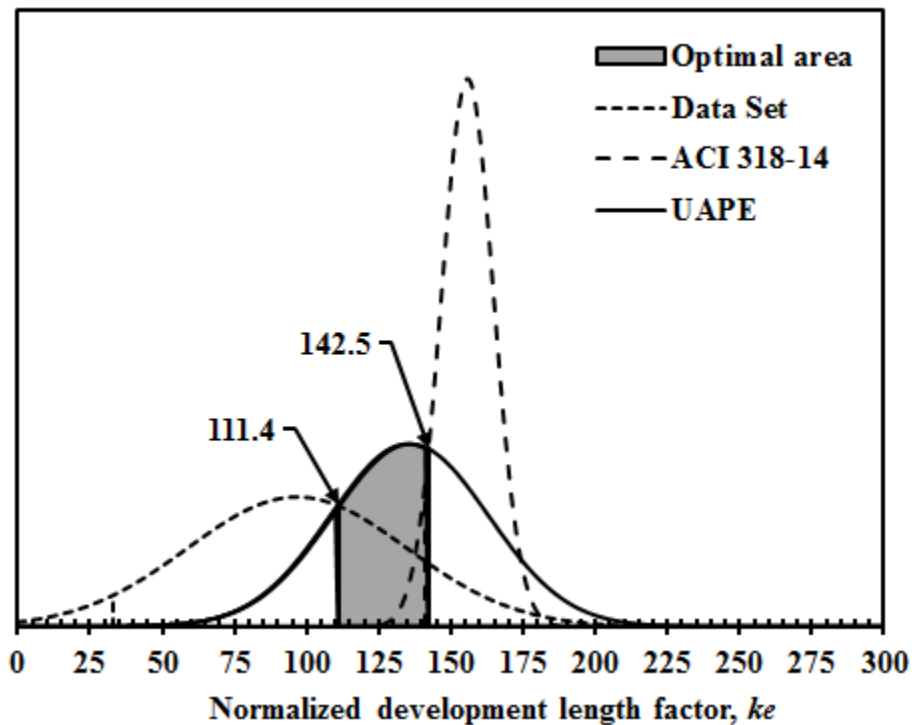
Figure 3-7. The normal distribution with different means and unequal standard deviation.

The ratio of the measured development lengths to predicted values to k_e values are plotted in **Figures 3-8** and 3-**9**. In **Figure 3-8**, the predicted value was obtained using ACI 318-14, and in **Figure 3-9** the predicted development length was calculated using UAPE. Shown in both figures are the average value (AV) of the ratio, its standard deviation (SD), the underestimation value (which are all ratios less than the average value), the overestimation value (which are all ratios that are greater than 1.0), the upper bound (AV+SD), and the lower bound (AV-SD). As shown in the **Figure 3-8**, the data follow a trend which is increasing k_e as the ratio of measured to predicted development length also increases. The AV for the data is 0.62 with a standard deviation of $\pm$ 0.25. Approximately 9 percent of data were considered overestimates because their ratio of measured to predict was greater than 1.0. Underestimated values accounted for 56 percent of the data and were those with a ratio less than 0.62, which was the average value.

The ratio of measured to predicted using the UAPE is plotted versus k_e in **Figure 3-9**. Although this data follows the same general trend as that shown in **Figure 3-8**, the trend is not as pronounced. The AV for the data is 0.72 with a standard deviation of $\pm$ 0.27. For this data, the amount of data classified as an overestimation and underestimation values represented 19% and 55% of data, respectively.

When comparing the two figures, 65 percent of the data fell between the upper and lower bounds for the UAPE compared to 60 percent of the data when using ACI 318-14. Based on those results, the UAPE better estimates development length for the data set than the ACI 318-14 equation.
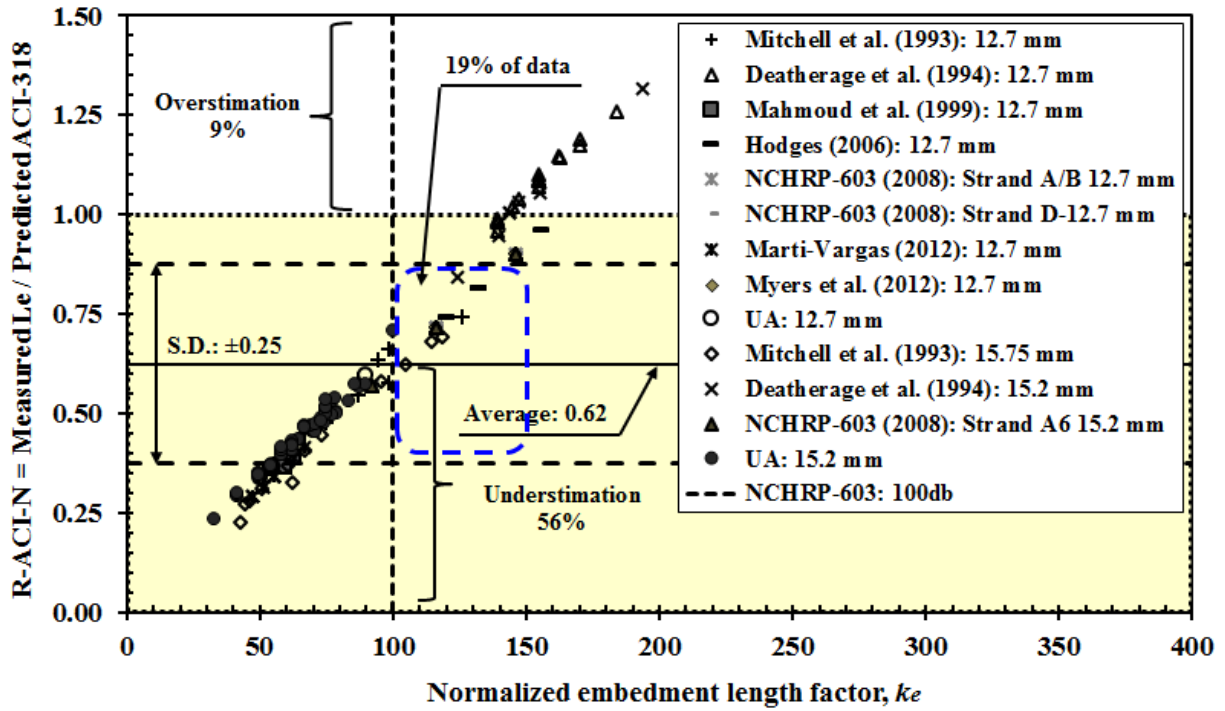
Figure 3-8. Relationship between ACI 318-14 ratio and the normalized embedment length factor.
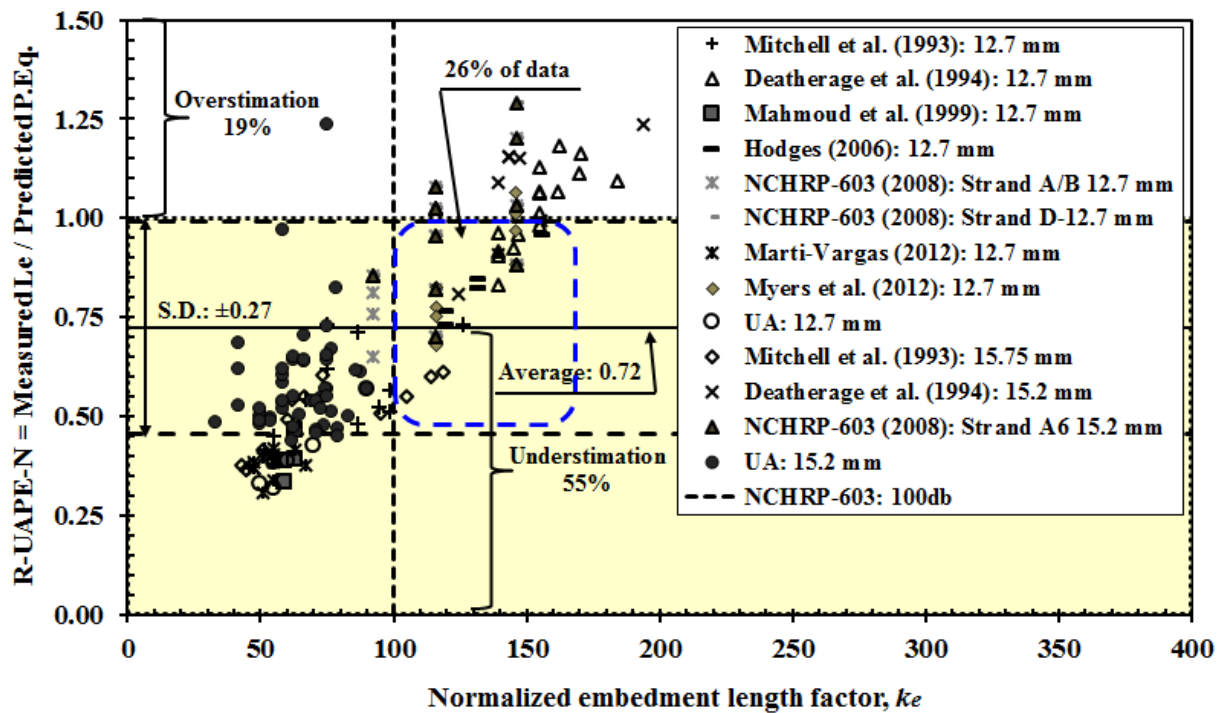
Figure 3-9. Relationship between UAPE ratio and the normalized embedment length factor.

In **Figures 3-8** and 3-**9**, a vertical line was plotted at a k_e of 100. This value was chosen because a normalized embedment length factor, k_e, of 100 is considered to be the lowest value for development length [10]. Using this vertical line along with the data in the figures, some conclusions were made. When using ACI 318-14 to predict development length, 19 percent of data set fell between the lower and upper bounds and to the right of the k_e of 100 vertical line. When the UAPE was used to predict development length, 26 percent of the data set fell between these bounds. A larger percentage of the data falls within the bounded area when using the UAPE. Therefore the UAPE better represents the data and more accurately represents the measured data than the predicted values from the ACI 318-14 equation.

3.3.5   Influence of Concrete Strength on Development Length

The development lengths predicted using the UAPE was compared to values predicted using the proposed equations in **Table 3-1**. For this analysis, some inputs were assumed to demonstrate the relationship between development lengths and compressive strength. Values of f_{pu}, f_{si}, and f_{se} had been assumed in previous tasks, but other values were required and were taken from Cousins et al. These included the plastic transfer bond stress coefficient ($U'_t = 0.556$), the plastic development bond stress coefficient ($U'_d = 0.110$), and the bond modulus ($B = 0.0815$ MPa/mm.). Using these values, the predicted development lengths from each author were calculated, normalized with respect to the nominal strand diameter, and plotted as shown in **Figure 3-10.** For each equation, the concrete compressive strength at release ranged from 28 MPa to 83 MPa while concrete strength at 28-days ranged from 41 MPa to 110 MPa. When the concrete strength at release and 28-days were 28 MPa and 41 MPa, respectively, 37.5 percent of the k_e were less than that predicted by the ACI 318-14 equation. At release strengths of 62 and

66

83 MPa, 75 percent of the k_e were less than those predicted by ACI 318-14. These results show that the ACI 318-14 equation better estimates development length at lower compressive strengths than at high compressive strengths.
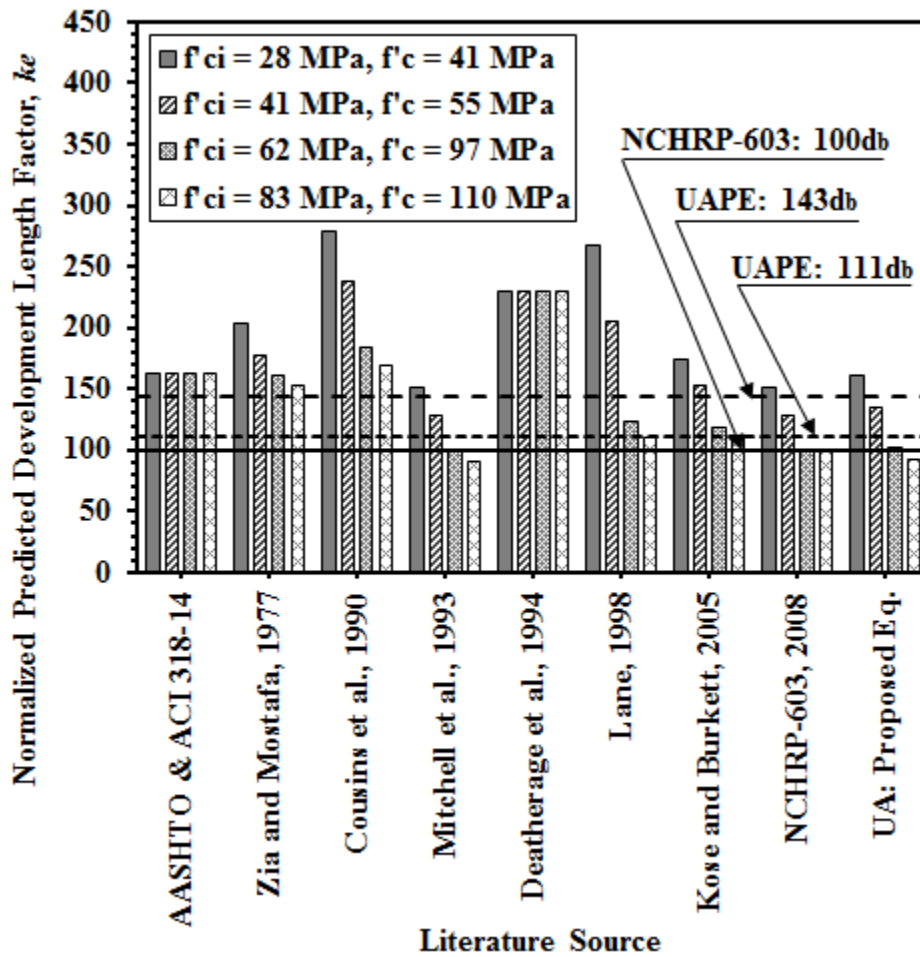
Figure 3-10. Comparison of normalized development length factors.

Figure 3-10 reveals two important conclusions. The first is when concrete strength at release and at 28-days increases, k_e decreases for all equations where concrete strength is a variable. For the ACI 318-14 and Deatherage et al. equations, the predicted values are constant because in those equations, the transfer length and flexural bond length are not dependent on concrete compressive strength. For the Zia and Mostafa and Deatherage et al. equations, there is little

www.manaraa.com

change in development length as concrete strength increases. In these two equations, concrete strength is only a factor in the transfer length portion of their development length equations. The second conclusion is related to the effect of high strength concrete on the development length. For all proposed equations which consider concrete strength at release and at 28 days, the predicted development length is less than or equal to the $111d_b$ that was proposed as the minimum development length in this investigation.

3.4   SUMMARY AND CONCLUSIONS

This study measured the embedment lengths and therefore determined the development lengths for 57 prestressed concrete beams. The beams were categorized into five groups. These groups included normal strength (NS), high strength (HS), self-consolidating concrete (SCC), ultra-high performance (UHP), and lightweight (LW) concrete that consisted of different types of aggregate and compressive strength. Fifty one beams were fabricated with 15.2 mm, Grade 270, seven wire low, relaxation prestressing strand. For all beams, the concrete strengths at release ranged from 23 MPa to 155 MPa. Six beams were fabricated using 12.7 mm diameter strand with concrete strengths at release between 24 MPa and 31 MPa. The University of Arkansas data was analyzed using linear and power regression in order to develop a new flexural bond length equation which is shown below in Eq, (5).

$$L_b = 66.5 \left(\frac{f_{ps} - f_{se}}{f_c^{'}} d_b \right)^{0.55} \tag{5}$$

In addition, data of measured embedment lengths from the literature was collected, analyzed, and compared with values predicted using ACI 318-14 and UAPE. Also, proposed development

68

length equations were taken from different researchers and compared with the UAPE equation. The results showed how development length is influenced by the concrete strength. Based on the following investigation, the following conclusions were made:

1. This investigation affirms that development length in prestressed concrete decreases as compressive strength increases. Therefore, concrete compressive strength should play a role in predicting transfer length and flexural bond length since the ACI 318 and AASHTO equations tend to overestimate development lengths for high compressive strengths.

2. The data set of measured embedment lengths collected from the literature were compared with values predicted by the ACI 318-14 and the UAPE equations. The standard normal distribution generated by the UAPE linked the area between the data set from the experimental data with the predicted values of ACI 318-14. The "linked area" represents a probability of 41 percent that a development length falls in that region. The lower intersection point, which is $111d_b$, between the normal distribution of the data set and the predicted values of the UAPE, is the proposed minimum value for development length.

3. The proposed UA equation (UAPE) was used to estimate the development length for concrete mixtures with a range of compressive strengths at release and at 28 days of age. The results showed that the UAPE better estimates the flexural bond length than the ACI 318-14 and AASHTO equations.

4. The analysis of the ratio of measured to predicted development lengths for the ACI 318-14 and UAPE equations indicates that 65 percent of the data set is found between the upper and lower bounds when using the UAPE to predict development length. When using the ACI 318-14 equation, 60 percent of data set is located between the bounds.

69

5.   Using the data set from the literature and that from the University of Arkansas, the study has shown that the current equations do not adequately estimate development length for higher strength concretes. Of the proposed equations, the UAPE best estimates the development length of prestressed members cast with high strength concrete.

NOTATION

A_s area of the prestressing strand (mm^2)

d_b diameter of the strand (mm)

f'_{ci} concrete compressive strength at prestress release (MPa)

f'_c concrete compressive strength at 28-days or time of testing (MPa)

f_{si} initial prestress (MPa)

f_{se} effective prestress (MPa)

f_{ps} stress at nominal strength of the member (MPa)

L_{fb} flexural bond length

L_e embedment length (mm)

L_d development length (mm)

k_e normalized embedment length factor

k_p normalized predicted development length factor

U'_t plastic transfer bond stress coefficient

U'_d plastic development bond stress coefficient

B bound modulus (MPa/mm)

71

REFERENCES

[1] ACI-318-14, Building code requirements for structural concrete and commentary, American Concrete Institute, Farmington Hills, MI, 2014.

[2] S.N. Lane, A new development length equation for pretensioned strands in bridge beams and piles, Federal Highway Administration, Turner-Fairbank Highway Research Center, 6300 Georgetown Pike, McLean, VA 22101 USA, 1998.

[3] C.D. Buckner, A review of strand development length for pretensioned concrete members, PCI Journal, 40 (1995) 84-105.

[4] J.H. Deatherage, E.G. Burdette, C.K. Chew, Development length and lateral spacing requirements of prestressing strands for prestressed concrete bridge girders, PCI Journal, 39 (1994) 70-83.

[5] N.W. Hanson, P.H. Kaar, Flexural bond tests of pretensioned prestressed beams, ACI Structural Journal, 55 (1959) 783-802.

[6] AASHTO, AASHTO LRFD Bridge Design Specifications, Customary U.S. Units, 6th ed., American Association of State Highway and Transportation Officials (AASHTO), Washington, D.C., 2012.

[7] B.W. Russell, Impact of High Strength Concrete on the Design and Construction of Pretensioned Girder Bridges, PCI Journal, 39 (1994) 76-89.

[8] T.E. Cousins, D.W. Johnston, P. Zia, Transfer and development length of epoxy coated and uncoated prestressing strand, PCI Journal, 35 (1990) 92-103.

[9] D. Mitchell, W.D. Cook, A.A. Khan, T. Tham, Influence of high strength concrete on transfer and development length of pretensioning strand, PCI Journal, 38 (1993) 52-66.

[10] J.A. Ramirez, B.W. Russell, Transfer, Development, and Splice Length for Strand/Reinforcement in High-Strength Concrete, Transportation Research Board, National Research Council (NCHRP-603), Washington, D.C., 2008.

[11] P. Zia, T. Mostafa, Development length of prestressing strands, PCI Journal, 22 (1977) 54-65.

[12] J.R. Martí-Vargas, P. Serna, J. Navarro-Gregori, J.L. Bonet, Effects of concrete composition on transmission length of prestressing strands, Construction and Building Materials, 27 (2012) 350-356.

[13] R.W. Floyd, E. Ruiz, D., N.H. Do, B.W. Staton, W.M. Hale, Development lengths of high-strength self-consolidating concrete beams, PCI Journal, 56 (2011) 36-53.

[14] Y.H. Kim, D. Trejo, M.B.D. Hueste, Bond performance in self-consolidating concrete pretensioned bridge girders, ACI Structural Journal, 109 (2012) 755-766.

[15] D.R. Rose, B.W. Russell, Investigation of standardized tests to measure the bond performance of prestressing strand, PCI Journal, 42 (1997) 56-80.

[16] E.E. John, E.D. Ruiz, R.W. Floyd, W.M. Hale, Transfer and Development Lengths and Prestress Losses in Ultra-High-Performance Concrete Beams, Transportation Research Record: Journal of the Transportation Research Board, 2251 (2011) 76-81.

[17] A.T. Ramirez-Garcia, R.W. Floyd, M. Hale, J.R. Martí-Vargas, Effect of concrete compressive strength on transfer length and development length, in: PCI-2013 Convention and National Bridge Conference: Discover High Performance Precast, PCI Journal, Gaylord Texan Resort-Grapevine, Texas, 2013.

[18] R.W. Floyd, Investigating the bond of prestressing strands in lightweight self-consolidating concrete, University of Arkansas, United States - Arkansas, 2012.

[19] R.W. Floyd, M.B. Howland, W. Micah Hale, Evaluation of strand bond equations for prestressed members cast with self-consolidating concrete, Engineering Structures, 33 (2011) 2879-2887.

[20] E.D. Ruiz Coello, Prestress losses and development length in pretensioned ultra high performance concrete beams, in, University of Arkansas, United States - Arkansas, 2007, pp. 181.

[21] D. Ward, Performance of prestressed double-tee beams cast with lightweight self-consolidating concrete, in, University of Arkansas, United States - Arkansas, 2010, pp. 133.

[22] B.W. Staton, Transfer lengths for prestressed concrete beams cast with self-consolidating concrete mixtures, in, University of Arkansas, United States - Arkansas, 2006, pp. 235.

[23] B.W. Staton, N.H. Do, E.D. Ruiz, W.M. Hale, Transfer lengths of prestressed bemas cast with self-consolidating concrete, PCI Journal, 54 (2009) 64-83.

[24] N.H. Do, B.W. Staton, W.M. Hale, Development of high strength self-consolidating concrete mixtures for use in prestressed bridge girders, in: The PCI National Bridge Conference, CD-ROM, Grapevine, Texas, 2006.

[25] M.M. Kose, W.R. Burkett, Formulation of new development length equation for 0.6 in. prestressing strand, PCI Journal, 50 (2005) 96-105.

73

[26] H. Park, Z.U. Din, J.-Y. Cho, Methodological Aspects in measurement of strand transfer length in pretensioned concrete, ACI Structural Journal, 109 (2012) 625-634.

[27] Z.I. Mahmoud, S.H. Rizkalla, E.-E.R. Zaghoul, Transfer and Development Lengths of Carbon Fiber Reinforced Polymers Prestressing Reinforcement, Structural Journal, 96 (1999) 594-602.

[28] A.T. Ramirez-Garcia, R.W. Floyd, W. Micah Hale, J.R. Martí-Vargas, Effect of concrete compressive strength on transfer length, Structures, 5 (2016) 131-140.

[29] J.J. Myers, J.S. Volz, E. Sells, K. Porterfield, T. Looney, B. Tucker, K. Holman, Self-Consolidating Concrete (SCC) for Infrastructure Elements: Report B-Bond, Transfer Length, and Development Length of Prestressing Strand, in, Missouri University of Science and Technology, Rolla, Missouri, MO, 2012.

[30] H.T. Hodges, Top Strand Effect and Evaluation of Effective Prestress in Prestressed Concrete Beams, in: Civil Engineering, Virginia Polytechnic Institute and State University, Blacksburg, VA, 2006.

[31] J.R. Martí-Vargas, P. Serna, J. Navarro-Gregori, L. Pallarés, Bond of 13 mm prestressing steel strands in pretensioned concrete members, Engineering Structures, 41 (2012) 403-412.

CHAPTER 4 : A HIGHER-ORDER EQUATION FOR MODELING STRAND BOND IN PRETENSIONED CONCRETE BEAMS

Alberto T. Ramirez-Garcia[1, 2], Canh N. Dang[3*], W. Micah Hale[2*], J.R. Martí-Vargas[4]

[1] Tatum Smith Engineers, Inc., 1108 Poplar PI, Rogers, AR 72756, USA
[2] The University of Arkansas, Department of Civil Engineering, 4190 Bell Engineering Center Fayetteville, AR 72701, USA
[3] Faculty of Civil Engineering, Ton Duc Thang University, Ho Chi Minh City, Vietnam
[4] Institute of Concrete Science and Technology (ICITECH), Universitat Politècnica de València, 4G, Camino de Vera s/n, 46022 Valencia, Spain

[*] Corresponding authors:
Phone +1-479-575-6348
Email: micah@uark.edu; canhdang@tdt.edu.vn

Abstract

In pretensioned concrete members, the bond between prestressing strands and concrete in the transfer zone is necessary to ensure the two materials can work as a composite material. This study develops a computer program based on the Thick-Walled Cylinder theory to predict the bond behavior within the transfer zone. The bond was modeled as the shearing stress acting at the strand-concrete interface, and this generated a normal stress to the surrounding concrete. The stresses developed in the concrete often exceeded its tensile strength, which resulted in radial cracks at the strand-concrete interface. These cracks reduced the concrete stiffness and redistributed the bond strength along the transfer zone. The developed program was able to determine the bond stress distribution, degree of cracking, and transfer length of the prestressing strands. The program was validated using a data set of transfer lengths measured at the University of Arkansas and a data set collected from the literature.

Keywords: pretensioned concrete, transfer length, strand bond, thick-walled cylinder, crack width.

4.1   INTRODUCTION AND BACKGROUND

Pretensioned concrete has been used extensively in buildings and bridge structures since the 1950's. In the design of pretensioned members, determining the transfer length is needed for calculating concrete stresses at release and quantifying shear strength at the ultimate state. Transfer length is the required length to transfer the prestress in the prestressing strands to the concrete. The prestressing force is transferred to the concrete by the bond between the two materials. The bond is a fundamental factor, which enables the strands and concrete to work as a composite material [1]. Studies have shown that bond strength is affected by many factors [1-8], including strand surface conditions [9], size of the strands [10], concrete compressive strength [11], type of release [4], concrete cover [12], cement content and water to cement ratio [8], and strand configuration [8, 13, 14]. The effects of these factors on strand bond have been validated by analytical and experimental studies [15]. While most studies have determined that the transfer length of prestressing strands is an indicator of strand bond, the number of studies that directly quantifies the bond-strength modeling at the strand-concrete interface is limited [16-21]. That existing numerical models and programs propose complex procedures to quantify the nonlinear interaction between the prestressing strands and concrete. Therefore, more research is needed to develop a simple a reliable technique to efficiently quantify the interaction and precisely predict the transfer length.

Prestressing steel can be considered as a homogeneous material in an analytical analysis, and its properties are generally well defined by ASTM-A416 / A416M-15 [22]. Concrete, on the other hand, is a heterogeneous material consisting of cement mortar and aggregates. Concrete properties depend on many variables and are difficult to define accurately. However, concrete can be assumed to be a homogeneous material for general applications in many civil engineering

76

structures, and this assumption is commonly accepted in the literature [23, 24]. The stress-strain relationship of concrete is nonlinear, and it is different in compression versus in tension. Prestressing steel is used exclusively in tension, and its stress-strain relationship is represented by a nonlinear curve [25].

The bond at the strand-concrete interface is dependent upon the properties of prestressing steel and concrete. The properties of the prestressing steel depend on the strain state of the material [25-27]. The concrete exhibits a high nonlinear behavior at higher compressive-stress levels and at the tensile state because of cracking, yielding and crushing [24]. Several investigations have assumed a perfect bond between the concrete and the prestressing steel since there is no slip at the contact surface of the concrete and strand. This assumption is used to simplify the calculation in pretensioned concrete structures using numerical methods, but it does not reflect the actual behavior of the materials.

For simplification, the design aspects related to strand bond are often solved without considering the bond stress distribution [7]. In this paper, the bond acting at the strand-concrete interface was modeled using the principles of solid mechanics. Previous studies determined that the stress level in the concrete after release often exceeds the concrete's tensile strength [28, 29], which is responsible for the concrete cracking within the transfer zone. Therefore, this study considered both cracked and uncracked regions adjacent to the strand within the transfer zone.

The research aims at predicting the bond behavior within the transfer zone using the Thick-Walled Cylinder theory. A second-order equation that represents the relationship of post-peak stress and crack width [30] was upgraded to a third-order equation. A computer program used to predict the transfer length and bond behavior was developed to analyze the cracked and fracture

77

zone. The accuracy of the developed program was validated using a data set of transfer lengths

measured at the University of Arkansas and a data set collected from the literature.

4.2 BACKGROUND

A thick-walled cylinder, which is shown in **Figure 4-1**, is widely used for estimating the transfer

length in pretensioned concrete beams [12, 28, 30].
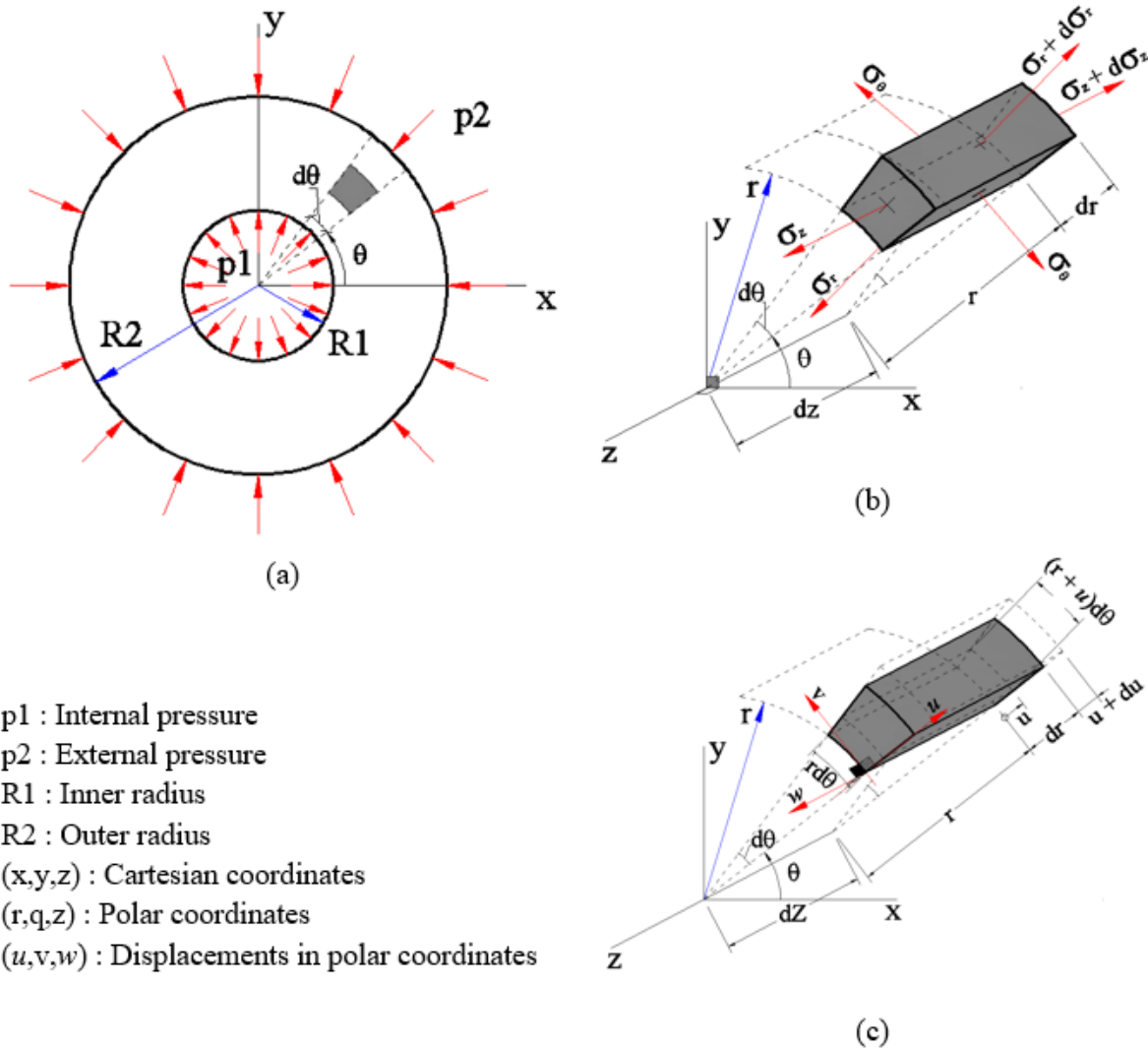
Figure 4-1 – Stress and displacements in thick-wall cylinder: (a) thick-wall cylinder (The z axis is perpendicular to the plane of the figure); (b) Stresses in cylindrical volume of thickness dz; (c) Radial displacement in cylindrical volume of thickness dz.

78

The cylinder thickness is constant and subjected to a uniform internal pressure p_1, a uniform external pressure p_2, and an axial load P. In 1939, Hoyer and Friedrich [31] idealized a pretensioned concrete beam as a thick-walled cylinder as shown in **Figure 4-2**.
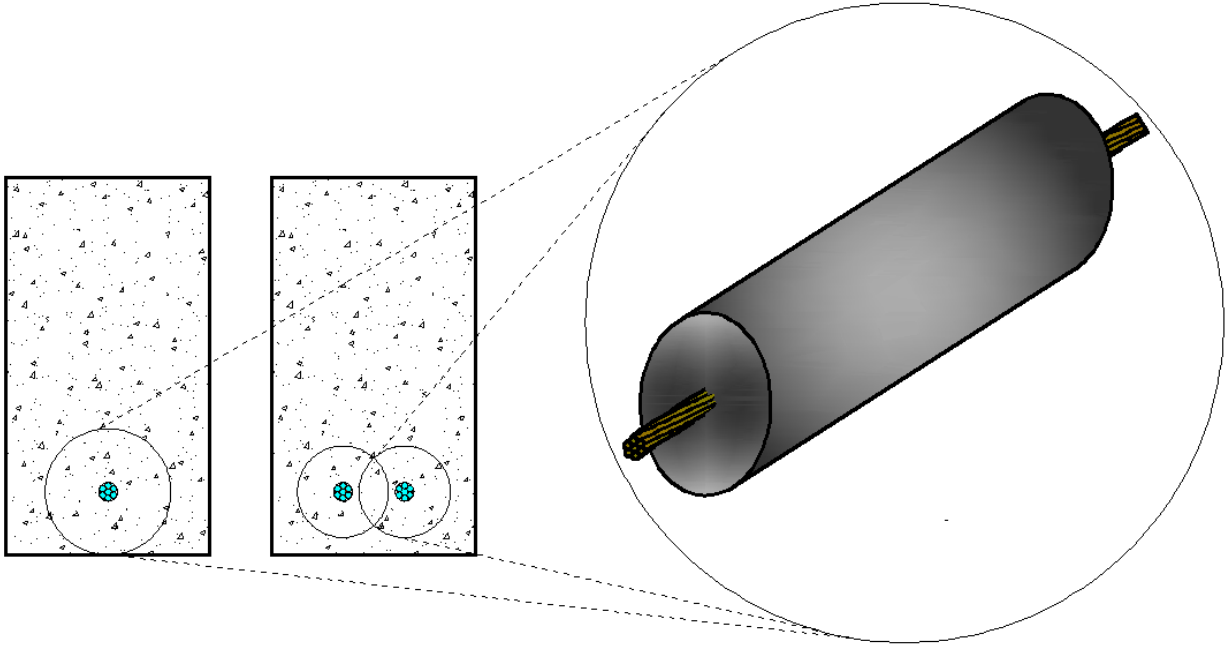
Figure 4-2 - Prestressed concrete beams idealized as thick-walled cylinder.

The researchers considered the anchorage to be a result of swelling of the prestressing steel or wires that were caused by Poisson's ratio and proposed an equation to predict the transfer length of prestressing strands as shown in **Eq. (1)**.

$$L_t = \frac{d_b}{2\mu}\left(1+v_c\right)\left(\frac{\eta}{v_p} - \frac{f_{si}}{E_c}\right)\frac{f_{se}}{2f_{si} - f_{se}} \tag{1}$$

where L_t = transfer length; d_b = strand diameter; μ = coefficient of friction between strand and concrete; v_c = Poisson's ratio of concrete; $\eta = E_p/E_c$ = modular ratio; v_p = Poisson's ratio of strand; f_{si} = initial prestress in strand; E_c = elastic modulus of concrete; f_{se} = effective prestress in strand after losses; E_p = elastic modulus of strand.

In the 1950s, Janney [21] developed an analytical model for the transfer length in which the prestressing steel was considered a solid cylinder, and the concrete was considered a hollow cylinder having the inner radius equal to the strand radius and an infinite outer radius. Janney's model was identical to Hoyer and Friedrich's model, which used the thick-walled cylinder theory. Based on this model, Janney developed an equation to predict transfer length as shown in **Eq. (2)**.

$$L_t = \frac{-d_b}{4\mu v_p}\left[1+(1+v_c)\frac{E_p}{E_c}\right]\ln\left(\frac{f_{si}-f_{se}}{f_{si}}\right) \tag{2}$$

Researchers have reported the applicability of using the thick-walled cylinder theory to predict the transfer length of prestressing strands [12, 17-19]. Most of the early investigations dealt with the transfer length of small wires of different sizes [21, 32]. Later studies [7, 17, 19, 31] on the bond of prestressing strands have dealt with multi-wire strands, including seven-wire, 12.7 mm and 15.2 mm diameter strand [11, 33]. Weerasekera [28] used these two strand sizes to develop a theory of bond action that used the principles of solid mechanics to predict the transfer length. The prestressing strand was considered as a solid cylinder, and the surrounding concrete was considered as a hollow cylinder. This was achieved through the consideration of elastic analysis (uncracked region) and a cracked region. The proposed transfer-length equation, **Eq. (3)**, considered a distributed crack zone around the strand, and the concrete in the affected region was analyzed as an anisotropic elastic material.

$$L_t = \frac{f_{si}A_b}{K_f f_t c_y} \tag{3}$$

$$K_f = B_0 - \frac{f_{si}A_b}{F_0 f_{ci}^{'m_0}} \tag{3a}$$

80

where f_{si} = initial prestress in strand (MPa); A_b = nominal area of strand (mm^2); K_f = constant factor depending on values of $B_0 = 3.055$, $F_0 = 52320$, $m_0 = 0.28$; f_t = concrete's tensile strength (MPa); c_y = clear concrete cover (mm); f'_{ci} = concrete's compressive strength at release of the strands (MPa).

Weerasekera [28] used Gopalaratnam and Shah's equation [29] in order to further investigate the partially cracked and fully cracked regions. Gopalaratnam and Shah [29] had investigated the tensile resistance of cracked concrete and proposed a power equation to calculate the tensile stress in the cracked regions. Their findings have been used to study the crack propagation of concrete elements subjected to tension by making some modifications. Mahmoud [30] assumed a simple second-order relationship between post-peak stress and crack width instead of using Gopalaratnam and Shah's relationship [29]. Mahmoud [30] concluded this second-order relationship provided a good agreement with the measured values.

A recent study conducted by Abdelatif et al. in 2015 [12] also affirmed the reliability of using the using the thick-walled cylinder theory to predict the transfer length of prestressing strands. The researchers proposed an equation for the transfer length as shown in **Eq. (4)**. In this equation, the prestressing strand and concrete were assumed to have elastic behavior, and the bond between the strand and concrete was modeled using Coulomb's friction law.

$$L_t = \frac{r_p}{2\mu}\left[\left(\frac{1}{B} + \frac{v_p}{B^2 E_p}\right)\ln\left(1 + 0.95 f_{se}\frac{B}{A}\right) - 0.95 f_{se}\left(\frac{1-v_p}{E_p} + \frac{v_p}{B^2 E_p}\right)\right] \tag{4}$$

where *A* and *B* are shown in **Eq. (4a)** and **(4b)** respectively

$$A = \frac{\left(r_p - r_{c,1}\right)}{\dfrac{1-\nu_p}{E_p} r_p + \dfrac{r_{c,1}}{E_c}\left[\nu_c + \dfrac{r_{c,2}^2 + r_{c,1}^2}{r_{c,2}^2 - r_{c,1}^2}\right]} \tag{4a}$$

$$B = \frac{-\left[\dfrac{\nu_p}{E_p} r_p + \dfrac{\nu_c}{E_c} r_{c,1}\left(\dfrac{A_p}{A_c}\right)\right]}{\dfrac{1-\nu_p}{E_p} r_p + \dfrac{r_{c,1}}{E_c}\left[\nu_c + \dfrac{r_{c,2}^2 + r_{c,1}^2}{r_{c,2}^2 - r_{c,1}^2}\right]} \tag{4b}$$

where r_p = nominal radius of prestressing steel (mm); $r_{c,1}$ = internal radius of concrete cylinder which equals to radius of strand after prestressing (mm); $r_{c,2}$ = external radius of concrete cylinder (mm); A_p = total area of strand (mm^2); A_c = cross sectional area of concrete (mm^2); E_c = elastic modulus of concrete (GPa); E_p = elastic modulus of strand (GPa); f_{se} = effective prestress in strand after losses (MPa); ν_p = Poisson's ratio of strand; ν_c = Poisson's ratio of concrete; and μ = coefficient of friction between prestressing steel and concrete

Although analytical models have been developed to predict the transfer length of prestressing strands, most models assume that the tension stress has a linear behavior, and they do not consider the fracture zones occurring along the concrete-strand bond interface. In this study, the behavior of the prestressing strands and the concrete in the transfer zone is evaluated. The variation of strand stress, which is dependent on the stiffness of the concrete adjacent to the strands, will also be examined. In this investigation, the proposed method by Mahmoud [30], which is a second-order equation to analyze the crack zone, is extended to the third-order because it better fits Gopalaratnam and Shah's relationship. Moreover, three type of cracks such as fully cracked, partially cracked, and uncracked are considered in the model, and the actual contact surface area and the effects of shrinkage are considered as well.

82

4.3 RESEARCH SIGNIFICANCE

A new method is proposed to improve the accuracy in quantifying the transfer length by considering several variables such as the number of cracks, concrete cover, and fracture criteria. A computer program was implemented based on the thick-walled cylinder theory to analyze the crack and fracture zone and predict the transfer length of prestressing strands. The relationship of post-peak stress and crack width proposed by Mahmoud [30] was upgraded from a second-order to a third-order equation. A data set of 24 transfer lengths measured at the University of Arkansas and collected from the literature was used to validate the computer program. The research findings are then synthesized and reported.

4.4 MATERIAL PROPERTIES

4.4.1 Concrete

Concrete compressive strength is a significant parameter in the design of pretensioned concrete structures. The presence of micro-cracks at the interfacial transition zone between the coarse aggregate and the cement matrix makes the prediction of concrete strength more complex [34]. However, the radial compressive stresses generated by the release of a tensioned strand normally do not exceed 60% of the concrete's compressive strength (f'_c) [25, 35, 36]. As a result, the concrete can be modeled as a linear elastic material in compression, and the elastic modulus (E_c) can be determined using **Eq. (5)** by [23, 24, 35, 36].

$$E_c = 0.043w^{1.5}\sqrt{f'_c} \tag{5}$$

where w = unit weight of concrete (kg/m^3); f'_c = concrete's compressive strength (MPa).

83

Concrete is stronger in compression than it is in tension. Concrete's tensile strength is approximately 10% of its compressive strength [24, 37]. This is a major factor that causes the nonlinear behavior of either conventionally reinforced or prestressed concrete structures. The stress-strain response of concrete in tension is assumed to be linear prior to cracking with the same elastic modulus (E_c), and the concrete's tensile strength at release of the prestressing strands is assumed to be equal to the modulus of rupture (f_t) [23-25, 35, 36].

$$f_t = 0.62\sqrt{f_c'} \tag{6}$$

where $f'c$ = concrete's compressive strength (MPa).

In this investigation, the allowable compressive stress after prestress transfer was $0.60 f_{ci}'$ (where f_{ci}' is the concrete's compressive strength at release of prestressing strands) as recommended by ACI 318 [35] and AASHTO LRFD [38], although a value of $0.70 f_{ci}'$ has also been recommended [36, 39, 40]. The Poisson's ratio of concrete is in the range of 0.15 to 0.20 [41] and is assumed to be equal to 0.15 when this ratio is not specified in the collected data.

4.4.2 Prestressing steel (strands)

The elastic modulus (E_p) and Poisson's ratio (v_p) of prestressing strands are assumed to be 197 GPa and 0.3 [38], respectively. This study used 12.7 mm and 15.2 mm, Grade 1860, low-relaxation prestressing strands. These strands were tensioned to 1,396 MPa prior to casting the concrete.

4.5 ANALYTICAL FORMULATION

A thick-walled cylinder equation was used in this investigation which can be derived from

Figure 4-1.b and **Figure 4-1.c** [42, 43] and detailed solutions are shown in **Appendix A**.

4.5.1 Bond Mechanisms in the Transfer Zone

Prestress is transferred to the concrete through adhesion, Hoyer´s effect, and mechanical

interlock [44, 45]. The two primary components of bond in the transfer region can be contributed

to Hoyer´s effect and mechanical interlock. Generally, adhesion is not included because it is lost

once slip occurs. Hoyer's effect is the first primary component of bond and is due to the lateral

expansion of the strand diameter, which induces frictional forces along the longitudinal axis of

the strand [45, 46]. Mechanical interlock depends on the twisting of the strand about its

longitudinal axis as it tries to slip through the concrete. It is the second primary component of

bond and occurs between the helical lay of the individual wires in the 7-wire strand and the

surrounding concrete [45, 47].

In the transfer zone, the bond between concrete and prestressing strand is generated by high

radial pressures due to Hoyer's effect as shown in **Figure 4-3**. Using Coulomb's friction law,

bond stress (τ) can be expressed as a function of interface pressure (σ_i) and the coefficient of

friction (μ) as shown in **Eq. (7)** [7, 12].

$$\tau = \mu\sigma_i \tag{7}$$
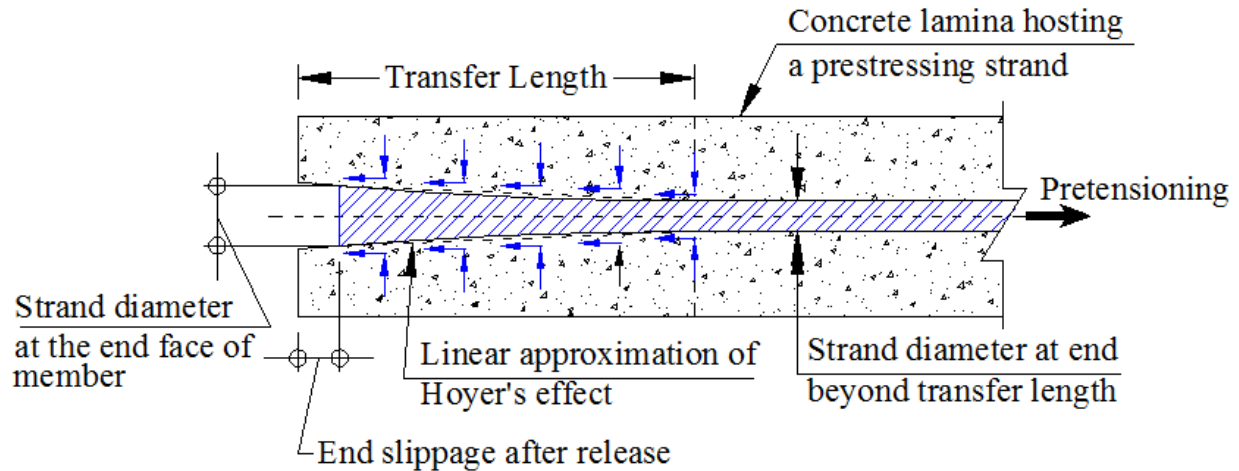
Figure 4-3 - Hoyer's effect along the transfer length.

Janney (1954) used the coefficient of friction values in prestressing steel wires that ranged from 0.20 to 0.60 [21], whereas a coefficient of friction of 0.75 was used for seven-wire steel strands [28]. The coefficient of friction used in this investigation, however, has been collected from the authors reported in this investigation, and for the pretensioned concrete beams tested at the University of Arkansas, those values have been assumed as 0.45 and 0.50.

4.5.2 Uncracked Analysis

In this analysis, both the concrete and strands are considered isotropic materials (elastic analysis). The strand is modeled as a solid cylinder having a radius R_1 while the concrete is modeled as a thick-walled cylinder having the inner radius R_1 and the outer radius R_2. The radius R_2 is equal to the clear concrete cover [7, 28].

Using the assumption of thick-walled cylinder theory, the expressions of stresses, strains, and displacements can be developed and solved using the constitutive law (stress–strain relationship), equilibrium and compatibility equations, and imposing boundary conditions. The outer surface of the concrete cylinder is assumed to behave as a free surface (stress at this point will be zero)

86

while the stresses produced by the strand's expansion are considered as a pressure developed at the strand-concrete interface. Moreover, the drying shrinkage of concrete (ε_{sh}) produces a normal stress acting on the strand before prestress release, and the release generates longitudinal compressive stresses in the concrete at the level of strand (f_{cz}). This effect can reduce the contact pressure due to the Hoyer's effect. The compatibility of displacements, therefore, in the radial direction at the prestressing steel and the concrete can be used to develop the interfacial pressure as shown by:

$$\Delta_{fp}^{p} + \Delta_{\sigma i}^{p} = \Delta_{\sigma i}^{c} + \Delta_{fcz}^{c} + \Delta_{sh}^{c} \tag{8}$$

where: Δ_{fp}^{p} = increase in radius of strand due to the reduction in longitudinal stress from initial prestress f_{si} to effective prestress f_{se}; $\Delta_{\sigma i}^{p}$ = reduction in strand radius due to the uniform radial compression at interface σ_i; $\Delta_{\sigma i}^{c}$ = increase in the inner radius of the thick-walled concrete cylinder due to the interface pressure σ_i; Δ_{fcz}^{c} = increase in the inner radius of the thick-walled concrete cylinder due to the longitudinal compressive stress at the level of strand f_{cz}; Δ_{sh}^{c} = reduction in the inner radius of the thick-walled concrete cylinder due to drying shrinkage ε_{sh}.

Each of the following parameters described above was extensively described by Mahmoud [30] and those parameters are explained in **Appendix B**. Knowing all the parameters, **Eq. (8)** can be solved by the following equation as given below:

$$\sigma_i = \frac{\dfrac{\left(f_{si} - f_{se}\right)}{E_p}v_p - \dfrac{f_{cz}}{E_c}v_c - \varepsilon_{sh}}{\dfrac{\left(1 - v_p\right)}{E_{pr}} + \dfrac{K_c}{E_c}} \tag{9}$$

87

where f_{si} = initial prestress in strand; f_{se} = effective stress in strand after all losses; E_p = elastic modulus of strand in the longitudinal direction; E_{pr} = elastic modulus of strand in the transversal direction (in this investigation this value is taken as E_p); v_c = Poisson's ratio for concrete; v_p = Poisson's ratio for strand; ε_{sh} = drying shrinkage coefficient as derived in **Eq. (9.b)**; f_{cz} = compressive stress in concrete at the level of the strand as derived in **Eq. (9.c)**; K_c = a parameter shown in **Eq. (9.a)**.

$$K_c = \frac{(1 - v_c) R_1^2 + (1 + v_c) R_2^2}{(R_2^2 - R_1^2)} \tag{9.a}$$

The drying shrinkage coefficient can be estimated using AASHTO-LRFD [38] as shown below

$$\varepsilon_{sh} = -k_s k_{hs} k_f k_{td} 0.48 \times 10^{-3} \tag{9.b}$$

where

k_s = factor for the effect of the volume-to-surface ratio, $k_s = 1.45 - 0.0051 \left(V/S \right) \geq 1.0$ (V in mm^3 and S in mm^2)

k_{hs} = humidity factor for shrinkage, $k_{hs} = (2.00 - 0.014H)$; the relative humidity (H) was assumed as 70%.

k_f = factor for the effect of concrete strength, $k_f = \dfrac{35}{7 + f_{ci}'}$ (f'_{ci} in MPa)

k_{td} = time-development factor, $k_{td} = \left(\dfrac{t}{61 - 0.58 f_{ci}' + t} \right)$; t in days (t = 1-day at time of release)

The concrete compressive stress at the level of the prestress strand (f_{cz}) varies from zero at the end of the beam to a maximum value at the end of the transfer length and is estimated by:

$$f_{cz} = -f_{se} A_p \left(\frac{1}{A_g} + \frac{e_c^2}{I_g} \right) \tag{9.c}$$

88

where f_{se} = effective prestress in strand after losses; A_p = total area of the strand; A_g = cross section area of the concrete member; e_c = eccentricity of the prestressing force; and I_g = moment of inertia of concrete section.

4.5.3 Cracked Analysis

4.5.3.1 Behavior of Concrete in Tension

Concrete is weak in tension. The tensile stresses generated by Hoyer's effect normally exceed the concrete's tensile strength [28, 29]. Within the transfer zone, the concrete adjacent to the prestressing strand exhibits cracking at different stress levels. The relationship between the post-peak stress and crack width is shown below [29]:

$$\sigma = \sigma_p e^{-k w_{cr} \lambda} \tag{10}$$

where σ = post-peak tensile stress; σ_p = tensile strength (peak value of σ); $\lambda = 1.01$ (assumed value in [29]); $k = 64.18$ mm^{-1} [48]; w_{cr} = crack width in mm; $w_o = 0.05$ mm, which is the initial crack width at the shear plane.

Eq. (10) can be re-written as shown in **Eq. (11)** [30]. In this equation, n is a degree polynomial equation. Mahmoud [30] proposed a second-order equation ($n = 2$), and the corresponding curve is shown in **Figure 4-4**. In this study, a third-order equation ($n = 3$) is proposed to increase the accuracy in predicting transfer length as discussed in later sections.

$$\sigma = \sigma_p \left(1 - \frac{w_{cr}}{w_o} \right)^n \tag{11}$$

89
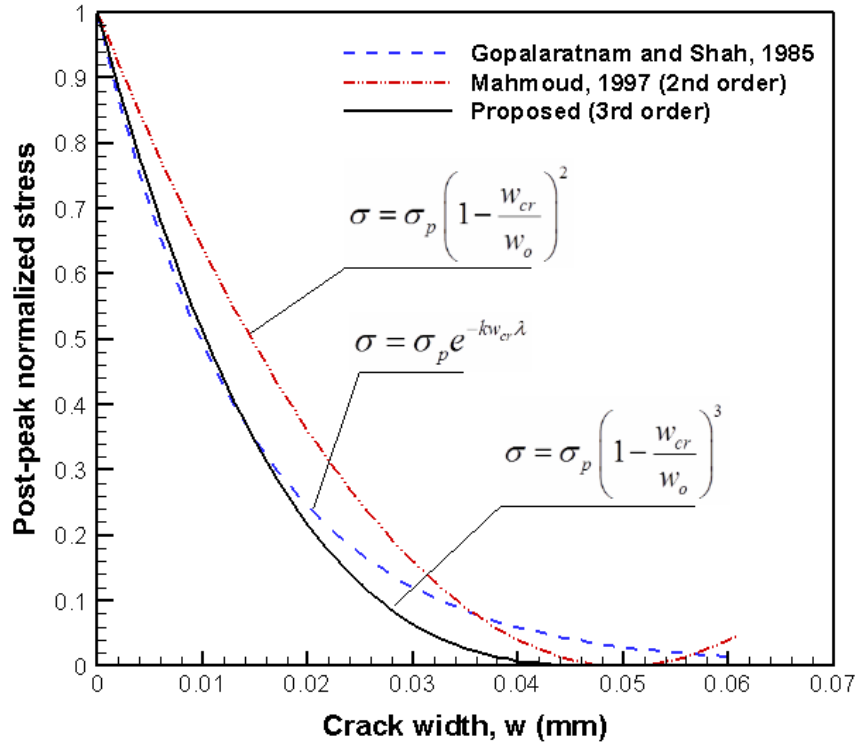
Figure 4-4 – Analytical expressions used for modeling the stress-crack width relationship.

4.5.3.2 Considerations of Fracture Zones Surrounding the Prestressing Steel

The state of cracking around the strand caused by the internal pressure after strand release is shown in **Figure 4-5**.

The state of cracking is divided into three zones, which includes the real cracked zone, the fracture zone, and the uncracked zone. The first zone may occur as soon as the strand is released, so the concrete region adjacent to the strand is cracked due to high internal pressure. This region is defined as the distance from the strand surface to the radial crack at $r = R_{cr}$ at which the crack width is 0.05 mm, and the hoop stress is considered to be zero for crack widths greater than 0.05 mm. The fracture zone is the distance from R_{cr} to R_{fr} at which the hoop stress, which is transferred across the crack, varies from zero at $r = R_{cr}$ and $w_o = 0.05$ mm to the maximum value of f_t, concrete's tensile strength, at the effective crack tip where $r = R_{fr}$ and $w_o =$

90

0. In this case, at a certain distance from the end, the concrete around the prestressing steel is considered partially cracked because of the decrease in pressure. The uncracked zone extends from the effective crack tip ($r = R_{fr}$) to the outer surface of the concrete ($r = R_2$), and the hoop stress decreases when the radius increases from $r = R_{fr}$ to $r = R_2$ according to the elastic theory of the thick-walled cylinder. At further distances from the end of the strand, also, the surrounding concrete is not cracked because the pressure in this part is negligible.
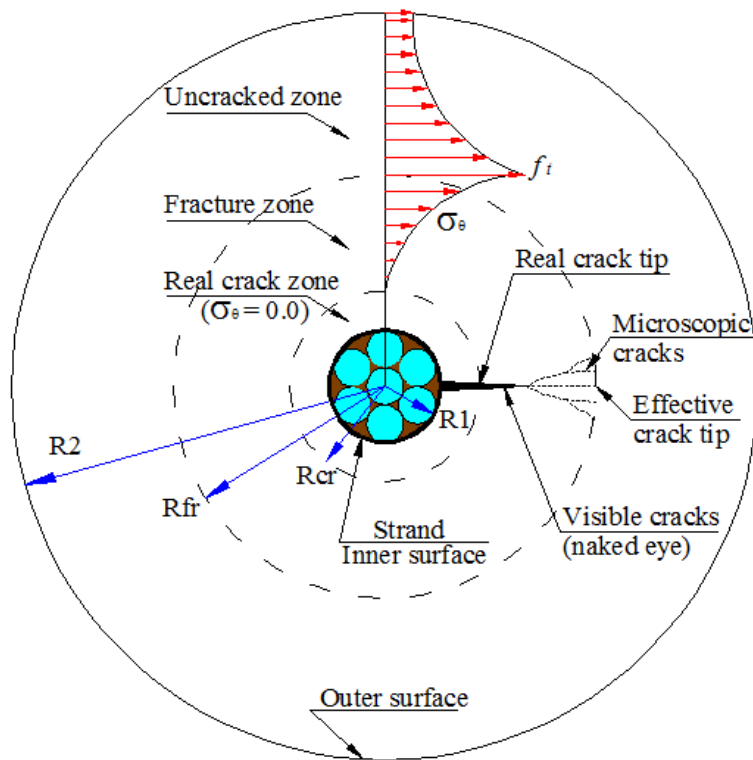
Figure 4-5 – Fracture zones around the prestressing steel.

In this analysis, Mahmoud's theory [30] was applied for the crack width (w_a), which is assumed at the strand-concrete interface of the thick-walled cylinder and depends on the variations of strand radius ($\Delta_{fp}^{p} + \Delta_{\sigma i}^{p}$) [where Δ_{fp}^{p} = increase in strand radius due to reduction in longitudinal stress from initial prestress f_{si} to effective prestress f_{se}; and $\Delta_{\sigma i}^{p}$ = reduction in radius of strand

due to the uniform radial compression at interface σ_i] and the assumed number of radial cracks

(N_{rc}), which varies from 1 to 6 [30]. The crack width equation, therefore, is given by:

$$w_a = \frac{2\pi R_1}{N_{rc}} \left[\frac{\left(f_{si} - f_{se}\right)}{E_p} v_p - \frac{\sigma_i}{E_{pr}} \left(1 - v_p\right) \right]$$ (12)

4.5.3.3 Compatibility Condition

The cracked analysis is solved using an elastic analysis as discussed previously [30]. **Eq. (8)** is

rewritten as:

$$\Delta_{fp}^p + \Delta_{\sigma i}^p = \left(\Delta_{cr}^c + \Delta_{fr}^c + u_{R_{fr}}^c\right) + \Delta_{fcz}^c + \Delta_{sh}^c$$ (13)

where Δ_{cr}^c = deformation of the real crack zone; Δ_{fr}^c = deformation of the fracture zone; and $u_{R_{fr}}^c$ =

radial displacement at $r = R_{fr}$.

The elastic modulus of concrete in the cracked regions was assumed to be elastic. The micro-

cracks generally occur around the strand, and the crack depth is less than a concrete cover of 75

mm, as shown in **Table 4-2**. There is no crack propagation through the prestressed concrete

beam (from bottom to the top) because the initial prestress is transferred to the concrete along the

strand. The mechanical properties of concrete were calculated using the given equations in

Section 4.1.

4.5.3.3.1 Deformation of the real crack zone, Δ_{cr}^c

The real crack zone is characterized by the condition where the tensile stress (σ_θ) is not

transmitted across this zone because the crack width is greater than w_o (initial crack width at the

92

shear plane). The thick-walled cylinder equation for this zone can be written as **Eq. (14)** [28, 30].

$$\frac{d\sigma_r}{dr} + \frac{\sigma_r}{r} = 0 \tag{14}$$

Solving the first order differential equation and applying the boundary condition of $\sigma_r = -\sigma_i$ at $r = R_1$, an expression of radial stress (σ_r) is obtained as shown below:

$$\sigma_r = -\frac{R_1}{r}\sigma_i \tag{15}$$

The deformation of the real crack zone (Δ_{cr}^c) can be calculated using the following equations:

$$\Delta_{cr}^c = -\int_{R_1}^{R_{cr}} \varepsilon_r dr \tag{15.a}$$

$$\varepsilon_r = \frac{\sigma_r}{E_c} \tag{15.b}$$

$$\Delta_{cr}^c = R_1 \frac{\sigma_i}{E_c} \ln \frac{R_{cr}}{R_1} \tag{15.c}$$

where Δ_{cr}^c = deformation of the real crack zone; R_1 : inner radius; σ_i = interface pressure; E_c = elastic modulus of concrete; and R_{cr} = crack radius.

4.5.3.3.2 Deformation of the fracture zone, Δ_{fr}^c

In this zone, two cases, Case A and Case B, were considered in the analysis. The second-order equation was explained by Mahmoud [30], and that idea was used to develop the third-order equation ($n = 3$). The maximum hoop stress (σ_θ) at the edge of the fracture zone (R_{fr}) is considered to be equal to the rupture strength of concrete (f_t). Thus, the hoop stress can be expressed by **Eq. 16**.

93

$$\sigma_\theta = f_t \left(\frac{r - R_{cr}}{R_{fr} - R_{cr}} \right)^3 \tag{16}$$

where σ_θ = hoop stress; f_t = concrete tensile strength; R_{fr} = fracture radius; r = radius in the radial direction; and R_{cr} = crack radius.

CASE A: the hoop stress is obtained by solving the third-order equation (**Eq. 16**) which is shown below:

$$\sigma_\theta = k_t \left(r^3 - 3r^2 R_{cr} + 3rR_{cr}^2 - R_{cr}^3 \right) \tag{16.a}$$

$$k_t = \frac{f_t}{\left(R_{fr} - R_{cr} \right)^3} \tag{16.b}$$

Substituting **Eq. 16.a-b** into **Eq. A.1** (see Appendix A) and using a boundary condition of radial stress $\sigma_r = -\sigma_i R_1 / R_{cr}$ at $r = R_{cr}$, an expression of radial stress (σ_r) is given as:

$$\sigma_r = -\sigma_i \frac{R_1}{r} + k_t \left(\frac{r^3}{4} - r^2 R_{cr} + \frac{3}{2} rR_{cr}^2 - R_{cr}^3 + \frac{R_{cr}^4}{4r} \right) \tag{16.c}$$

Where σ_i = interface pressure; r = radius in the radial direction; R_1 = inner radius; k_t = radial stress; and R_{cr} = crack radius.

The total deformation of the fracture zone in the radial direction, therefore, is the integration of the radial strain ε_r (**Eq. A.2**) from $r = R_{cr}$ to $r = R_{fr}$ where the longitudinal stress σ_z has been neglected.

$$\Delta_{fr}^c = R_1 \frac{\sigma_i}{E_c} \left(\ln \frac{R_{fr}}{R_{cr}} \right) - k_1 \tag{16.d}$$

94

where:

$$k_1 = \frac{k_t}{E_c} \left\{ \begin{array}{l} \dfrac{R_{fr}^4 - R_{cr}^4}{16}(1-4v_c) - \dfrac{R_{cr}\left(R_{fr}^3 - R_{cr}^3\right)}{3}(1-3v_c) + \dfrac{3R_{cr}^2\left(R_{fr}^2 - R_{cr}^2\right)}{4}(1-2v_c)... \\ \\ -R_{cr}^3\left(R_{fr} - R_{cr}\right)(1-v_c) + \dfrac{R_{cr}^4}{4}\left(\ln\dfrac{R_{fr}}{R_{cr}}\right) \end{array} \right\} \tag{16.e}$$

CASE B: if the crack width at the strand-concrete interface (w_a) is less than or equal to 0.05 mm, then the real crack zone would not be formed, and the hoop stress is calculated using **Eq. (12)**. The relationship between the crack width (w_{cr}) at any point on the interface, the radius r, and the crack width w_a can be expressed by:

$$w_{cr} = w_a \frac{R_{fr} - r}{R_{fr} - R_1} \tag{17.a}$$

where R_{fr} = fracture radius; R_1 = inner radius; and r = radius in the radial direction.

Using this value of w_{cr} in **Eq. (11)** with $n = 3$, the hoop stress or tensile stress can be expressed by:

$$\sigma_\theta = f_t + k_2\left(R_{fr} - r\right) + k_3\left(R_{fr} - r\right)^2 + k_{23}\left(R_{fr} - r\right)^3 \tag{17.b}$$

Where the constant factors are the following:

$$k_2 = -\left(\frac{3w_a}{w_o}\right)\frac{f_t}{\left(R_{fr} - R_1\right)} \tag{17.c}$$

$$k_3 = 3\left(\frac{w_a}{w_o}\right)^2 \frac{f_t}{\left(R_{fr} - R_1\right)^2} \tag{17.d}$$

$$k_{23} = -\left(\frac{w_a}{w_o}\right)^3 \frac{f_t}{\left(R_{fr} - R_1\right)^3} \tag{17.e}$$

95

Substituting **Eq. (17.b)** into **Eq. (A.1)** and using a boundary condition of radial stress $\sigma_r = -\sigma_i$ at

$r = R_1$, an expression for radial stress (σ_r) is shown below:

$$\sigma_r = -\frac{R_1}{r}\sigma_i + \left\{ f_t + k_2\left(R_{fr} - \frac{r}{2}\right) + k_3\left(R_{fr}^2 - rR_{fr} + \frac{r^2}{3}\right) + k_{23}\left(R_{fr}^3 - \frac{3}{2}R_{fr}^2 r + R_{fr}r^2 - \frac{r^3}{4}\right)\right\} - \frac{k_4}{r}$$

$$(17.f)$$

where:

$$k_4 = f_t R_1 + k_2 R_1\left(R_{fr} - \frac{1}{2}R_1\right) + k_3 R_1\left(R_{fr}^2 - R_{fr}R_1 + \frac{1}{3}R_1^2\right) + k_{23}R_1\left(R_{fr}^3 - \frac{3}{2}R_{fr}^2 R_1 + R_{fr}R_1^2 - \frac{1}{4}R_1^3\right)$$

$$(17.g)$$

The deformation of the fracture zone in the radial direction is the integration of the radial strain ε_r

from $r = R_1$ to $r = R_{fr}$. Thus, **Eqs. (17.b-17.f)** are used to calculate the deformation of the

fracture zone as shown as:

$$\Delta_{fr}^c = R_1 \frac{\sigma_i}{E_c}\left(\ln\frac{R_{fr}}{R_1}\right) - k_5 \tag{17.h}$$

where:

$$k_5 = \frac{f_t}{E_c}\left(R_{fr} - R_1\right)\left(1 - v_c\right) + \frac{k_2}{E_c}\left\{R_{fr}\left(R_{fr} - R_1\right)\left(1 - v_c\right) - \frac{1}{4}\left(R_{fr}^2 - R_1^2\right)\left(1 - 2v_c\right)\right\}$$

$$+ \frac{k_3}{E_c}\left\{R_{fr}^2\left(R_{fr} - R_1\right)\left(1 - v_c\right) - \frac{1}{2}R_{fr}\left(R_{fr}^2 - R_1^2\right)\left(1 - 2v_c\right) + \frac{1}{9}\left(R_{fr}^3 - R_1^3\right)\left(1 - 3v_c\right)\right\}$$

$$+ \frac{k_{23}}{E_c}\left\{R_{fr}^3\left(R_{fr} - R_1\right)\left(1 - v_c\right) - \frac{3R_{fr}^2}{4}\left(R_{fr}^2 - R_1^2\right)\left(1 - 2v_c\right) + \frac{R_{fr}}{3}\left(R_{fr}^3 - R_1^3\right)\left(1 - 3v_c\right) - \frac{\left(R_{fr}^4 - R_1^4\right)}{16}\left(1 - 4v_c\right)\right\}$$

$$- \frac{k_4}{E_c}\left(\ln\frac{R_{fr}}{R_1}\right)$$

$$(17.i)$$

4.5.3.3.3 Radial displacement of the uncracked zone, $u^c_{R_{fr}}$

The tensile stress σ_θ at the inner surface of the uncracked zone must be taken as the value of rupture strength of concrete f_t. So that, the radial stress at $r = R_{fr}$ can be given by:

$$\sigma_{R_{fr}} = f_t \frac{R_{fr}^2 - R_2^2}{R_{fr}^2 + R_2^2} \tag{18.a}$$

The radial displacement, then, at $r = R_{fr}$ can be calculated using **Eqs. A.2-A.3**.

$$u^c_{R_{fr}} = R_{fr}\varepsilon_{\theta_{fr}} = R_{fr} \frac{\left(f_t - \nu_c \sigma_{R_{fr}}\right)}{E_c} \tag{18.b}$$

where $\varepsilon_{\theta_{fr}}$ = the circumferential strain at $r = R_{fr}$.

4.5.3.4 Contact Pressure, σ_i

Knowing the displacement components of the compatibility **Eq. 13**, the contact pressure at the strand-concrete interface can be developed for the case of cracked analysis as following:

$$\sigma_i = \frac{1}{k_j}\left(\Delta^p_{fp} + k_i - u^c_{R_{fr}} - \Delta^c_{fcz} - \Delta^c_{sh}\right) \tag{19}$$

where:

$$k_6 = \frac{R_1}{E_{pr}}\left(1 - \nu_p\right) + \frac{R_1}{E_c}\left(\ln\frac{R_{cr}}{R_1} + \ln\frac{R_{fr}}{R_{cr}}\right) = R_1\left(\frac{1-\nu_p}{E_{pr}} + \frac{1}{E_c}\ln\frac{R_{fr}}{R_1}\right) \tag{19.a}$$

$$k_7 = \frac{R_1}{E_{pr}}\left(1 - \nu_p\right) + \frac{R_1}{E_c}\left(\ln\frac{R_{cr}}{R_1} + \ln\frac{R_{fr}}{R_1}\right) = R_1\left(\frac{1-\nu_p}{E_{pr}} + \frac{1}{E_c}\ln\left(\frac{R_{cr}R_{fr}}{R_1^2}\right)\right) \tag{19.b}$$

Case A: $k_i = k_1$ and $k_j = k_6$

Case B: $k_i = k_5$ and $k_j = k_7$

97

4.6   ANALYTICAL PREDICTION OF TRANSFER LENGTH

Measuring the transfer length of prestressing strands is time-consuming, and errors from the method of taking the readings and from the instrument calibration can exist. Numerical modeling using the thick-walled cylinder theory is an alternative technique to predict the transfer length and calculate the contact pressures for different fracture zones at the strand-concrete interface. Since the contact pressure σ_i is known, the bond stress τ can be calculated for a particular Δx increment using Coulomb's friction law. **Figure 4-6** shows the stresses on the prestressing strand and the finite-element idealization used in this analysis. The incremental Δx required to transfer an incremental stress Δf_{pxi} to the concrete can be calculated as following:

$$\Delta x = \frac{A_p \Delta f_{pxi}}{\left(\frac{4}{3}\pi d_b\right)\mu\sigma_i} \tag{20}$$

Using a finite-element analysis, this expression can be expressed by:

$$\Delta f_{bi} = k_{bi}\Delta x \tag{21}$$

where A_p = strand area, Δf_{bi} = bond stress around the strand surface.
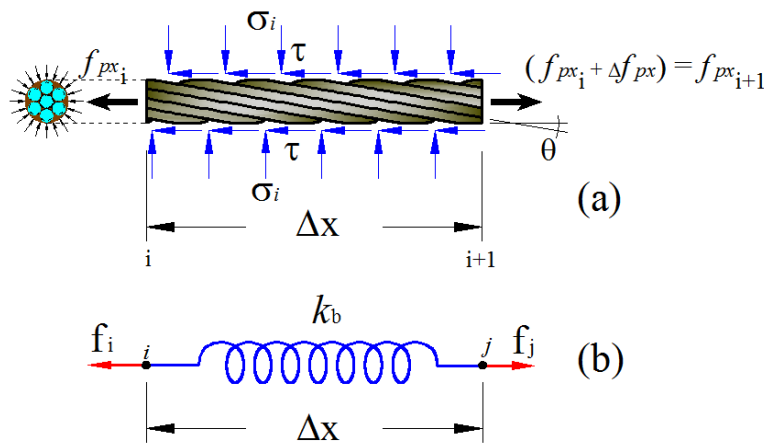
Figure 4-6 – Stresses on the prestressing strand: (a) Discretization of prestressing steel; (b) Finite element idealization for prestressing steel (k_b is the bond stiffness).

98

The bond surface stiffness is represented by $k_{bi} = \lambda_b \left(\frac{4}{3} \pi d_b \right) \mu \sigma_i$. The coefficient λ_b is a bond

factor that depends on strand diameter, number of radial cracks, and twisting angle of helical

wire with respect to the center wire [49], strand surface and mechanical interlocking [50], axial

and helical strain [49, 51], and concrete strength [17, 18]. This study found that the coefficient

λ_b varied from 0.50 to 1.55. As the variation of strand stress is equal to $\Delta f_{pxi} = \Delta f_{bi} / A_p$, the

strand stress at section $i+1$, therefore, is calculated by the relation:

$$f_{px(i+1)} = f_{px(i)} + \Delta f_{pxi} \tag{22}$$

As a result, prestressing force and stress in the concrete at the level of the strand at section $i+1$

are shown in the following equations, respectively:

$$P_{x(i+1)} = A_p f_{px(i+1)} \tag{23}$$

$$f_{cz(i+1)} = P_{x(i+1)} \left(\frac{1}{A_g} + \frac{e_c^2}{I_g} \right) \tag{24}$$

Transfer length, therefore, can be obtained from the summation of the calculated increments of

Δx from the free end of the beam.

4.7 IMPLEMENTATION OF A COMPUTER PROGRAM

Equations presented in previous sections were implemented in a computer program due time

necessary to complete the calculations by hand. Using the computer program, the equations can

be solved in a matter of seconds. **Figure 4-7** shows the major steps of the program that was

developed to calculate the transfer length using the thick-walled cylinder theory. **Table 4-1**

presents the program notation and input data used in the program. The program results are

shown in **Figure 4-8.a.**

99

Numerical modeling of the transfer length in pretensioned concrete members generally consists of two important considerations: the constitutive laws and the finite-element method (FEM). The constitutive laws control the elastoplastic response of the simulated thick-walled concrete cylinder after the strand is released. The compatibility of displacements in the radial direction at the interface of the prestressing steel and the concrete were assumed equal, and from this relationship, the interfacial contact pressure between strand and concrete can be calculated. This calculation is an iterative process, therefore, a numerical procedure to calculate the internal contact pressure and the FEM in one dimension were implemented to calculate the bond, strand stress, prestressing force, and concrete stress at each iteration.
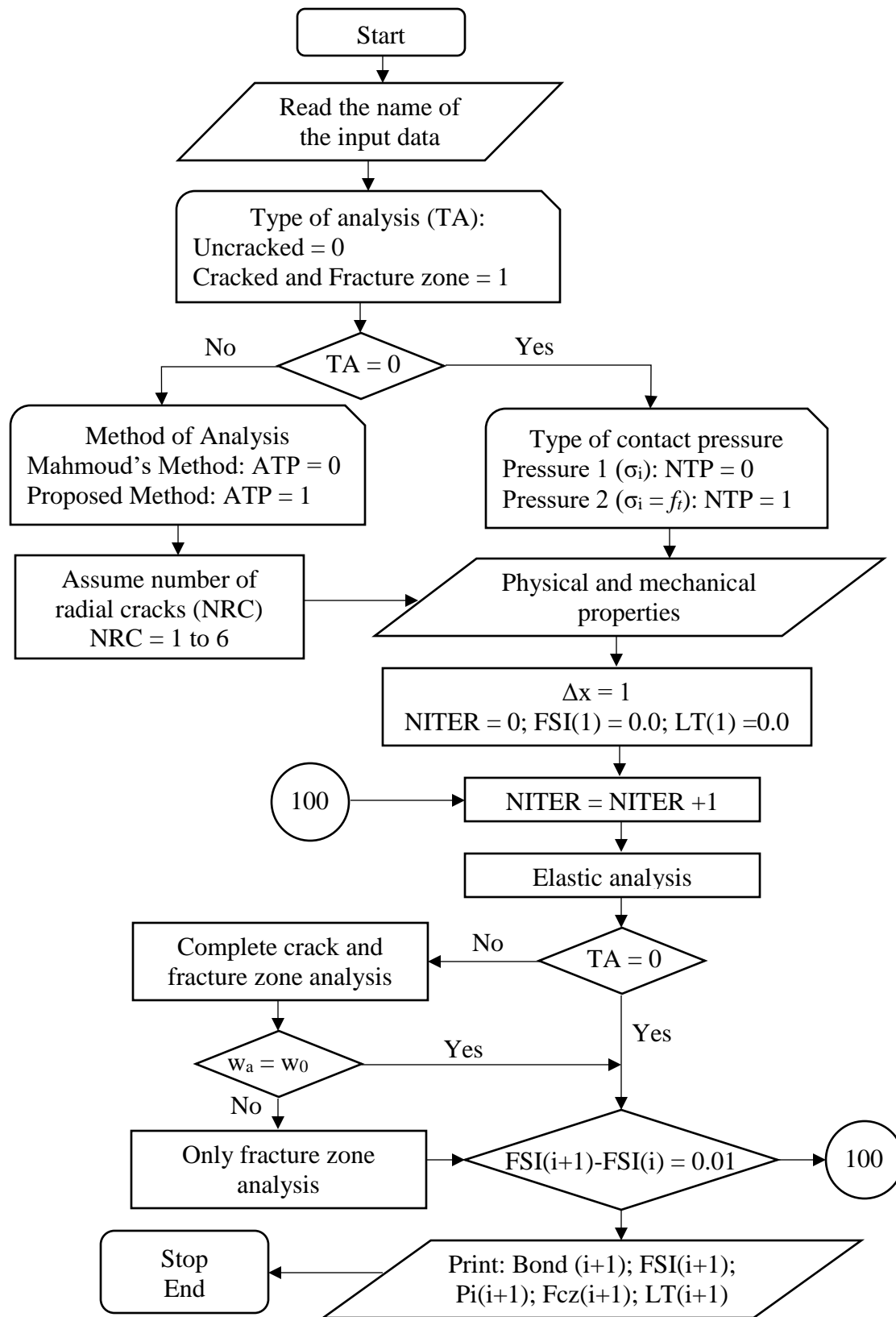
Figure 4-7 – Flowchart of the analytical model.

Table 4-1 –Program notation and input data

Identifier	Definition	Identifier	Definition
NDB	Number of strands	BLNG	Length of the beam
DB	Strand diameter	FRICT	Coefficient of friction
FSI	Initial prestressing stress	W0	Initial crack width
EP	Elastic modulus of strand	NI	Number of iteration
PR_P	Poisson's ratio of strand	HR	Relative humidity
UNIT	Type of analysis (0 for U.S. units and 1 for international units)	TM	Time in days
		TA	Type of analysis
		NRC	Number of radial cracks
FCI	Concrete compressive strength at release	Δx	Incremental of transfer zone
		NITER	Number of iterations
EC	Elastic modulus of concrete	w_a	Crack width
FT	Concrete tension strength	Bond(i+1)	Bond stress at section i+1
PR_C	Poisson's ratio of concrete	FSI(i+1)	Effective stress at section i+1
CX	Concrete cover at x axes	Pi(i+1)	Prestressing force at section i+1
CY	Concrete cover at y axis	Fcz(i+1)	Concrete stress at level of the strand at section i+1
S	Spacing between strands		
B	Width of the beam	LT(i+1)	Transfer length at section i+1
H	Deep of the beam		

Input Data:

Row 1: NDB, DB, FSI, EP, PR_P, UNIT	(Strand Properties)
Row 2: FCI, PR_C	(Concrete Properties)
Row 3: CX, CY, S	(Position of a Strand, see Fig. 10)
Row 4: B, H, BLNG	(Beam Section)
Row 5: FRICT, W0, NI	(Factors for Fracture)
Row 6: HR, TM	(Factors for Shrinkage)

(a)

(b)

Figure 4-8 – (a) Numerical analysis of transfer length using the program TWC_LTDXv1; (b) Mechanical interlocking considered in the analysis.

Another consideration implemented in this program is that the perimeter of a strand is not equal to πd_b, which is for a perfect circle (see **Fig. 4-8.b**). Therefore, the solid cylinder of radius R_1 has been defined from the nominal strand diameter, whereas bond stresses have been computed by considering the actual strand perimeter of $4/3 \, \pi d_b$ (where d_b is the nominal strand diameter). In addition, the clear concrete cover (c_y) and the effective strand cover (c_{eff}, as defined in [7]) were taken from bottom fiber or lateral fiber to the surface of strand as shown in **Figure 4-9**. Also, the bond mechanism was multiplied by a factor (λ_b) which depends on the mechanical interlocking and other factors as explained previously. The mechanical interlocking was idealized as a constant normal pressure around the strand (**Figure 4-8.b**). Transfer length is calculated through an iterative process. At each iteration, corresponding to a certain length, a contact pressure is calculated in order to calculate the bond stress, the strand stress, and the concrete stress at this length. Having these values, concrete and strand strains can be calculated.
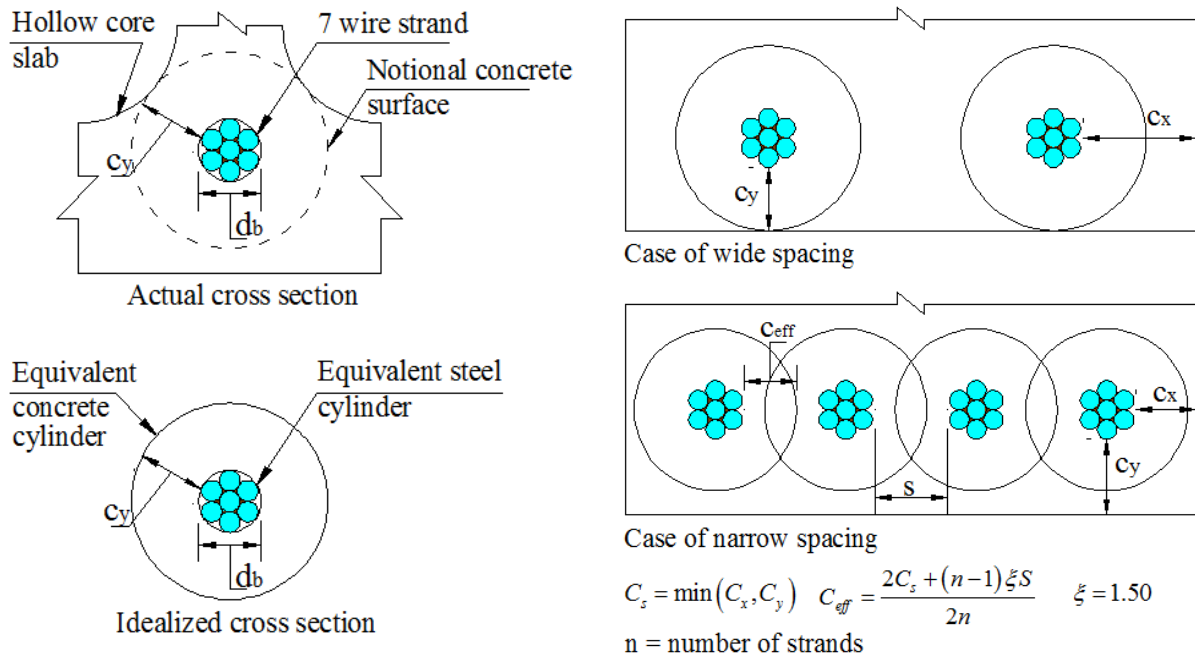
Figure 4-9 – Idealization of the thick-walled cylinder.

4.8   MODEL VALIDATION

4.8.1   Numerical example

A data set of 24 beams obtained through experimental investigations conducted by several

researchers is summarized in **Table 4-2** [2, 4, 5, 8, 14, 15, 17, 18, 30, 51-54]. This table also

includes the input data for the developed computer program. For the pure-elastic analysis,

variables needed for the input data were taken from Mahmoud [30] and Weerasekera [28] as

follows: strand diameter d_b = 12.7 mm, initial prestress f_{si} = 1300 MPa, elastic modulus of the

strand E_p = 200 GPa, Poisson's ratio for strand v_p = 0.30, concrete strength at release f'_{ci} = 30

MPa, Poisson's ratio for concrete v_c = 0.15, concrete cover c_y = 46.35 mm, and beam cross

section of 100 x 200 mm. The distributions of radial and hoop stress at the free end of the beam

are obtained using **Eq. 18** and shown in **Figure 4-10.a**. This figure shows that the tensile stress

near the strand and along the circumferential direction is approximately 11 times greater than the

concrete's tensile strength at release while the radial stress is approximately 2.2 times greater

than the concrete's compressive strength at release. However, cracking in the concrete around

the strand occurs after release, which required a more refined analysis, was implemented in this

investigation as shown in **Figure 4-10.b**. This figure shows the three zones considered in this

investigation for the case of specimen SS160-6 (see **Table 4-2**). The result presented from this

figure is calculated at station 200 (a distance of 199 mm from the free end), which gives the

effective strand stress of 502.1 MPa. The station represents the number of iterations in the

program and for this example the increment is 1 mm. At this station, the cracked zone, fracture

zone, and uncracked zone are shown. The cracked zone is where the hoop stress is zero, the

fracture zone is where the hoop stress is increasing from zero to the concrete's tensile strength at

release, and the uncracked zone is where the hoop stress begins to decrease from the allowable

105

tensile strength at release. Although this analysis may be complicated for beams with several

strands, this analysis was simplified using the idealization of thick-walled cylinder (see **Fig. 4-9**).

For instance, the stress presented in the overlapped region, which is the case for narrow strand

spacing, was not considered in this analysis. This region was treated as a simple, thick-walled

cylinder with an effective thickness as shown in **Figure 4-9**.

Table 4-2 – Input data used in the program

Beam	f'_{ci}, MPa	E_c, GPa	v_c	C_{eff}, mm	μ	f_{pi}, MPa	E_p, GPa	d_b, mm	A_s, mm^2	Number of strands
SS150-4 [52]	26.0	22.9	0.20	63.50	0.45	1299.0	194.4	12.7	99.0	1
13/31-1200 [5]	21.0	20.6	0.20	50.00	0.55	1442.0	204.9	12.7	99.0	1
13/75-950 [5]	50.0	31.8	0.20	50.00	0.50	1367.0	204.9	12.7	99.0	1
BS5 [30, 53]	35.0	26.6	0.15	50.00	0.75	1227.6	200.0	12.7	99.0	1
M12-N-C3-1&2 [4, 54]	33.6	26.1	0.20	36.35	0.40	1402.1	200.0	12.7	99.0	1
N-12-5 [18, 54]	35.0	26.6	0.15	56.35	0.50	1210.0	200.0	12.7	99.0	1
C350/0.50 [2, 8, 14, 15]	26.1	23.0	0.20	50.00	0.60	1326.0	192.6	13.0	99.7	1
C350/0.40 [2, 8, 14, 15]	46.7	30.8	0.20	50.00	0.60	1328.0	192.6	13.0	99.7	1
C400/0.50 [2, 8, 14, 15]	24.2	22.1	0.20	50.00	0.60	1303.0	192.6	13.0	99.7	1
C500/0.30 [2, 8, 14, 15]	54.8	33.3	0.20	50.00	0.60	1295.0	192.6	13.0	99.7	1
SS160-6 [52]	28.9	24.2	0.20	63.50	0.45	1287.0	194.4	15.2	140.0	1
S1 [17, 51]	45.0	30.2	0.20	75.00	0.45	1347.5	200.0	15.2	140.0	1
M15-N-C4-1&2 [4, 54]	33.6	26.1	0.20	47.60	0.40	1392.5	200.0	15.2	140.0	1
N-15-5 [18, 54]	35.0	26.6	0.15	57.20	0.50	1210.0	200.0	15.2	140.0	1
16/31-1865 [5]	21.0	20.6	0.20	50.00	0.60	1286.0	204.9	15.7	146.4	1
16/65-1150 [5]	48.0	31.2	0.20	50.00	0.60	1218.0	204.9	15.7	146.4	1
T12-N-S3 [4, 54]	34.0	26.2	0.20	42.46	0.40	1398.4	200.0	12.7	99.0	2
T15-N-S3 [4, 54]	37.6	27.6	0.20	45.90	0.40	1357.4	200.0	15.2	140.0	2
NSC-I-01 (*)	38.8	28.0	0.15	44.63	0.45	1396.6	204.8	15.2	140.0	2
NSC-I-03 (*)	26.8	23.3	0.15	44.63	0.45	1396.6	204.8	15.2	140.0	2
NSC-I-07 (*)	64.8	36.2	0.15	44.63	0.45	1396.6	204.8	15.2	140.0	2
NSC-II-01 (*)	29.0	24.2	0.15	44.63	0.50	1396.6	199.9	15.2	140.0	2
NSC-II-08 (*)	30.7	24.9	0.15	44.63	0.50	1396.6	199.9	15.2	140.0	2
NSC-II-12 (*)	48.8	31.4	0.15	44.63	0.50	1396.6	199.9	15.2	140.0	2

(*) experimental program performed at the University of Arkansas to validate the analytical
method

106
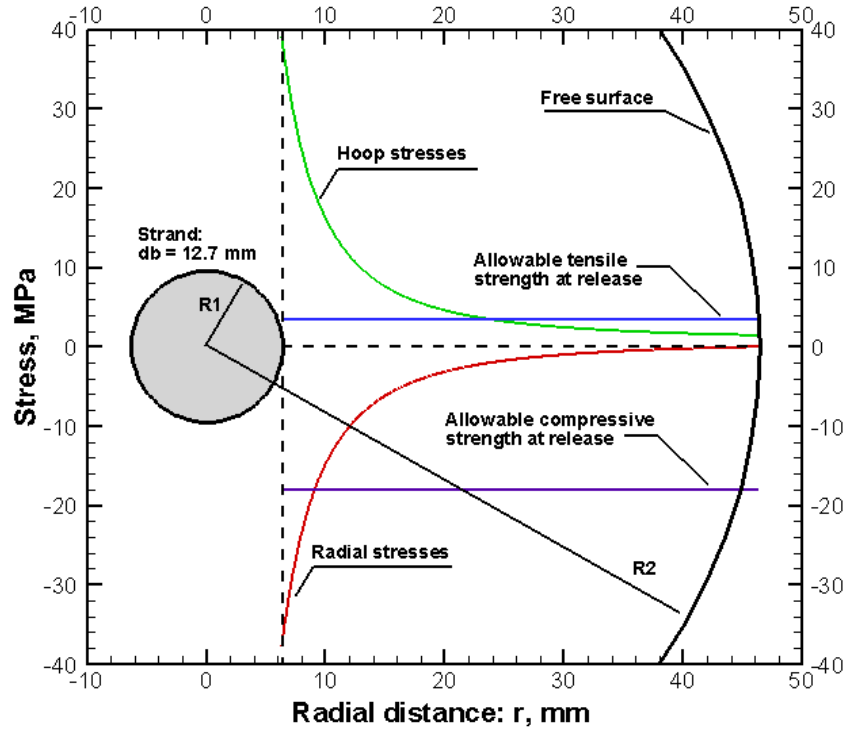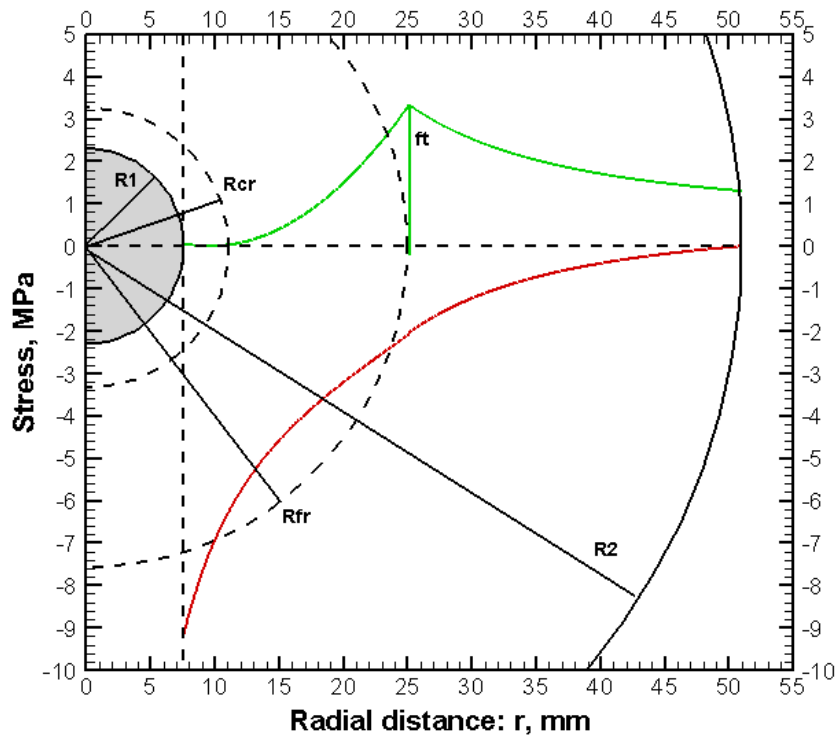
Figure 4-10 – Transverse stress distribution: (a) Isotropic elastic analysis at station 1 (free end); (b) Anisotropic and isotropic analysis at fracture zone at station 200 (a distance of 199 mm of the free end) and at effective stress of 502.1 MPa (specimen SS160-6).

107

4.8.2 Transfer length comparison from measured and numerical analysis

Table 4-3 compares the experimental and numerical results. The numerical results presented in this table are plotted in **Figure 4-11.a-b.**

Table 4-3 – Transfer length comparison between experimental and numerical results

Specimen	Beam Section b x h x L, mm	Transfer length L_t, mm		
		Measured	Mahmoud's Method (2nd order)	Proposed Method (3rd order)
SS150-4 [52]	102x127x3668	737	738	771
13/31-1200 [5]	150x225x1200	710	729	772
13/75-950 [5]	100x200x950	405	466	490
BS5 [30, 53]	100x250x1900	550	557	588
M12-N-C3-1&2 [4, 54]	112.7x200x3000	851	857	894
N-12-5 [18, 54]	112.7x112.7x1900	617	639	652
C350/0.50 [2, 8, 14, 15]	100x100x2000	550	626	651
C350/0.40 [2, 8, 14, 15]	100x100x2000	550	557	497
C400/0.50 [2, 8, 14, 15]	100x100x2000	650	657	682
C500/0.30 [2, 8, 14, 15]	100x100x2000	400	421	394
SS160-6 [52]	102x127x3668	762	778	808
S1 [17, 51]	150x150x3000	1092	1047	1062
M15-N-C4-1&2 [4, 54]	115.2x200x3000	839	870	903
N-15-5 [18, 54]	115.2x115.2x1900	727	749	715
16/31-1865 [5]	200x250x1865	872	848	896
16/65-1150 [5]	200x250x1150	427	486	435
T12-N-S3 [4, 54]	150.8x200x3000	808	806	840
T15-N-S3 [4, 54]	160.8x200x3000	997	998	1030
NSC-I-01 (*)	165x305x5500	709	655	686
NSC-I-03 (*)	165x305x5500	830	867	903
NSC-I-07 (*)	165x305x5500	565	554	581
NSC-II-01 (*)	165x305x5500	768	834	739
NSC-II-08 (*)	165x305x5500	816	799	834
NSC-II-12 (*)	165x305x5500	612	584	612

(*) experimental program performed at the University of Arkansas to validate the analytical method

These figures show scattered data around the mean values because this analysis was not refined as needed. However, the figures show affirmations from other researchers in this matter [18, 54]. For instance, the linear analysis shows that the transfer length decreases when the coefficient of friction and concrete cover increase.
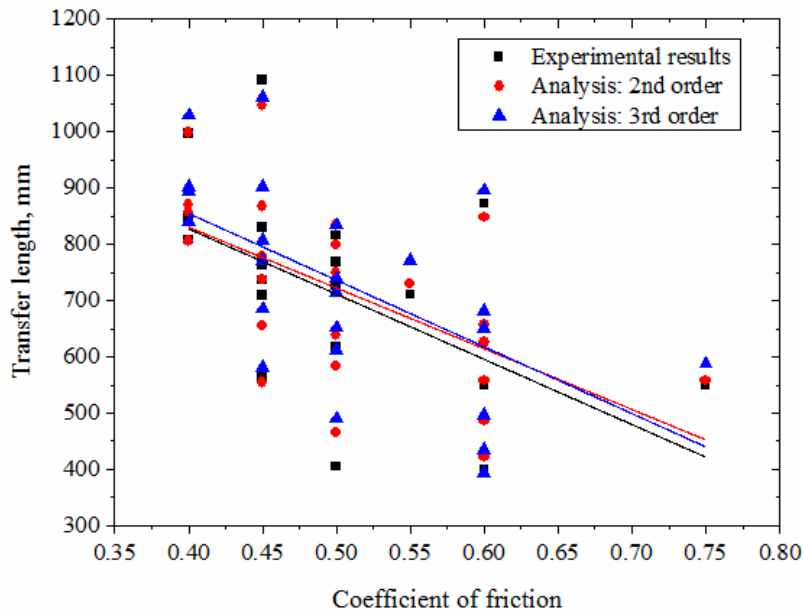
(a) Coefficient of friction against transfer length
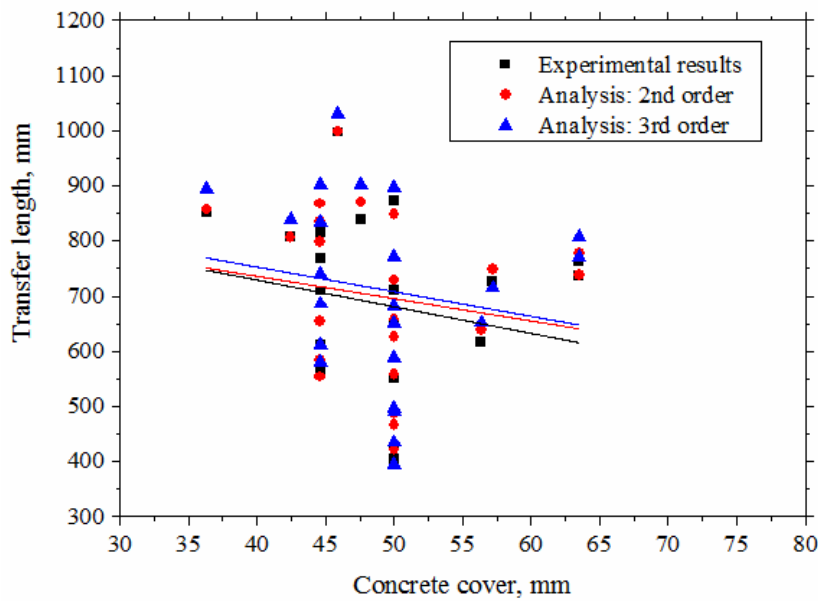
(b) Concrete cover against transfer length

Figure 4-11 – Correlation of between coefficient of friction and concrete cover with transfer length.

109

Additionally, Lim et al. [18] affirmed that the transfer length decreases not only with increasing concrete strength but also with increasing concrete cover [54]. If transfer length decreases when the coefficient of friction increases, this coefficient can be proportional to the concrete strength. In other words, the coefficient of friction is high for high-strength concrete. Therefore, the bond between strand and high-strength concrete is greater than that of low-strength concrete. The trend lines of experimental and proposed method (3rd order) are parallel while the trend line of Mahmoud´s method (2nd order) presents a different slope than others. This is a result of the higher order equation for modeling transfer length using the thick-walled cylinder model.

Figure 4-12 provides a comparison of transfer length for mono strand series, which are strand diameters of 12.7 mm and 13 mm (**Figure 4-12.a**) and strand diameters of 15.2 mm and 15.7 mm (**Figure 4-12.b**). **Figure 4-12.a** includes six results for strand diameter 12.7 mm and four results from strand diameter 13 mm. The upper and lower calculated values using the proposed method are 21% greater than the measured value for specimen 13/75-950 and 10% less than the measured value for specimen C350/0.40, respectively. On the other hand, **Figure 4-12.b** shows the four results for 15.2 mm strand and two results for the 15.7 mm. The upper and lower given values by the proposed method are 8% greater than the measured value for specimen M15-N-C4-1&2 and 3% less than the measured values for specimen S1, respectively. In addition, **Figure 4-13** provides a comparison of transfer length for eight specimens that contained two strands. The strand diameter was either 12.7 mm or 15.2 mm. The upper and lower values are 9% greater than the measured value for specimen NSC-I-03 and 4% less than the measured value for specimen NSC-II-01, respectively.

110
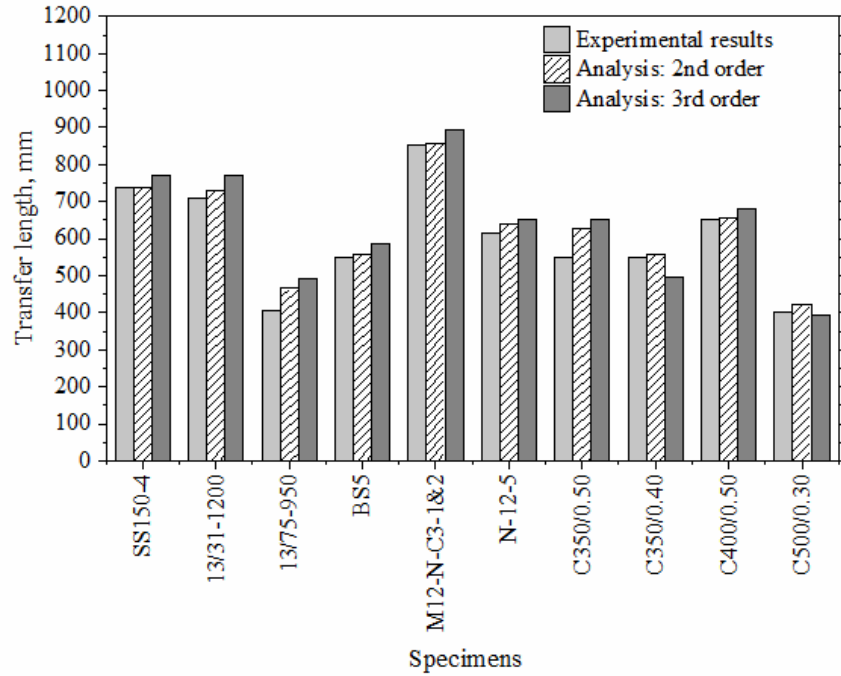
(a) Strand diameter 12.7 mm and 13 mm
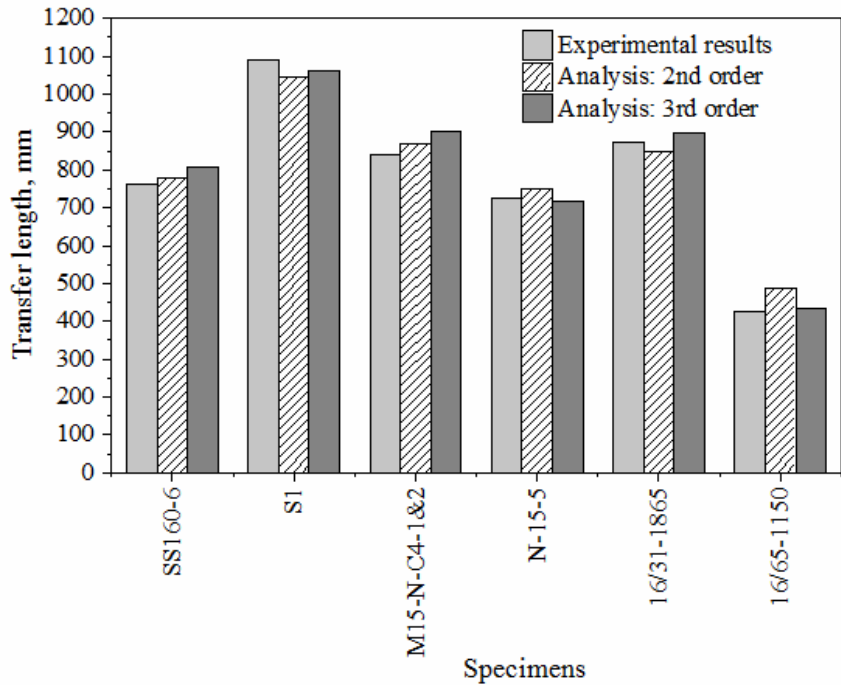
(b) Strand diameter 15.2 mm and 15.7 mm

Figure 4-12 – Transfer length comparison between measured and calculated for mono strand test series.
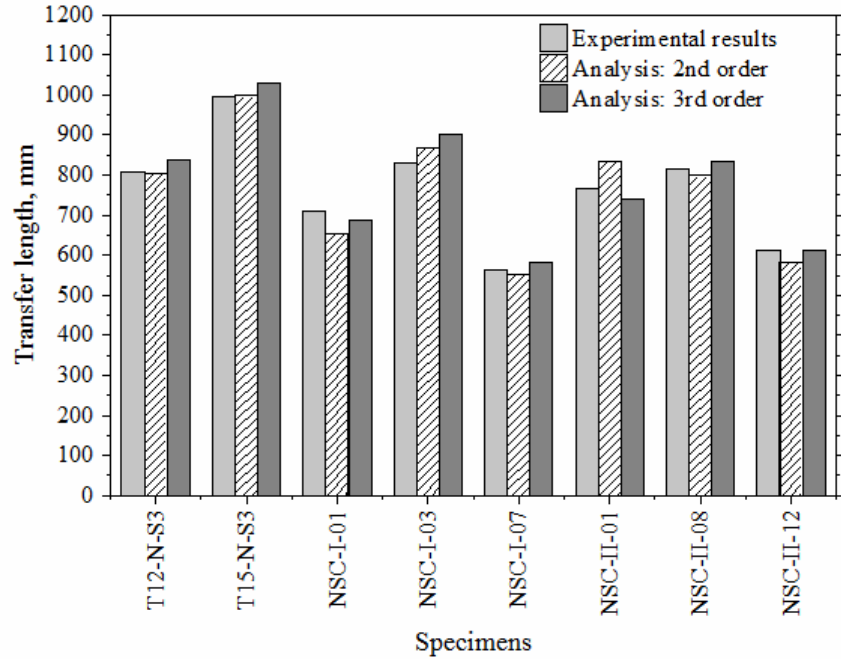
Figure 4-13 – Transfer length comparison between measured and calculated for twin strand test series.

The concrete strain profile along the beam can be obtained using this program, as shown in **Figure 4-14.a**, and can be compared with the experimental concrete strain measurements as shown in **Figure 4-14.b**. The figures summarize the concrete strains for specimen NSC-II-12 along with the measured transfer lengths and the transfer lengths calculated using the 2nd order and 3rd order numerical analysis. In this analysis, the measured transfer length and the transfer length calculated using the 3rd order method are the same as the 95% average maximum strain (AMS) trend line. In addition to this analysis, the concrete and strand stress distribution along the beam are plotted in **Figure 4-15**. The intersection between the 95% AMS trend line and the linear trend line gives the transfer length for 95% AMS, which is 612 mm as shown in **Figure 4-15.a**.
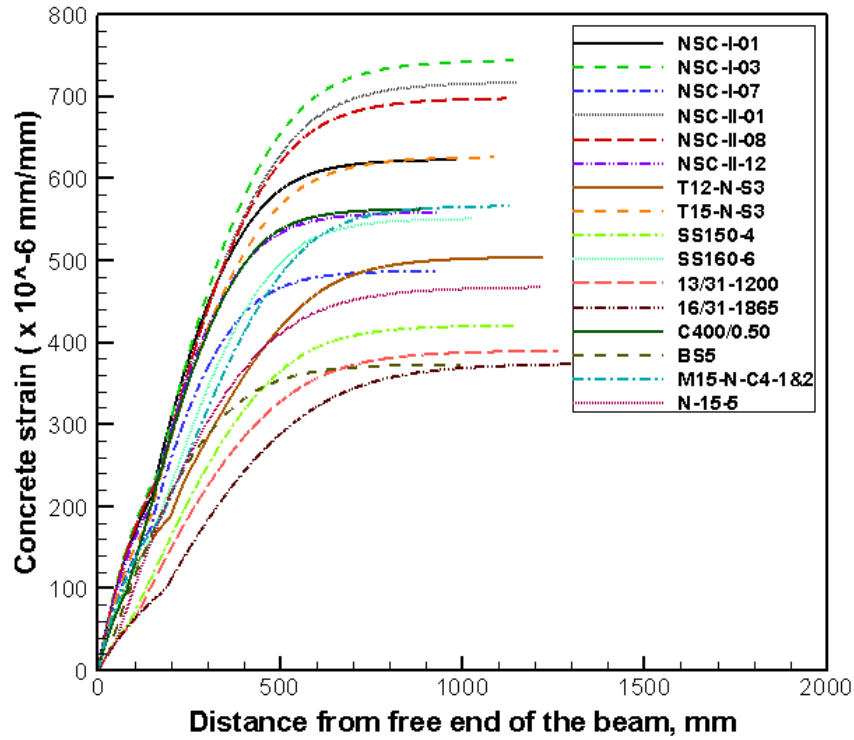
(a)
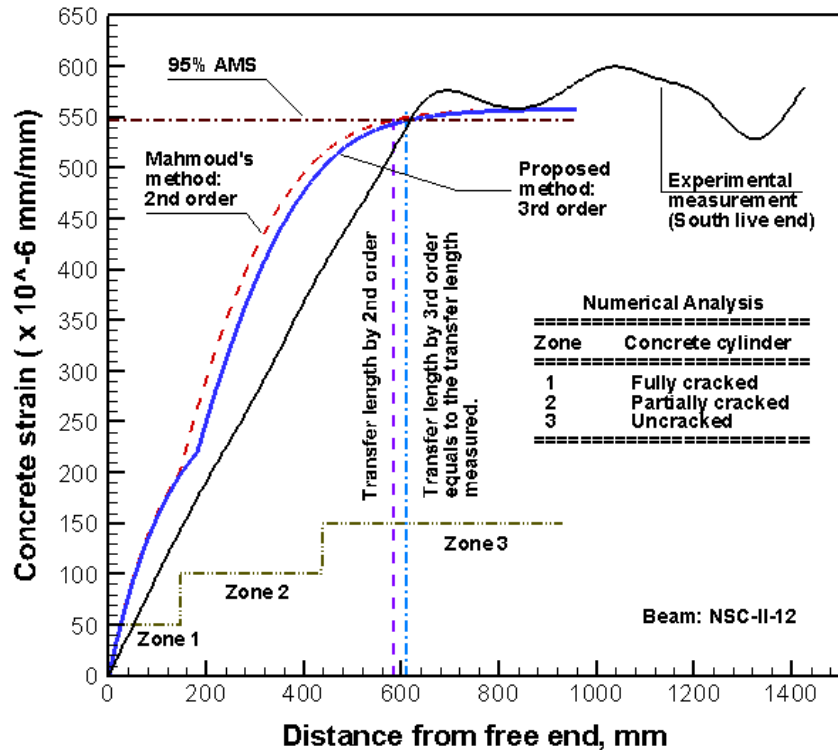
(b)

Figure 4-14 – Concrete strain distribution: (a) From the numerical analysis; (b) Comparison between numerical analysis and experimental measurement using DEMEC gauges (specimen NSC-II-12).

113

Figure 4-15.b shows three zones, and each zone presents a different type of analysis as following: Zone 1 requires a nonlinear analysis, and a specimen in this zone is at the fully cracked condition along the 180 mm. The cracking is due the hoop stress along this length being greater than allowable tensile strength. Zone 2 is known as partially cracked zone and requires linear and nonlinear analysis, and along this 305 mm, a specimen presents visible and microscopic cracks. Zone 3 is known as the uncracked zone. This zone only requires a linear analysis because the hoop stress is less than allowable tensile strength, and the transfer length is found within this length (475 mm). All zones are shown in **Figure 4-10.b** and **Figure 4-14.b**. In summary, it is expected that the use of the 3rd order equation provides a better prediction of the measured transfer lengths when compared to the 2nd order equation. The predicted values presented in **Table 4-3** are greater than or equal to the measured values. These results could be related to the drastic change from zone 1 to zone 2 as shown in **Figure 4-14.b** while the 2nd order equation did not present this issue. The consideration of additional variables into the analysis, typically including drying shrinkage coefficient and bond surface stiffness, possibly contributes to the over-estimation of the predicted values. Further studies are needed to investigate this issue.

114
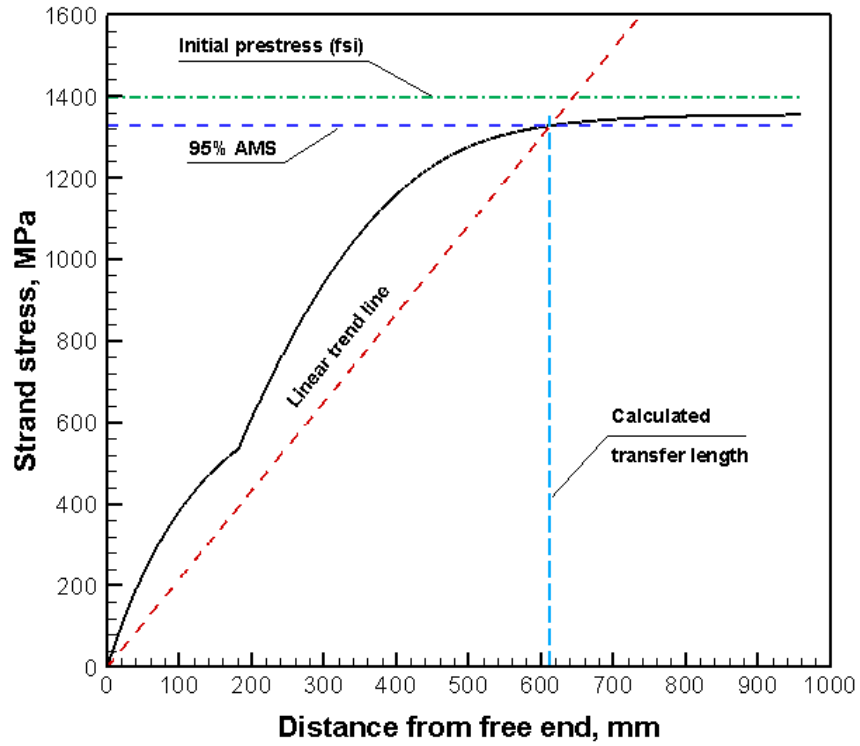
(a)
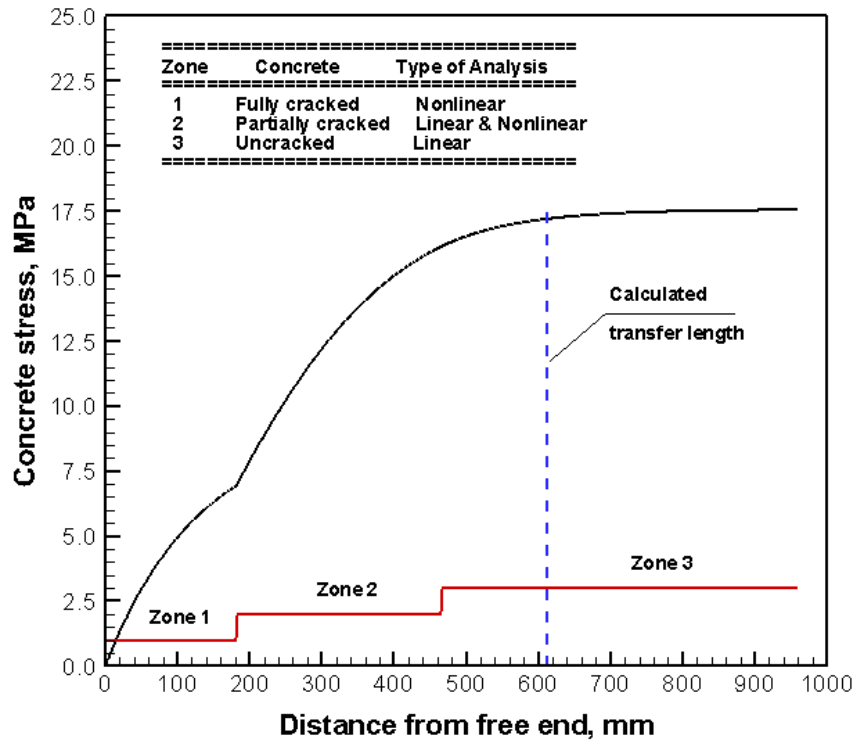
(b)

Figure 4-15 – Stress distribution along the beam NSC-II-12 using the proposed method: (a) Strand stress and transfer length calculation; (b) Concrete stress and zones of analysis.

115

4.9   SUMMARY AND CONCLUSIONS

This paper develops a computer program using the thick-walled cylinder theory to model strand bond in pretensioned concrete beams. An expression between post-peak and crack width proposed by Mahmoud in 1997 has been upgraded from a second-order to the third-order equation because the hoop stress is related to the post-peak stress. Hoop stress is an important key in this matter and affects the crack and fracture zone because of the contact pressure between strand and concrete, which have been analyzed in this investigation. A data set of 24 transfer lengths collected from the literature was used to validate the program. This data set consists of various pretensioned concrete beams that were cast with one strand or two prestressing strands. The beams with one strand were cast using 12.7 mm, 13 mm, 15.2 mm, and 15.7 mm diameter strands while beams with two strands were cast using 12.7 mm and 15.2 mm diameter strands. The developed computer program can be used to improve the accuracy in predicting the transfer length by considering the number of cracks, concrete cover, fracture criteria, and elastic analysis. Based on the investigation, the following conclusions can be drawn:

1.   Using the thick-walled cylinder theory with the third-order equation (proposed in this investigation), the predicted transfer length for all specimens with one strand, including 12.7 or 13 mm diameter strands, are between 90% and 121% of the measured values. The predicted transfer lengths using the second-order equation ranged from 100% to 114% when compared to the measured values. The predicted transfer lengths for specimens with one, 15.2 mm strand ranged from 97% to 108% of the measured values while the predicted transfer lengths due to second-order equation ranged from 96% to 114%. The predicted transfer length for specimens with two strands (either 12.7 mm or 15.7 mm) ranged from 96% and 109 % while the predicted transfer lengths using the second-order equation are in

116

the range of 92% and 109%. The results show that the third-order equation provides a reasonable transfer length estimate when compared to the second-order equation for beams containing either one 15.2 mm strand or two strands of either diameter.

2. Transfer length is directly related to the bond between the strand and concrete. The strand bond can be modeled using the Coulomb's friction law and depends on several variables, including the coefficient of friction, bond factor, strand diameter, strand surface, internal pressure, and concrete strength.

3. The complexity of the proposed equations to completely and partially model the concrete cracking most likely results in the difference in the predicted and the measured transfer lengths, which varies between 94% and 121%. This increment of 21% of transfer length could be associated with (1) the variation in concrete strains between zone 1 and zone 2, which is attributed to the post-peak and crack-width relationship, and (2) the bond surface stiffness, which is directly proportional to the transfer length.

4. Concrete strength, coefficient of friction, and concrete cover influence transfer length. The results shown in Tables 1 and 2 indicate that transfer length decreases when these variables increase.

5. The presence of the enhanced variables, including the bond surface stiffness and bond factor coefficient, can provide a better prediction of transfer length. However, additional research is need to calibrate these parameters with experimental data because these parameters are directly proportional to the transfer length of prestressing strands.

117

ACKNOWLEDGEMENT

118

NOTATION

A_s nominal strand area

A_b nominal area of strand

A_g cross section area of concrete member

A_p total area of strand

A_c cross sectional area of concrete

c_y clear concrete cover

d_b strand diameter

e_c eccentricity of the prestress force

E elastic modulus of element

E_c elastic modulus of concrete

E_p elastic modulus of strand

E_{pr} elastic modulus of strand in the transversal direction

f_{si} initial prestress in strand

f_{se} effective prestress in strand after losses

f'_{ci} concrete's compressive strength at release of strand

f'_c concrete's compressive strength

f_t concrete's tensile strength

f_{cz} concrete compressive stress due to effective prestress

f_{pu} ultimate tensile strength

f_{py} yield strength

f_{pi} initial prestressing stress

I_g moment of inertia of concrete section

119

ν Poisson's ratio of element

ν_p Poisson's ratio of strand

ν_c Poisson's ratio of concrete

$\eta = E_p / E_c$ modular ratio

n integer number (2 for second-order equation and 3 for third-order equation)

λ_b bond factor

λ_{sp} strand perimeter factor (1 is for solid strand and 4/3 for strand seven wire)

λ_{uscE} factor of unit system conversion for elastic modulus

λ_{uscT} factor of unit system conversion for tensile strength

L_t transfer length of prestressing steel in pretensioned concrete members

w unit weight of concrete

μ coefficient of friction between prestressing steel and concrete

σ_i interface pressure

σ_r radial stress at concrete and strand interface

σ_θ hoop stress

σ_z longitudinal stress

ε_r radial strain

ε_θ hoop strain

ε_z longitudinal strain

ε_{sh} drying shrinkage coefficient

K_f constant factor

k_t radial stress

120

k_{ii} constant factor (ii = 1,2,3,..,7)

k_{bi} bond surface stiffness

r_p nominal radius of strand

$r_{c,1}$ internal radius of concrete cylinder which equals to radius of strand after prestressing

$r_{c,2}$ external radius of concrete cylinder

r radius in the radial direction

R_1 inner radius

R_2 outer radius

R_{cr} crack radius

R_{fr} fracture radius

τ bond stress

(r, θ, z) polar coordinates stresses

(u, v, w) polar coordinates displacements

Δ_{fp}^{p} increase in radius of strand due to reduction in longitudinal stress from initial prestress f_{si}

            to effective prestress f_{se}

$\Delta_{\sigma i}^{p}$ reduction in radius of strand due to the uniform radial compression at interface σ_i

$\Delta_{\sigma i}^{c}$ increase in inner radius of the thick-walled concrete cylinder due to the interface pressure

            σ_i

Δ_{fcz}^{c} increase in inner radius of the thick-walled concrete cylinder due to the longitudinal

            compressive stress at the level of strand f_{cz}

Δ_{sh}^{c} reduction in inner radius of the thick-walled concrete cylinder due to drying shrinkage ε_{sh}

Δ_{cr}^{c} deformation of the real crack zone

121

Δ_{fr}^{c} deformation of the fracture zone

$u_{R_{fr}}^{c}$ radial displacement at $r = R_{fr}$

Δx incremental of transfer zone

Δf_{bi} bond force around the strand surface

Δf_{pxi} strand stress incremental

w_{cr} crack width at any point

w_{a} crack width

w_{o} initial crack width at the shear plane

122

APPENDIX A

This section presents procedures to solve the thick-walled cylinder equations, and the governing equation of the thick-walled cylinders can be derived from **Figure 4-1.b**. The stresses σ_r and σ_θ are only functions of *r* and the shear stress on the element must be zero. By solving the radial force equilibrium shown in **Figure 4-1.b** and ignoring second-order terms, a governing equation is given by [42, 43]:

$$\frac{d\sigma_r}{dr} + \frac{\sigma_r - \sigma_\theta}{r} = 0 \tag{A.1}$$

where σ_r = normal stress in radial direction; σ_θ = hoop stress in the circumferential direction; *r* = radius in the radial direction.

Stresses and displacements represented in the polar coordinates as (r, θ, z) and (u, v, w) are shown in **Figure 4-1.b-c**, respectively. The ends of the cylinder are assumed to be open and unconstrained ($\sigma_z = 0$). The cylinder is in a condition of plane stress, and Hooke's law used in elastic and plastic analysis offers the strains given as following:

$$
\begin{aligned}
\varepsilon_r &= \frac{1}{E}\left[\sigma_r - \nu\left(\sigma_\theta + \sigma_z\right)\right] \\
\varepsilon_\theta &= \frac{1}{E}\left[\sigma_\theta - \nu\left(\sigma_r + \sigma_z\right)\right] \\
\varepsilon_z &= \frac{1}{E}\left[\sigma_z - \nu\left(\sigma_r + \sigma_\theta\right)\right]
\end{aligned}
\tag{A.2}
$$

where ε_r = radial strain; ε_θ = hoop strain; ε_z = longitudinal strain; σ_r = radial stress at concrete and strand interface; σ_θ = hoop stress; σ_z = longitudinal stress; and ν = Poisson's ratio.

Strain-displacement compatibility equation derived from **Figure 4-1.c** is defined as:

123

$$\varepsilon_r = \frac{\partial u}{\partial r} \qquad \varepsilon_\theta = \frac{u}{r} \qquad \varepsilon_z = \frac{\partial w}{\partial z} \tag{A.3}$$

Using the compatibility equations and Hook's law are sufficient to obtain a unique solution to any axisymmetric problem with specific boundary conditions [42, 43]. Thus, **Eq. (A.1)** can be rewritten as following:

$$\frac{\partial^2 u}{\partial r^2} + \frac{1}{r}\frac{du}{dr} - \frac{u}{r^2} = 0 \tag{A.4}$$

A general solution to this differential equation is given by:

$$u = C_1 r + \frac{C_2}{r} \tag{A.5}$$

$$\frac{\partial u}{\partial r} = \varepsilon_r = C_1 - \frac{C_2}{r^2} \tag{A.6}$$

$$\frac{u}{r} = \varepsilon_\theta = C_1 + \frac{C_2}{r^2} \tag{A.7}$$

Subtracting **Eq. (A.6)** and **Eq. (A.7)**, σ_θ is obtained in a function of C_2 and σ_r:

$$\sigma_\theta = \frac{2EC_2}{r^2(1+v)} + \sigma_r \tag{A.8}$$

This equation is substituted into **Eq. (A.7)**, and σ_r is represented by:

$$\sigma_r = \frac{E}{1-v}C_1 - \frac{E}{r^2(1+v)}C_2 + \frac{v\sigma_z}{1-v} \tag{A.9}$$

where C_1 and C_2 are constants of integration and their values can be obtained using **Eq. (A.9)**; σ_r = radial stress; E = elastic modulus of element; v = Poisson's ratio; and r = radius in the radial direction.

To find C_1 and C_2, two boundary conditions were used: (1) at the inner radius: $r = R_1$ and $\sigma_r = -\sigma_i$; and (2) at the outer radius: $r = R_2$ and $\sigma_r = 0$.

124

$$-\sigma_i = \frac{E}{1-\nu}C_1 - \frac{E}{R_1^2(1+\nu)}C_2 + \frac{\nu\sigma_z}{1-\nu} \tag{A.10}$$

$$0 = \frac{E}{1-\nu}C_1 - \frac{E}{R_2^2(1+\nu)}C_2 + \frac{\nu\sigma_z}{1-\nu} \tag{A.11}$$

Subtracting **Eq. (A.10)** and **Eq. (A.11)**, C_2 is given below:

$$C_2 = \frac{R_1^2 R_2^2 (1+\nu)}{E\left(R_2^2 - R_1^2\right)}\sigma_i \tag{A.12}$$

Then C_1 shown below is obtained by replacing **Eq. (A.12)** into **Eq. (A.11)**:

$$C_1 = \frac{R_1^2(1-\nu)}{E\left(R_2^2 - R_1^2\right)}\sigma_i - \frac{\nu}{E}\sigma_z \tag{A.13}$$

Replacing C_1 and C_2 in **Eq. (A.9)**, **Eq. (A.8)**, and **Eq. (A.5)**, the radial stress (σ_r), hoop stress (σ_θ), and radial displacement (u) written in **Eq. (A.14-16)** were derived, respectively, and the longitudinal stress (σ_z) was replaced by the concrete compressive stress due to the effective prestress (f_{cz}).

$$\sigma_r = \sigma_i \frac{R_1^2}{R_2^2 - R_1^2}\left(1 - \frac{R_2^2}{r^2}\right) \tag{A.14}$$

$$\sigma_\theta = \sigma_i \frac{R_1^2}{R_2^2 - R_1^2}\left(1 + \frac{R_2^2}{r^2}\right) \tag{A.15}$$

$$u = \sigma_i \frac{R_1^2 r}{E_c\left(R_2^2 - R_1^2\right)}\left[(1-\nu_c) + (1+\nu_c)\frac{R_2^2}{r^2}\right] - \frac{\nu_c f_{cz} r}{E_c} \tag{A.16}$$

where R_1 = inner radius; R_2 = outer radius; σ_i : interface pressure; E_c = elastic modulus of concrete; ν_c = Poisson's ratio of concrete; and r = radius in the radial direction.

125

APPENDIX B

This section presents procedures to solve the uncracked equation as shown in **Eq. (8)** which was widely explained by Mahmoud [30], and an equation to solve this relationship as shown in **Eq. (9)** is explained below by the following procedures:

Each of the following parameters described in **Eq. (8)** can be expressed in **Eq. (B.1-5)**.

$$\Delta_{fp}^{p} = \frac{v_p \left(f_{si} - f_{se} \right)}{E_p} R_1 \tag{B.1}$$

$$\Delta_{\sigma i}^{p} = -\frac{\sigma_i \left(1 - v_p \right)}{E_{pr}} R_1 \tag{B.2}$$

$$\Delta_{\sigma i}^{c} = \frac{\sigma_i R_1}{E_c} \frac{\left[\left(1 - v_c \right) R_1^2 + \left(1 + v_c \right) R_2^2 \right]}{\left(R_2^2 - R_1^2 \right)} \tag{B.3}$$

$$\Delta_{fcz}^{c} = \frac{v_c f_{cz}}{E_c} R_1 \tag{B.4}$$

$$\Delta_{sh}^{c} = \varepsilon_{sh} R_1 \tag{B.5}$$

Substituting **Eqs. (B.1-5)** into **Eq. (8)**, the interfacial pressure (σ_i) is shown below:

$$\sigma_i = \frac{\dfrac{\left(f_{si} - f_{se} \right)}{E_p} v_p - \dfrac{f_{cz}}{E_c} v_c - \varepsilon_{sh}}{\dfrac{\left(1 - v_p \right)}{E_{pr}} + \dfrac{K_c}{E_c}} \tag{B.6}$$

126

REFERENCES

[1] Dang CN, Murray CD, Floyd RW, Hale WM, Martí-Vargas JR. Analysis of bond stress distribution for prestressing strand by Standard Test for Strand Bond. Engineering Structures. 2014;72:152-9.

[2] Martí-Vargas JR, Serna P, Navarro-Gregori J, Pallarés L. Bond of 13 mm prestressing steel strands in pretensioned concrete members. Engineering Structures. 2012;41:403-12.

[3] Dang CN, Floyd RW, Murray CD, Hale WM, Martí-Vargas JR. Bond Stress-Slip Model for 0.6 in. (15.2 mm) Diameter Strand. ACI Structural Journal. 2015;112:625-34.

[4] Oh BH, Kim ES. Realistic Evaluation of Transfer Lengths in Pretensioned, Prestressed Concrete Members. ACI Structural Journal. 2000;97:821-30.

[5] Mitchell D, Cook WD, Khan AA, Tham T. Influence of high strength concrete on transfer and development length of pretensioning strand. PCI Journal. 1993;38:52-66.

[6] Oh BH, Kim ES, Choi YC. Theoretical Analysis of Transfer Lengths in Pretensioned Prestressed Concrete Members. Journal of Engineering Mechanics. 2006;132:1057-66.

[7] Den Uijl JA. Bond Modelling of Prestressing Strand. ACI Special Publication. 1998;180:145-69.

[8] Martí-Vargas JR, Serna P, Navarro-Gregori J, Bonet JL. Effects of concrete composition on transmission length of prestressing strands. Construction and Building Materials. 2012;27:350-6.

[9] Dang CN, Murray CD, Floyd RW, Hale WM, Martí-Vargas JR. A Correlation of Strand Surface Quality to Transfer Length. ACI Structural Journal. 2014;111:1245-52.

[10] Dang CN, Floyd RW, Hale WM, Martí-Vargas JR. Measured Transfer Lengths of 0.7 in. (17.8 mm) Strands for Pretensioned Beams. ACI Structural Journal. 2016;113:85-94.

[11] Ramirez-Garcia AT, Floyd RW, Micah Hale W, Martí-Vargas JR. Effect of concrete compressive strength on transfer length. Structures. 2016;5:131-40.

[12] Abdelatif AO, Owen JS, Hussein MFM. Modelling the prestress transfer in pre-tensioned concrete elements. Finite Elements in Analysis and Design. 2015;94:47-63.

[13] Zia P, Mostafa T. Development length of prestressing strands. PCI Journal. 1977;22:54-65.

[14] Martí-Vargas JR, Serna P, Hale WM. Strand bond performance in prestressed concrete accounting for bond slip. Engineering Structures. 2013;51:236-44.

127

[15] Martí-Vargas JR, Arbelaez CA, Serna-Ros P, Navarro-Gregori J, Pallares-Rubio L. Analytical model for transfer length prediction of 13 mm prestressing strand. Structural Engineering and Mechanics. 2007;26:211-29.

[16] Kim YH, Trejo D, Hueste MBD. Bond performance in self-consolidating concrete pretensioned bridge girders. ACI Structural Journal. 2012;109:755-66.

[17] Park H, Cho J-Y. Bond-Slip-Strain Relationship in Transfer Zone of Pretensioned Concrete Elements. ACI Structural Journal. 2014;111:503-14.

[18] Lim SN, Choi YC, Oh BH, Kim JS, Shin S, Lee MK. Bond characteristics and transfer length of prestressing strand in pretensioned concrete structures. In: Van Mier JGM, Ruiz G, Andrade C, Yu RC, Zhang XX, editors. VIII International Conference on Fracture Mechanics of Concrete and Concrete Structures. Toledo (Spain): FraMCoS; 2013. p. 1-8.

[19] Benítez JM, Gálvez JC. Bond modelling of prestressed concrete during the prestressing force release. Mater Struct. 2011;44:263-78.

[20] Benítez JM, Gálvez JC, Casati MJ. Study of bond stress–slip relationship and radial dilation in prestressed concrete. International Journal for Numerical and Analytical Methods in Geomechanics. 2013;37:2706-26.

[21] Janney JR. Nature of Bond in Pre-Tensioned Prestressed Concrete. ACI Journal Proceedings. 1954;50:717-36.

[22] ASTM-A416/A416M-15. Standard Specification for Low-Relaxation, Seven-Wire Steel Strand for Prestressed Concrete. West Conshohocken, PA: ASTM International; 2015.

[23] Kang YJ. Nonlinear geometric, material and time dependent analysis of reinforced and prestressed concrete frames. Berkeley, CA: University of California; 1977. p. 252.

[24] Greunen JV. Nonlinear Geometric, Material and Time Dependent Analysis of Reinforced and Prestressed Concrete Slabs and Panels. Berkeley, CA: University of California; 1979. p. 286.

[25] Bazant ZP, Nilson AH. State-of-the-art report on finite element analysis of reinforced concrete. New York, NY: American Society of Civil Engineers; 1982.

[26] Naaman AE. Prestressed Concrete Analysis and Design: Fundamentals. 2nd ed. Ann Arbor, Michigan: Techno Press 3000; 2004.

[27] Benaim R. The Design of Prestressed Concrete Bridges: Concepts and principles. New York, NY: Taylor & Francis; 2008.

128

[28] Weerasekera IRA. Transfer and flexural bond in pretensioned prestressed concrete [Ph.D.]. Ann Arbor: University of Calgary (Canada); 1991.

[29] Gopalaratnam VS, Shah SP. Softening Response of Plain Concrete in Direct Tension. Journal Proceedings. 1985;82:310-23.

[30] Mahmoud ZI. Bond characteristics of fibre reinforced polymers prestressing reinforcement [Ph.D.]: Alexandria University (Egypt); 1997.

[31] Lin TY, Burns NH. Design of prestressed concrete structures. 3rd ed. New York: John Wiley & Sons, Inc.; 1981.

[32] Hoyer E, Friedrich E. Beitrag zur Frage der Haftspannung in Eisenbetonbauteilen. Beton und Eisen (Berlín). 1939;50:717-36.

[33] Carroll JC, Cousins TE, Roberts-Wallmann CL. A practical approach for finite-element modeling of transfer length in pretensioned, prestressed concrete members using end-slip methodology. PCI Journal. 2014;59:110-29.

[34] ACI-446.1R-91. Fracture Mechanics of Concrete: Concepts, Models and Determination of Material Properties (Reapproved 1999). Reported by ACI Committee 446, Fracture Mechanics; 1991. p. 146.

[35] ACI-318-11. Building code requirements for structural concrete and commentary. Farmington Hills, MI: American Concrete Institute; 2011.

[36] ACI-318-14. Building code requirements for structural concrete and commentary. Farmington Hills, MI: American Concrete Institute; 2014.

[37] Mehta PK, Monteiro PJM. Concrete microstructure, properties, and materials. 3rd ed. New York: Tata McGraw-Hill Companies, Inc.; 2006.

[38] AASHTO. AASHTO LRFD Bridge Design Specifications, U.S. Customary Units. 7th ed. Washington, D.C.: American Association of State Highway and Transportation Officials (AASHTO); 2014.

[39] Hale WM, Russell BW. Effect of Allowable Compressive Stress at Release on Prestress Losses and on the Performance of Precast, Prestressed Concrete Bridge Girders. PCI Journal. 2006;51:14-25.

[40] Dolan CW, Krohn JJ. A Case for Increasing the Allowable Compressive Release Stress for Prestressed Concrete. PCI Journal. 2007;52:102-5.

[41] Park R, Paulay T. Reinforced Concrete Structures. New York, NY: John Wiley & Sons; 1975.

[42] Ugural AC, Fenster SK. Advanced Mechanics of Materials and Applied Elasticity. 5th ed. New York, NY: Pearson Education, Inc.; 2012.

[43] Fenner RT. Mechanics of Solids. John Street, London: Black Well Scientific Publications; 1989.

[44] Briere V, Harries KA, Kasan J, Hager C. Dilation behavior of seven-wire prestressing strand – The Hoyer effect. Construction and Building Materials. 2013;40:650-8.

[45] Burgueño R, Sun Y. Stress transfer characteristics of sheathed strand in prestressed concrete beams: computational study. PCI Journal. 2014;59:95-109.

[46] Gross SP, Burns NH. Transfer and development length of 15.2 mm (0.6 in.) diameter prestressing strand in high performance concrete: Results of the Hoblitzell-Buckner beam tests. National Technical Information Service, Springfield, VA 22161: Center for Transportation Research, The University of Texas at Austin; 1995. p. 106.

[47] Chao S-H, Naaman AE, Parra-Montesinos GJ. Bond Behavior of Reinforcing Bars in Tensile Strain-Hardening Fiber-Reinforced Cement Composites. ACI Structural Journal. 2009;106: 897-906.

[48] Wu KR, Yao W, Li ZJ. Damage and strain softening of soncrete under uniaxial tension. FRAMCOS-3 - Fracture Mechanics of Concrete Structures. Japan: AEDIFICATIO Publishers; 1998. p. 357-65.

[49] Moon DY, Zi G, Kim J-H, Lee S-J, Kim G. On strain change of prestressing strand during detensioning procedures. Engineering Structures. 2010;32:2570-8.

[50] Arab AA, Badie SS, Manzari MT. A methodological approach for finite element modeling of pretensioned concrete members at the release of pretensioning. Engineering Structures. 2011;33:1918-29.

[51] Park H, Din ZU, Cho J-Y. Methodological Aspects in measurement of strand transfer length in pretensioned concrete. ACI Structural Journal. 2012;109:625-34.

[52] Russell BW, Burns NH. Measured of transfer lengths of pretensioned concrete elements. Journal of Structural Engineering. 1997;123:541-9.

[53] Mahmoud ZI, Rizkalla SH, Zaghoul E-ER. Transfer and Development Lengths of Carbon Fiber Reinforced Polymers Prestressing Reinforcement. Structural Journal. 1999;96:594-602.

[54] Oh BH, Lim SN, Lee MK, Yoo SW. Analysis and Prediction of Transfer Length in Pretensioned, Prestressed Concrete Members. ACI Structural Journal. 2014;111:549-60.

131

CHAPTER 5 : CONCLUSIONS, CONTRIBUTIONS, AND FUTURE WORKS

5.1   CONCLUSIONS

The principal goal of this dissertation is to examine the effect of concrete compressive strength on transfer and development length. The second objective of the research program is to develop an equation for predicting transfer and development length that includes concrete compressive strength. The conclusions from the research program are listed below.

1. The results showed that transfer lengths were larger in magnitude when the compressive strength at release was less than 34.5 MPa (5000 psi). However, when the compressive strength at release was greater than 34.5 MPa (5000 psi), there was little difference in transfer length. Similar trends were apparent in the development length results.

2. Research results also show that the ACI 318-14 and AASHTO equations overestimate transfer lengths in members containing concrete with high compressive strengths. Therefore, concrete compressive strength should be a factor in predicting transfer length.

3. Based on the results of the study, the proposed transfer length equation and the ACI 318-14 equation are recommended when the concrete compressive strength at release is less than 34.5 MPa. Based on the UA experimental data, $40d_b$ should be used as minimum transfer length for members containing concrete with compressive strengths at release greater than 34.5 MPa but less than 55 MPa. When the concrete compressive strength at release is greater than 55 MPa, transfer length can be taken as $33d_b$. There is little change in transfer length as concrete compressive strength at release increases beyond 55 MPa.

4. The data set of measured embedment lengths collected from the literature were compared with values predicted by the ACI 318-14 and the University of Arkansas's proposed

132

equation (UAPE). The standard normal distribution generated by the UAPE linked the area between the data set from the experimental data with the predicted values of ACI 318-14. The "linked area" represents a probability of 41 percent that a development length falls in that region. The lower intersection point, which is $111d_b$, between the normal distribution of the data set and the predicted values of the UAPE, is the proposed minimum value for development length.

5. Using the thick-walled cylinder theory with the third-order equation (proposed in this investigation), the predicted transfer length for all specimens with one strand, including 12.7 or 13 mm diameter strands, are between 90% and 121% of the measured values. The predicted transfer lengths using the second-order equation ranged from 100% to 114% when compared to the measured values. The predicted transfer lengths for specimens with one, 15.2 mm strand ranged from 97% to 108% of the measured values while the predicted transfer lengths due to second-order equation ranged from 96% to 114%. The predicted transfer length for specimens with two strands (either 12.7 mm or 15.7 mm) ranged from 96% and 109 % while the predicted transfer lengths using the second-order equation are in the range of 92% and 109%. The results show that the third-order equation provides a reasonable transfer length estimate when compared to the second-order equation for beams containing either one 15.2 mm strand or two strands of either diameter.

6. Strand bond can be modeled using the Coulomb's friction law and depends on several variables, including the coefficient of friction, bond factor, strand diameter, strand surface, internal pressure, and concrete strength.

7. The presence of the enhanced variables, including the bond surface stiffness and bond factor coefficient, can provide a better prediction of transfer length. However, additional research is need to calibrate these parameters with experimental data.

8. Much of the published literature is based on the finite element analysis of either 2-D or 3-D. That research analyzed the bond between the strand and concrete as a perfect bond which is not true because of cracks around the strand. These cracks affect the bond, and the perfect bond assumption between the strand and concrete cannot be used. The program developed in this investigation with a crack criteria to address this matter provides comparable results to the experimental results.

5.2   CONTRIBUTION TO THE BODY OF KNOWLEDGE

Several investigations have investigated the transfer and development lengths of prestressed concrete beams since the 1950s. However, the uniqueness of this research program lies in the types and strengths of concrete that were examined. Thus, the following contributions are pointed out:

1. A new equation for transfer length prediction was derived as shown below from the power regression analysis. This proposed equation depends on the variables such as: the initial prestress, the concrete strength at release, and the nominal strand diameter.

$$L_t = 25.7 \left(\frac{f_{si}}{f_{ci}'} d_b \right)^{0.55}$$

134

2. A new equation for development length prediction was developed which is a sum of the transfer length and the flexural bond length as shown below.

$$L_d = 25.7\left(\frac{f_{si}}{f_{ci}'}d_b\right)^{0.55} + 66.5\left(\frac{f_{ps} - f_{se}}{f_c'}d_b\right)^{0.55}$$

3. Based on the UA experimental data, $40d_b$ should be used as minimum transfer length for members containing compressive strengths at release greater than 34.5 MPa and less than 55 MPa. Transfer length can be predicted as $33d_b$ when the compressive strength at release is greater than 55 MPa. Moreover, based on the wide data analysis of data from the literature, the development length between $111d_b$ and $143d_b$ represents the 41% of the probability of the superimposed analysis of the normal distribution, and a minimum development length is proposed to be as $111d_b$.

4. A new method using the thick-walled cylinder theory has been proposed to model the bond between prestressing strand and concrete surface and estimate the transfer length. A bond surface stiffness (k_{bi}) and a bond factor (λ_b) coefficients were introduced. Although the proposed equation is complex due to concrete cracking around the strand surface, the transfer length estimation is reasonable for beams containing one strand or two strands.

$$k_{bi} = \lambda_b\left(\frac{4}{3}\pi d_b\right)\mu\sigma_i$$

135

5.3 FUTURE WORKS

Further numerical investigation is necessary to determine how cracks affect the bond between strand and concrete. Bond modeling between concrete and strand surface can be further improved so that a general equation which considers all of the parameters discussed in this investigation. Another area of future work is further examination of the variable bond factor which was introduced in the numerical analysis. The bond factor depends on the concrete strength, the coefficient of friction, the concrete cover, the number of cracks, and other variables like twisting angle of helical wire respect to the center wire.

APPENDIX

APPENDIX A: PROGRAM 1

A.1   Code

```fortran
C      CALCULATING NUMBER OF PARAMETERS
C      BRITTEN BY: ALBERTO RAMIREZ
C      UNIVERSITY OF ARKANSAS
C      AUGUST 13, 2014
C      MODIFIED ON FEBRUARY 20, 2015
C      RATIO = Le/Ld
C
C      ====================================================================
       PARAMETER (NND = 10000)
       IMPLICIT REAL*8 (A-H,O-Z)
       DIMENSION XD(NND) !,YD(NND)
       CHARACTER *80, FINP,FOUT
C      ====================================================================
C
C
       PRINT*, 'READ THE NAME OF THE INPUT FILE'
       READ(*,100) FINP
  100  FORMAT(A)
       PRINT*, 'READ THE NAME OF THE OUTPUT FILE'
       READ(*,100) FOUT
C       DATA INP/5/, OUT/4/
C
       OPEN (5, FILE = FINP)
       OPEN (2, FILE = FOUT, STATUS = 'NEW')
C
C      ====================================================================
C
C
       READ(5,*)ND,AVG,STD     ! TOTAL NUMBER OF DATA, AVERAGE, STDV

C
       AVG_UP = AVG+STD           ! AVG + STD   = UPPER
       AVG_DOWN = AVG-STD         ! AVG - STD   = LOWER
C
       WRITE(2,110) ND,AVG,STD,AVG_UP,AVG_DOWN
  110  FORMAT(//,4X,'TOTAL NUMBER OF DATA ANALYZED =',I6,/,
      &4X,'AVERAGE =',F10.2,/,4X,'STANDARD DEVIATION =',F10.2,/,
      &4X,'UPPER VALUE =',F10.2,/,4X,'LOWER VALUE =',F10.2)

       WRITE(2,115)
  115  FORMAT(//,7X,'NUM.',8X,'RATIO')
       DO I = 1,ND
       READ(5,*)XD(I)
       WRITE(2,120)I,XD(I)
       END DO
  120  FORMAT(4X,I6,4X,F10.2)
C
       ICOUNT1 = 0; ICOUNT2 = 0; ICOUNT3 = 0
       ICOUNT4 = 0; ICOUNT5 = 0; ICOUNT6 = 0; ICOUNT7 = 0
       DO I = 1,ND
```

138

```fortran
      IF(XD(I).GE.AVG_DOWN.AND.XD(I).LE.AVG_UP) ICOUNT1 = ICOUNT1 + 1
      IF(XD(I).LT.1.0) ICOUNT2 = ICOUNT2 + 1
      IF(XD(I).GT.AVG) ICOUNT3 = ICOUNT3 + 1
      IF(XD(I).LT.AVG_DOWN) ICOUNT4 = ICOUNT4 + 1
      IF(XD(I).GT.AVG_UP) ICOUNT5 = ICOUNT5 + 1
      END DO
C
      NA1 = ICOUNT1      ! VALUE BETWEEN OUTLINERS
      NB1 = ICOUNT2      ! VALUE LESS THAN 1
      NC1 = ICOUNT3      ! VALUE GREATER THAN AVG.
      ND1 = ICOUNT4      ! LESS THAN LOWER OUTLINE
      NE1 = ICOUNT5      ! GREATER THAN UPPER OUTLINE
      NF1 = ND-NB1       ! VALUES GREATER THAN 1
C
      NA2 = ABS(NC1-NF1)     ! BETWEEN AVEG AND 1
      NA3 = ABS(ND-ND1-NF1)  ! BETWEEN LOWER AND 1
      NA4 = ABS(NA3-NA1)     ! BETWEEN UPPER AND 1
      NA5 = ABS(ND-NC1)      ! LESS THAN AVG.
      NA6 = ABS(NA2-NA4)     ! BETWEEN AVG AND UPPER
      NA7 = ABS(NA1-NA6)     ! BETWEEN AVG AND LOWER
C     PORCENTAGES
      PNA1 = 100.D0*NA1/ND; PNB1 = 100.D0*NB1/ND; PNC1 = 100.D0*NC1/ND;
      PND1 = 100.D0*ND1/ND; PNE1 = 100.D0*NE1/ND; PNF1 = 100.D0*NF1/ND;
      PNA2 = 100.D0*NA2/ND; PNA3 = 100.D0*NA3/ND; PNA4 = 100.D0*NA4/ND;
      PNA5 = 100.D0*NA5/ND; PNA6 = 100.D0*NA6/ND; PNA7 = 100.D0*NA7/ND;

      WRITE(2,130)NA1,PNA1,NB1,PNB1,NF1,PNF1,NC1,PNC1,NA5,PNA5,ND1,PND1,
     &NE1,PNE1,NA2,PNA2,NA3,PNA3,NA4,PNA4,NA6,PNA6,NA7,PNA7
  130 FORMAT(//,4X,'TOTAL NUMBERS CALCULATED FOR EACH CASE',//,
     &4X,'========================================================',/,
     &9X,'CASE OF ANALYSIS',6X,'No POINTS',4X,'PERCENTAGE (%)',/,
     &4X,'========================================================',/,
     &4X,'BETWEEN THE OUTLINERS ... =',I6,6X,F10.2,/,
     &4X,'LESS THAN 1.0 ........... =',I6,6X,F10.2,/,
     &4X,'GREATER THAN 1.0 ........ =',I6,6X,F10.2,/,
     &4X,'GREATER THAN AVG. ....... =',I6,6X,F10.2,/,
     &4X,'LESS THAN AVG. .......... =',I6,6X,F10.2,/,
     &4X,'LESS THAN: LOWER ........ =',I6,6X,F10.2,/,
     &4X,'GREATER THAN: UPPER ..... =',I6,6X,F10.2,/,
     &4X,'BETWEEN AVG. AND 1.0 .... =',I6,6X,F10.2,/,
     &4X,'BETWEEN LOWER AND 1.0 ... =',I6,6X,F10.2,/,
     &4X,'BETWEEN UPPER AND 1.0 ... =',I6,6X,F10.2,/,
     &4X,'BETWEEN AVG. AND UPPER .. =',I6,6X,F10.2,/,
     &4X,'BETWEEN AVG. AND LOWER .. =',I6,6X,F10.2,/,
     &4X,'========================================================')
C
C
      STOP
      END
```

139

A.2   Input Data File

Name of the input file: ACI-M152.txt

The first row to be read by the program is: the total data to be analyzed (188), the average of data

(0.72), and the standard deviation (0.27).

After the second row the program reads the total data to be analyzed.

188, 0.72, 0.27
0.47
0.61
0.50
0.57
0.45
0.48
0.46
0.51
0.46
.
.
.
1.47
1.22
0.97

A.3   Output Data File

  TOTAL NUMBER OF DATA ANALYZED =   188
  AVERAGE =   0.72
  STANDARD DEVIATION =   0.27
  UPPER VALUE =   0.99
  LOWER VALUE =   0.45

   NUM.   RATIO
    1   0.47
    2   0.61
    3   0.50
    4   0.57
    5   0.45
    6   0.48

140

7	0.46
8	0.51
9	0.46
10	0.46
11	0.54
12	0.43
13	0.61
.	.
.	.
.	.
180	0.87
181	0.69
182	1.05
183	1.08
184	0.90
185	0.71
186	1.47
187	1.22
188	0.97

TOTAL NUMBERS CALCULATED FOR EACH CASE

CASE OF ANALYSIS	No POINTS	PERCENTAGE (%)
BETWEEN THE OUTLINERS …. =	123	65.43
LESS THAN 1.0 .... =	152	80.85
GREATER THAN 1.0 .... =	36	19.15
GREATER THAN AVG.............. =	84	44.68
LESS THAN AVG...................... =	104	55.32
LESS THAN: LOWER ……........ =	29	15.43
GREATER THAN: UPPER …....... =	48	25.53
BETWEEN LOWER AND 1.0....... =	123	65.43
BETWEEN UPPER AND 1.0 ……. =	0	0.00
BETWEEN AVG. AND UPPER … =	48	25.53
BETWEEN AVG. AND LOWER... =	75	39.89

B.1 Code

```
C       SUBPROGRAM TWC_LTDXv1
C       BY INCREMENTING DX THE LT IS CALCULATED
C       WRITTEN BY ALBERTO RAMIREZ
C       UNIVERSITY OF ARKANSAS
C       DECEMBER 02, 2013
C       MODIFIED: MARCH 12, 2014
C       MODIFIED: JUNE 21, 2014
C       MODIFIED: MARCH 9, 2015
C
C
C       ======================================================================
        PARAMETER (NNS=10000)
        IMPLICIT REAL*8 (A-H,O-Z)
        DIMENSION XC(NNS),DL(NNS),ZA(NNS),BOND(NNS),FSE1(NNS),P1(NNS),
       &FCZ1(NNS),XL(NNS),DATAR(NNS,NNS),FSEL(NNS,3),DINTP(2,2),
       &PLINE(NNS,4)
        CHARACTER *80, FINP,TINP,FOUT,PLLT,ROUT,SOUT,FINP1   !FOUT
        CHARACTER *80, PLBOND,PLSTRD,PLCONC,DREAD
        CHARACTER *5, TEXT,RTXT,PLT1,RTX1,RSTS,LTPL,BNPL,STRN,CONC,REA1
C
C       ======================================================================
C
        WRITE(*,120)
 120    FORMAT(/,17X,'UNIVERSITY OF ARKANSAS',/,
       &13X,'DEPARTMENT OF CIVIL ENGINEERING',//,
       &1X,'PROGRAM: TWC_LT (NUMERICAL ANALYSIS OF TRANSFER LENGTHS)',/,
       &1X,'WRITTEN BY: ALBERTO T. RAMIREZ',/,
       &1X,'=======================================================',/)
C
C       ======================================================================
        PRINT*,' '
        PRINT*, 'READ THE NAME OF THE INPUT FILE (WITHOUT .TXT)'
        READ(*,100) FINP
 100    FORMAT(A)
C       PRINT*, 'READ THE NAME OF THE OUTPUT FILE'
C       READ(*,100) FOUT
C       DATA INP/5/,OUT/6/
C
        TEXT = '.TXT'
        PLT1 = '.PLT'
        RTXT = '_OUT'
        RTX1 = '_RSL'
        RSTS = '_STRS'
        LTPL = '_LT'
        BNPL = '_BS'
        STRN = '_STRD'
        CONC = '_CONC'
        REA1 = '_READ'
C       MAKE FILES
        TINP = TRIM(FINP)       !
```

142

```fortran
      FINP1 = FINP             !
      FINP = TRIM(FINP)//TEXT             ! INPUT FILE
      FOUT = TRIM(FINP1)//RTXT//TEXT    ! OUTPUT FILE
      ROUT = TRIM(FINP1)//RTX1//TEXT    ! RESULTS
      SOUT = TRIM(FINP1)//RSTS//TEXT    ! STRESSES
      PLLT = TRIM(FINP1)//LTPL//PLT1    ! PLOT LT
      PLBOND = TRIM(FINP1)//BNPL//PLT1   ! PLOT BOND STIFFNESS
      PLSTRD = TRIM(FINP1)//STRN//PLT1  ! PLOT STRAND FORCES & LT
      PLCONC = TRIM(FINP1)//CONC//PLT1  ! PLOT CONCRETE STRESS & FORCES
      DREAD = TRIM(FINP1)//REA1//TEXT   ! READ THE INFORMATION

      OPEN (10, FILE = FINP)
      OPEN (7, FILE = FOUT)
      OPEN (2, FILE = ROUT)
      OPEN (3, FILE = SOUT)
      OPEN (1, FILE = PLLT)
      OPEN (4, FILE = PLBOND)
      OPEN (9, FILE = PLSTRD)
      OPEN (11, FILE = PLCONC)
      OPEN (12, FILE = DREAD)
C      OPEN (7,FILE='RES.TXT')
C
C      =======================================================================
C
      PI = 4.D0*ATAN(1.D0)
C
      WRITE(7,200)
 200  FORMAT(//,'ANALYSIS OF TRANSFER LENGTH IN PRESTRESSED CONCRETE',/,
     &11X,'DEPARTMENT OF CIVIL ENGINEERING',/,
     &15X,'UNIVERSITY OF ARKANSAS',//,
     &'Written by: Alberto Ramirez',/,
     &'Email: axr031@uark.edu',/,
     &'Professor: Dr. Micah Hale',/,
     &'Email: micah@uark.edu',//)
C
C      ############### READ STEEL PROPERTIES ##########################
C
C      DB: DIAMETER OF STRAND
C      FSI: INITIAL JACKING STRESS
C      EP: ELASTIC MODULUS OF STRAND
C      PR_P: POISSON'S RATIO OF STRAND
C
C      ################## READ CONCRETE PROPERTIES ##################
C
C      CY: CLEVER COVER
C      FCI: COMPRESSIVE STRENGT AT RELEASE
C      EC: ELASTIC MODULUS OF CONCRETE
C      PR_C: POISSON'S RATIO OF CONCRETE  (0.15 - 0.20)
C
C      ================== READ INPUT FILES =============================
C
      READ(10,*) NDB,DB,FSI,EP,PR_P,UNIT  ! STRAND PROPERTIES
      READ(10,*) FCI,PR_C                 ! CONCRETE PROPERTIES
      READ(10,*) CX1,CY1,S1               !cx(mm),cy(mm),S(mm)  C-COVER
      READ(10,*) B,H,BLNG                 ! CROSS SECTION OF THE BEAM
      READ(10,*) FRICT,WO,NI              ! FACTORS OF FRACTURE
      READ(10,*) HR,TM                    ! FACTORS FOR SHRINKAGE
```

143

```fortran
C        READ(10,*) IV1,IV2,IV3,IV4,IV5,IV6,IV7,IV8,IV9,IV10,IV11,IV12,
C       &IV13,IV14,IV15,IV16,IV17,IV18,IV19,IV20,IV21
C
         ! FACTOR FOR DATA PRINTING
         IV1 = 1; IV2 = 5; IV3 = 10; IV4 = 15; IV5= 20; IV6 = 25; IV7 = 30
         IV8 = 35; IV9 = 40; IV10 = 45; IV11 = 50; IV12 = 55; IV13 = 60
         IV14 = 65; IV15 = 70; IV16 = 75; IV17 = 80; IV18 = 85; IV19 = 90
         IV20 = 95; IV21 = 100

C
       IF(NI.GE.100) NIF = NI/100
       IV2 = NIF*IV2; IV3 = NIF*IV3; IV4 = NIF*IV4; IV5 = NIF*IV5
       IV6 = NIF*IV6; IV7 = NIF*IV7; IV8 = NIF*IV8; IV9 = NIF*IV9
       IV10 = NIF*IV10; IV11 = NIF*IV11; IV12 = NIF*IV12; IV13 = NIF*IV13
       IV14 = NIF*IV14; IV15 = NIF*IV15; IV16 = NIF*IV16; IV17 = NIF*IV17
       IV18 = NIF*IV18; IV19 = NIF*IV19; IV20 = NIF*IV20; IV21 = NIF*IV21
C
C       =============== TYPE OF ANALYSIS AND No CRACKS ================
       WRITE(*,205)
 205   FORMAT(/,4X,'TYPE OF ANALYSIS UPON THE ZONES',/,
      &4X,'=============================',//,
      &4X,'UNCRACKED ZONE: ELASTIC ANALYSIS              (0)',/,
      &4X,'CRACK AND FRACTURE ZONE: NONLINEAR ANALYSIS  (1)')
       READ(*,*)TA
       IF(TA.EQ.0) GO TO 211
C
       WRITE(*,210)
 210   FORMAT(/,4X,'METHOD OF ANALYSIS',/,
      &4X,'==================',//,
      &4X,'MAHMOUDiS METHOD: SECOND ORDER     (0)',/,
      &4X,'PROPOSED METHOD: THIRD ORDER       (1)')
       READ(*,*)ATP
C
 211   CONTINUE
       IF(TA.EQ.0) THEN
       NRC = 0
       WRITE(*,212)
 212   FORMAT(/,4X,'TYPE OF CONTACT PRESSURE:',/,
      &4X,'===========================',//,
      &4X,'PRESSURE 1 : SIG(i) ........ WRITE (0)',/,
      &4X,'PRESSURE 2 : SIG(i) = ft ... WRITE (1)')
       READ(*,*) NTP
       ELSE
C 190  CONTINUE
       WRITE(*,215)
 215   FORMAT(/,4X,'NUMBER OF RADIAL CRACKS TO BE CONSIDERED IN:',/,
      &4X,'==========================================',//,
      &4X,'CRACK ANALYSIS:       1-6 (RECOMENDED 3-4)')
       READ(*,*)NRC
       NTP = 1
       END IF

C       ================ PREVIOUS CALCULATION =========================
C
C       US UNITS LOW RELAXATION STRAND
       IF(DB.EQ.0.50D0) AP = 0.153D0
       IF(DB.EQ.0.60D0) AP = 0.217D0
```

144

```fortran
      IF(DB.EQ.0.70D0) AP = 0.294D0   ! IN.^2
C     SI UNITS LOW RELAXATION STRAND
      IF(DB.EQ.12.7D0) AP = 99.0D0      ! MM^2
      IF(DB.EQ.13.0D0) AP = 99.69D0
      IF(DB.EQ.15.2D0) AP = 140.D0
      IF(DB.EQ.15.7D0) AP = 146.4D0
      IF(DB.EQ.17.8D0) AP = 190.D0
C
C     #################### DEFINE TYPE OF UNIT  #####################
C
      IF(UNIT.EQ.0) THEN
      WRITE(7,*) 'CUSTOMARY U.S. UNITS'
      FVS = 1.D0
      FFCI = 1.D0
      ELSE
      WRITE(7,*) 'CUSTOMARY S.I. UNITS'
      FVS = 25.4D0     ! 1in. = 25.4mm
      FFCI = 0.145D0  !1MPa = 0.145 ksi, 25.4D0*25.4D0/(9.81D0*0.4536D0)
      END IF
C
C     ========================= PRINT STRAND PROPERTIES ===============
C     FOR SEVEN WIRE STRAND
C
      PSTD = 4.D0*PI*DB/3.D0       ! STRAND PERIMETER OR 2*PI*R1 = PI*DB
C
      WRITE(7,300)NDB,DB,AP,FSI,EP,PR_P
 300  FORMAT(//,4X,'STRAND PROPERTIES',/,'=========================',//,
     &'STRAND NUMBER(S) ........... =',I4,/,
     &'DIAMETER ................... =',F10.2,/,
     &'AREA ....................... =',F10.3,/,
     &'INTIAL JACKING STRESS ...... =',F10.2,/,
     &'ELASTIC MODULUS ............ =',F10.2,/,
     &'POISSONS RATIO ............. =',F10.2)
C
C     ================= CONCRETE PROPERTIES CALCULATION ===============
C
C      READ(10,*) CY,FCI,PR_C,TA
C
      FCI_R = FCI
      IF(UNIT.EQ.0) THEN
C      EC = 33000.D0*UWC**(1.5)*SQRT(FCI)   ! KSI
      EC = 57.D0*SQRT(FCI*1000.D0)       ! KSI
      FT = 7.5D0*SQRT(FCI*1000.D0)/1000.D0     ! KSI, LIMIT IN TENSION
      FT_L = 0.6D0*FCI        ! LINEAR LIMIT IN COMPRESSION
      ELSE
      EC = 4500*SQRT(FCI)      ! MPa
      FT = 0.62D0*SQRT(FCI)    ! LIMIT IN TENSION
      FT_L = 0.6D0*FCI         ! LIMIT IN COMPRESSION
      END IF
C     EFECTIVE CONCRETE COVER
      SFACT = 1.5D0      ! ASSUMED BY UIJL
      CCS = MIN(CX1,CY1)
      CEFF =(2.D0*CCS+(NDB-1)*SFACT*S1)/(2.D0*NDB)
      CCV = CEFF
C
      WRITE(7,400)FCI,EC,PR_C,CCV,FT,FT_L
 400  FORMAT(//,3X,'CONCRETE PROPERTIES',/,
```

145

```
     &'=========================',//,
     &'COMPRESSIVE STRENGTH AT RELEASE..... =',F10.2,/,
     &'ELASTIC MODULUS.................... =',F10.2,/,
     &'POISSONS RATIO .................... =',F10.2,/,
     &'CONCRETE COVER .................... =',F10.2,/,
     &'LIMIT TENSILE STRENGTH ............ =',F10.2,/,
     &'LIMIT COMPRESSION STRENGTH ........ =',F10.2)
C
C      ================== THICK WALLED ASSUMPTIONS ====================
C
C      THICK-WALLED CYLINDER ASSUMPTION
C
       R1 = DB/2          ! INNER RADIUS OF THICK-WALLED
       CY = CCV-R1        ! THICK WALL OR CLEVER COVER
       R2 = R1+CY         ! OUTER RADIUS OF THICK-WALLED
       NR = 1000          ! NUMBER OF RADIAL PARTS
       DR = (R2-R1)/NR    ! INCREMENT OF RADIUS
C
       WRITE(7,500)R1,R2,NR,DR
 500   FORMAT(//,3X,'THICK-WALLED CYLINDER',/,
     &'============================',//,
     &'INNER RADIUS .......... =',F6.2,/,
     &'OUTER RADIUS .......... =',F6.2,/,
     &'NUMBER OF RADIAL PARTS =',I5,/,
     &'INCREMENT OF RADIUS ... =',F6.5)
C
C      =====================================================================
C            CROSS-SECTION OF A PRESTRESSED CONCRETE BEAM
C      =====================================================================
C
C      B: WIDTH OF THE BEAM
C      H: HIGHT OF THE BEAM
C
C       READ(10,*) B,H
C
       BI = B*H**3/12.D0    ! INERTIA
       BA = B*H             ! AREA OF THE CROSS-SECTION OF THE BEAM
       ECC = H/2.D0-CY1     ! ECCENTRICITY FROM NA TO THE STRAND
       VS = BA/(2.D0*(B+H)) ! V/S : VOLUME SURFACE
C       PRINT*,VS,HR
C
       WRITE(7,600)B,H,BA,BI,ECC
 600   FORMAT(//,3X,'PRESTRESSED CONCRETE BEAM',/,
     &'==============================',//,
     &'WIDTH OF THE BEAM .......... =',F10.2,/,
     &'HIGHT OF THE BEAM .......... =',F10.2,/,
     &'AREA ....................... =',F10.2,/,
     &'INERTIA .................... =',E12.3,/,
     &'ECCENTRICITY ............... =',F10.2)
C
C      =====================================================================
C        NUMBER OF RADIAL CRACKS & FRICTION COEFFICIENT ON THE BOND
C      =====================================================================
C
C      NRC: NUMBER OF RADIAL CRACKS
C      FRICT: FRICTION ASSUMED
C
```

146

```fortran
C        READ(10,*) NRC,FRICT,WO,NI,ATP
C
         WRITE(7,700)NRC,FRICT,WO,NI
 700     FORMAT(//,3X,'VALUES ASSUMED',/,
     &'==============================',//,
     &'NUMBER OF RADIAL CRACK .......... =',I5,/,
     &'COEFFICIENT OF FRICTION ........ =',F6.2,/,
     &'WIDTH OF THE CRACK ............. =',F6.4,/,
     &'NUMBER OF ITERATIONS ........... =',I5,//)
C
C        READ(INP,*) ATP      ! ANALYSIS TYPE: QUADRATIC (0) & CUBIC (1)
C
         IF(TA.EQ.0) THEN
         WRITE(7,*) 'UNCRACKED ZONE: ELASTIC ANALAYSIS'
         ELSE
         WRITE(7,*) 'COMPLETE CRACK AND FRACTURE ZONE ANALYSIS'
         IF(ATP.EQ.0) THEN
         WRITE(7,*) 'ANALYSIS TYPE: SECOND ORDER'
         ELSE
         WRITE(7,*) 'ANALYSIS TYPE: THIRD ORDER'
         END IF
         END IF
C        ======================================================================
C
C        READ(10,*)HR,TM
C
C        READ(10,*)IV1,IV2,IV3,IV4,IV5,IV6
C
C     SET UP XL(I) TO ZERO
         DO I = 1,NNS
         XL(I) = 0.D0
         P1(I) = 0.D0
         FCZ1(I) = 0.D0
         FSE1(I) = 0.D0
         BOND(I) = 0.D0
         END DO          ! POSITION
C     LENGTH OF EACH ELEMENT
         DX = 1.D0 !     0.001D0   !1.D0/N   ! LENGTH OF EACH ELEMENT
C        ======================================================================
C
         FSE95 = 0.95D0*FSI  ! 95% AMS
C        PRINT*,FSE95
C
C        ======================================================================
C
C        COEFFICIENT OF SHRINKAGE
C
         CALL SHRINKAGE(FVS,FFCI,VS,FCI,HR,TM,EPS_SH)
C        EPS_SH = 0.D0      ! -KS*KH*(T/(T+35))*0.51*10**(-3)
         WRITE(7,*) 'STRAIN DUE TO SHRINKAGE:',EPS_SH
C
C        ======================================================================
C
         EPR = EP      ! ELASTIC MODULUS IN THE TRANSVERSAL DIRECTION
C
         WRITE(1,750)
         WRITE(2,800)
```

147

```
 750  FORMAT(6X,'Lt(i)',6X,'Fse',6X,'FSE95',4X,'SIG(i)',3X,'SFr',5X,
     *'Fcz',5X,'Rfr',5X,'Rcr',6X,'Wa',5X,'WO',5X,'STAGE')
 800  FORMAT(2X,'INC.#',5X,'Lt(i)',6X,'Fse',6X,'FSE95',4X,'SIG(i)',3X,
     *'SFr',5X,'Fcz',5X,'Rfr',5X,'Rcr',6X,'Wa',5X,'WO',5X,'STAGE')
C
C     =========================================================================
C     ====================== MAIN PROGRAM STARTS FROM HERE =============
C     =========================================================================
C
      FSE1(1) = 0.0
C
      INJJ = 0
 850  INJJ = INJJ+1
      I = INJJ
C      PRINT*,I
C      DO 50 I = 1,NI+1
      FSE = FSE1(I)       ! INCREMENT OF EFFECTIVE STRESS
C       FSE = DFSE*(I-1)
C
C      IF(FSE.GT.FSI) FSE = FSI
      FCZ = -NDB*FSE*AP*(1.D0/BA + ECC**2/BI)
C
C     ===================== ELASTIC ANALYSIS =========================
C
      DPFP = (FSI-FSE)*PR_P/EP     ! INCREASE IN RADIUS OF STRAND
      FFCZ = -PR_C*FCZ/EC          ! FACTOR OF COMPRESSIVE STRESS
C
      IF(DPFP.LT.0.D0) DPFP = 0.D0
C
      CALL ELSTRESS(R1,R2,PR_C,DPFP,FFCZ,EC,EPS_SH,PR_P,EPR,SIG_I)
C
C       PRINT*,SIG_I
      IF(SIG_I.LT.0.D0) GO TO 50
C
C       WRITE(7,*)'SIG_E =',SIG_I                 !%%%%%%%%%%%%
C
      SIGR = (-1.D0)*FT*(R2**2-R1**2)/(R2**2+R1**2)
      RCR = R1       ! CRACKED RADIUS EQUAL TO INNER RADIUS
      RFR = R1       ! FRACTURE RADIUS EQUAL TO INNER RADIUS
      XC(I) = 3      ! UNCRACKED CASE  ===== CONDITION ======
C
      IF(SIG_I.LT.ABS(SIGR).OR.TA.EQ.0) GO TO 40
C
C     =========================================================================
C     =============== BOTH COMPLETE CRACK & FRACTURE ZONE =============
C
      RCR = R1
      LC = 0
  30  LC = LC+1
      RFR = R1+(0.0001D0*LC)*(R2-R1)   ! RADIUS AT FRACTURE ZONE
C       IF(RFR.GT.1.001D0*R2) GO TO 20
      IF(RFR.GT.R2) GO TO 40     !**** FROM 20 TO 40
C       IF(RCR.LT.R1) RCR = R1     ! MAYBE IT IS NOT NECESARY... CHECK IT!
C
      IF(ATP.EQ.0) THEN
       CALL CRSTRESS(R1,R2,PR_C,DPFP,FFCZ,EC,EPS_SH,PR_P,EPR,FT,
     &FT_L,RFR,RCR,SIG_IR,DPFP_R,SKT)
```

148

```fortran
C
      ELSE
       CALL CRSTRESS3(R1,R2,PR_C,DPFP,FFCZ,EC,EPS_SH,PR_P,EPR,FT,
     &FT_L,RFR,RCR,SIG_IR,DPFP_R,SKT)
C
      END IF
C
C      IF(SIG_IR.GT.FT_L) SIG_IR = 0.4D0*FT_L        ! $$$$$$
C
C      WRITE(7,*)'SIG_CR =',SIG_IR,'  RFR =',RFR        !%%%%%%%%%%%
C
C      =====================================================================
C
      RCR_I = RCR
C     CRACK WIDTH
      WA = (2.D0*PI/NRC)*(DPFP_R-SIG_IR*(1.D0-PR_P)*R1/EPR)
      IF(WA.LT.WO) WA = WO        !******************* ADDED***********
      RCR = RFR-(WO/WA)*(RFR-R1)     ! RADIUS AT CRACKED ZONE
C
      SFR1 = -SIG_IR*R1/RFR
C
      IF(ATP.EQ.0) THEN
      SIG_FR = SFR1+SKT*(RFR**2/3.D0-RCR*RFR+RCR**2-RCR**3/(3.D0*RFR))
C
      ELSE
      SIG_FR = SFR1+SKT*(RFR**3/4.D0-RCR*RFR**2+1.5D0*RCR**2*RFR-
     &        RCR**3+RCR**4/(4.D0*RFR))
      END IF
C
      SIG_RFR = FT*(RFR**2-R2**2)/(R2**2+RFR**2)  ! RUPTURE STRENGTH C
      SIG_I = SIG_IR
      XC(I) = 1      ! CRACKED ZONE
C
      IF(WA.LT.WO) RCR = R1
      IF(ABS(SIG_RFR/SIG_FR).LT.0.98) GO TO 30   ! LESS THAN 97% MSA
C
C  20  IF(WA.GT.WO) GO TO 40     !*****??????????????????
      IF(WA.LT.WO) GO TO 40        !FROM GT TO LT
C
C     ===================== ONLY FRACTURE ZONE =========================
C
      INC = 0
      LC = 0
 10   LC = LC+1
      RFR = R1+(0.0001D0*LC)*(R2-R1)   ! RADIUS AT FRACTURE ZONE
      INC = INC+1
C
      IF(RFR.GE.R2) RFR=R2
      IF(INC.GT.5000) GO TO 40
C
      IF(ATP.EQ.0) THEN
      CALL FRSTRESS(R1,R2,PR_C,DPFP,FFCZ,EC,EPS_SH,PR_P,EPR,FT,
     &FT_L,RFR,RCR,WA,WO,SIG_IR,DPFP_R,SK2,SK3,SK4)
C
      ELSE
      CALL FRSTRESS3(R1,R2,PR_C,DPFP,FFCZ,EC,EPS_SH,PR_P,EPR,FT,
     &FT_L,RFR,RCR,WA,WO,SIG_IR,DPFP_R,SK2,SK3,SK23,SK4)
```

149

```fortran
C
      END IF
C
C        IF(SIG_IR.GT.FT_L) SIG_IR = 0.4D0*FT_L          ! $$$$$$
C
C        WRITE(7,*)'SIG_FR =',SIG_IR,'  RFR =',RFR          !%%%%%%%%%%%%
!%%%%%%%%%%%%
C     ======================================================================
      R = RFR
      CK1 = -(R1*SIG_IR+SK4)/R
C
      IF(ATP.EQ.0) THEN
      SIG_FR = CK1+(FT+SK2*(RFR-0.5D0*R)+SK3*(RFR**2-RFR*R+R**2/3.D0))
      ELSE
      SIG_FR = CK1+(FT+SK2*(RFR-0.5D0*R)+SK3*(RFR**2-RFR*R+R**2/3.D0)+
     &        SK23*(RFR**3-1.5D0*RFR**2*R+RFR*R**2-R**3/4.D0))
      END IF
C
      SIG_RFR = FT*(RFR**2-R2**2)/(RFR**2+R2**2)
C     CRACK WIDTH
      WA = (2.D0*PI/NRC)*(DPFP_R-SIG_IR*(1.D0-PR_P)*R1/EPR)
C
      IF(WA.LT.WO) RCR = R1       !; WA = WO
      SIG_I = SIG_IR
C
      XC(I) = 2       ! FRACTURE ZONE
C
      IF(ABS(SIG_RFR/SIG_FR).LT.0.98) GO TO 10    ! LESS THAN 97% MSA
C
C     ======================================================================
C
C     ======================================================================
  40  CONTINUE
C
C        IF(RFR.GE.R2) WRITE(*,900)RFR,XC(I)
      IF(RFR.GE.R2) RFR = R2
C 900  FORMAT(2X,F10.4,5X,'INSUFICIENT COVER STAGE',3X,F8.2,//,
C     &4X,'PROBABLY THE NUMBER OF CRACKS NEEDS TO BE INCREASED',//)
C        IF(RFR.GE.R2) STOP
C        IF(RFR.GE.R2) GO TO 190
C
C     ============== BOND BETWEEN CONCRETE AND STRAND ==================
C
      IF(DB.LT.15.OR.DB.LT.0.6D0) THEN
         IF(NRC.EQ.0) FBND1 = 1.00D0
         IF(NRC.EQ.1) FBND1 = 1.10D0    ! OK
         IF(NRC.EQ.2) FBND1 = 0.90D0    ! OK
         IF(NRC.EQ.3) FBND1 = 0.75D0    ! OK
         IF(NRC.EQ.4) FBND1 = 0.60D0    ! OK
         IF(NRC.EQ.5) FBND1 = 0.55D0    ! OK
         IF(NRC.EQ.6) FBND1 = 0.50D0 !1.25/NRC ! DUE TO SOME FACT..
         INCR = 1
      ELSE
C        IF(DB.GT.15.OR.DB.GT.0.6D0) FBND = 0.90D0*NRC
         IF(NRC.EQ.0) FBND1 = 1.00D0
         IF(NRC.EQ.1) FBND1 = 1.45D0    ! OK
```

150

```fortran
        IF(NRC.EQ.2) FBND1 = 1.15D0
        IF(NRC.EQ.3) FBND1 = 0.95D0   ! OK
        IF(NRC.EQ.4) FBND1 = 0.85D0   ! OK
        IF(NRC.EQ.5) FBND1 = 0.65D0   ! OK
        IF(NRC.EQ.6) FBND1 = 0.55D0   ! OK
        INCR = 2
      END IF
C       PRINT*,FBND1,INCR
C
C      STRESSES AND FORCES AT ONE THICK WALLED CYLINDER
C
C       BOND(I) = FBND*2.D0*PI*R1*FRICT*SIG_I
      BOND(I+1) = FBND1*PSTD*FRICT*SIG_I          ! PSTD > 2.D0*PI*R1
      BONDT = NDB*BOND(I+1)
C
      DFSE = BONDT*DX/AP        ! AP = AREA OF ONE STRAND
C
      FSE1(I+1) = FSE1(I)+DFSE
C
      IF(FSE1(I+1).GT.FSI) FSE1(I+1) = FSI
      P1(I+1) = NDB*FSE1(I+1)*AP
      FCZ1(I+1) = -P1(I+1)*(1.D0/BA + ECC**2/BI)
C      FCZ = -FSE*AP*(1.D0/BA + ECC**2/BI)
C      END IF
C      IF(DL(I).LT.0.D0) GO TO 50
C
C      XL = XL+DL(I)     ! POSITION
      XL(I+1) = XL(I)+DX      ! POSITION
C
C      ====================================================================
C      ================= WRITE TRANSFER LENGTH ===========================
C      ====================================================================
C
C
      NJD = I
      DATAR(I,1) = I; DATAR(I,2) = XL(I); DATAR(I,3) = FSE
      DATAR(I,4) = FSE95; DATAR(I,5) = SIG_I; DATAR(I,6) = SIG_IR
      DATAR(I,7) = FCZ; DATAR(I,8) = RFR; DATAR(I,9) = RCR_I
      DATAR(I,10) = WA; DATAR(I,11) = WO; DATAR(I,12) = XC(I)
C
C      WRITE(1,1000)XL(I),FSE,FSE95,SIG_I,SIG_IR,FCZ,RFR,RCR_I,WA,WO,
C     &XC(I)
C      WRITE(2,1050)I,XL(I),FSE,FSE95,SIG_I,SIG_IR,FCZ,RFR,RCR_I,WA,WO,
C     &XC(I)
C1000  FORMAT(3F11.3,11F8.3)
C1050  FORMAT(I5,3F11.3,11F8.3)
C
C      IF(FSE95.LT.FSE1(I)) WRITE(7,1100)I,XL(I),FSE1(I),SIG_I
C1100  FORMAT(/,'95% of Fsi',/,I5,7F10.3)
C
C      ====================================================================
C
      DO J = 1,NI
      ZA(J) = 0
      END DO
C
      ZA(IV1) = 1; ZA(IV2) = 1; ZA(IV3) = 1; ZA(IV4) = 1; ZA(IV5) = 1
```

151

```fortran
      ZA(IV6) = 1; ZA(IV7) = 1; ZA(IV8) = 1; ZA(IV9) = 1; ZA(IV10) = 1
      ZA(IV11) = 1; ZA(IV12) = 1; ZA(IV13) = 1; ZA(IV14) = 1
      ZA(IV15) = 1; ZA(IV16) = 1; ZA(IV17) = 1; ZA(IV18) = 1
      ZA(IV19) = 1; ZA(IV20) = 1; ZA(IV21) = 1
C
      IF(ZA(I).NE.1) GO TO 50
      WRITE(3,*) 'RESULTS'
C      WRITE(4,*) 'RESULTS'
C
      IF(XC(I).EQ.3) GO TO 3
      IF(XC(I).EQ.2) GO TO 2
C
      IF(ATP.EQ.0) THEN
      CALL RCRSTRESS(R1,R2,DR,NR,SIG_I,RCR_I,RFR,FT,I,XL,XC,FINP1)
C
      ELSE
      CALL RCRSTRESS3(R1,R2,DR,NR,SIG_I,RCR_I,RFR,FT,I,XL,XC,
     &FINP1)
C
      END IF
C
C 200  FORMAT(I5,5F12.4)
C     ===================================================================
      GO TO 50
C
   2  CONTINUE
C
      IF(ATP.EQ.0) THEN
      CALL RFRSTRESS(R1,R2,DR,NR,SIG_IR,RFR,FT,SK2,SK3,SK4,
     &I,XL,XC,FINP1)
C
      ELSE
      CALL RFRSTRESS3(R1,R2,DR,NR,SIG_IR,RFR,FT,SK2,SK3,SK23,SK4,
     &I,XL,XC,FINP1)
C
      END IF
C
      GO TO 50
C
   3  CONTINUE
C
      CALL RELSTRESS(R1,R2,DR,NR,SIG_I,I,XL,XC,FT,FT_L,FINP1,NTP)
C
  50  CONTINUE
      DLT = FSE1(I+1)-FSE1(I)
      IF(DLT.GT.0.010) GO TO 850
C
      PRINT*,FBND1,INCR                 ! TO SEE WHERE IT OCCURS
C      PRINT*,NJD
C      DO I = 1,NJD
C      NJ = DATAR(I,1)
C      WRITE(7,1150)NJ,(DATAR(I,J),J=2,12)
C1150  FORMAT(I5,3F11.3,11F8.3)
C      END DO
C
      FSE95_1 = DATAR(NJD,3)
      IF(FSE95_1.LT.FSE95) THEN
```

152

```fortran
             FSE95 = 0.999D0*FSE95_1
               DO I = 1,NJD
               DATAR(I,4) = FSE95
               END DO
         ELSE
             FSE95 = FSE95
         END IF
C     PRINT*,FSE95
C
         DO I = 1,NJD
         NCOL = DATAR(I,1)
         WRITE(1,1000) (DATAR(I,J),J = 2,12)
         WRITE(2,1050) NCOL,(DATAR(I,J),J = 2,12)
C     WRITE(1,1000)XL(I),FSE,FSE95,SIG_I,SIG_IR,FCZ,RFR,RCR_I,WA,WO,
C     &XC(I)
C     WRITE(2,1050)I,XL(I),FSE,FSE95,SIG_I,SIG_IR,FCZ,RFR,RCR_I,WA,WO,
C     &XC(I)
         END DO
1000     FORMAT(3F11.3,11F8.3)
1050     FORMAT(I5,3F11.3,11F8.3)
C
C
         CALL PINFL(NNS,FSEL,NJD,DATAR,FSE95,DINTP)
C      PRINT*,FSEL(1,1),FSEL(1,2),FSEL(1,3)
C      PRINT*,DINTP(1,1),DINTP(1,2),DINTP(2,1),DINTP(2,2)
C
         X1 =DINTP(1,1); X2 = DINTP(1,2); Y1 = DINTP(2,1); Y2 = DINTP(2,2)
C
         Y = FSE95
         CALL INTERP(X1,X,X2,Y1,Y,Y2)
         WRITE(*,1125)FSI,FSE95,FCI_R,X,NRC
         WRITE(7,1125)FSI,FSE95,FCI_R,X,NRC
1125     FORMAT(//,4X,'RESULTS FROM THE ANALYSIS',/,
        &4X,'=========================',/,
        &4X,'INITIAL PRESSTRESS ............. =',F8.1,/
        &4X,'PRESTRESS AT 95% AMS METHOD .... =',F8.1,/,
        &4X,'CONCRETE STRENGHT AT RELEASE ... =',F8.1,/,
        &4X,'CALCULATED TRANSFER LENGTH ..... =',F8.1,/,
        &4X,'NUMBER OF RADIAL CRACKS ........ =',I5,/)
C
         CALL PSLOP(NNS,NJD,DATAR,PLINE,X,Y)


C
C     ==================== DATA PLOT FOR TECPLOT =====================
C     BOND
         DO I = 1,NJD
         STIFB = BOND(2)-BOND(I)
         IF(I.EQ.1) STIFB = BOND(I)
         BSTRAIN = STIFB/EP
         WRITE(4,1150)XL(I),BOND(I),STIFB,BSTRAIN
         END DO
1150     FORMAT(5F11.3)
C
C     CONCRETE
         DO I = 1,NJD
         CSTR = FCZ1(I)/EC*10**6      ! CONCRETE STRAIN BY 10^-6
         WRITE(11,1150)XL(I),-FCZ1(I),X,-CSTR,XC(I)
```

153

```fortran
      END DO
C
C     STRAND
      DO I = 1,NJD
      SSTR = FSE1(I)/EP
      WRITE(9,1200)XL(I),FSE1(I),P1(I),FSE95,FSI,X,PLINE(I,2),SSTR,XC(I)
      END DO
1200  FORMAT(10F11.3)
C
      WRITE(12,1250)
1250  FORMAT(/,
     &1X,'READ THIS DATA INFORMATION FOR EACH FILE BEFORE PLOTTING',/,
     &1X,'=======================================================',//,
     &1X,'(1): FILENAME_LT.PLT',//,
     &1X,'Lt(i);',2X,'Fse;',2X,'FSE95;',2X,'SIG(i);',2X,'SFr;',2X,
     *'Fcz;',2X,'Rfr;',2X,'Rcr;',2X,'Wa;',2X,'WO;',2X,'STAGE',///,
     &1X,'(2): FILENAME_BS.PLT',//,
     &1X,'DIST. FROM FREE END;',2X,'BOND;',2X,'BOND FROM ZERO',2X,
     &'BOND STRAIN',///,
     &1X,'(3): FILENAME_CONC.PLT',//,
     &1X,'DIST. FROM FREE END;',2X,'STRESS;',2X,'Lt;',2X,
     &'STRAIN by 10^-6;',2X,'FRACT. ZONES',///,
     &1X,'(4): FILENAME_STRD.PLT',//,
     &1X,'DIST. FROM FREE END;',2X,'STRESS;',2X,'FORCE;',2X,'95% AMS;',
     &2X,'Fsi;',2X,'Lt;',2X,'EQ. LINE Lt;',2X,'STRAIN;',2X,
     &'FRACT. ZONES',///,
     &1X,'(5): FILENAME_RFRXXXX.PLT  OR  FILENAME_RCRXXXX.PLT',//,
     &1X,'RADIAL INCR.;',2X,'RADIAL STRESSES;',2X,'HOOP STRESSES;',2X,
     &'Lti;',2X,'FRACT. ZONES',///,
     &1X,'(6): FILENAME_RELXXXX.PLT',//,
     &1X,'RADIAL INCR.;',2X,'RADIAL STRESSES;',2X,'HOOP STRESSES;',2X,
     &'TENSILE LIMIT Ft;',2X,'COMPRESS. LIMIT Ft_L;',2X,'Lti;',2X,
     &'FRACT. ZONES',///)
C
      STOP
      END
C
C     =======================================================================
C                           SUBROUTINES
C     =======================================================================
C
C     ================== SUBROUTINE ELSTRESS ========================
C     ELASTIC CONTACT PRESSURE INTERFACE
C
      SUBROUTINE ELSTRESS(R1,R2,PR_C,DPFP,FFCZ,EC,EPS_SH,PR_P,EPR,SIG_I)
      IMPLICIT REAL*8 (A-H,O-Z)
C
      SKC = ((1.D0-PR_C)*R1**2+(1.D0+PR_C)*R2**2)/(R2**2-R1**2)
      SIG_I = (DPFP-FFCZ-EPS_SH)/((1-PR_P)/EPR+(SKC/EC))
      RETURN
      END
C
C     ================== SUBROUTINE CRSTRESS ========================
C     CRACKED CONTACT PRESSURE INTERFACE
C
      SUBROUTINE CRSTRESS(R1,R2,PR_C,DPFP,FFCZ,EC,EPS_SH,PR_P,EPR,FT,
     &FT_L,RFR,RCR,SIG_IR,DPFP_R,SKT)
```

154

```fortran
      IMPLICIT REAL*8 (A-H,O-Z)
C
      DPFP_R = DPFP*R1
      DCFCZ = FFCZ*RFR    !RFR       !R1  (FCZ*(PR_C/EC)*RFR)
      DCSH = EPS_SH*R1
C
      SKT = FT/(RFR-RCR)**2
C     CONSTANT K1
      SK11 = (RFR**3-RCR**3)*(1.D0-3.D0*PR_C)/9.D0
      SK12 = RCR*(RFR**2-RCR**2)*(1.D0-2.D0*PR_C)/2.D0
      SK13 = (RCR**2)*(RFR-RCR)*(1.D0-PR_C)
      SK14 = (RCR**3)*(LOG(RFR/RCR))/3.D0
C
      SK1 = (SKT/EC)*(SK11-SK12+SK13-SK14)
C     RADIAL DISPLACEMENT FRACTURE : RDCFR
      SIG_FR = (-1.D0)*FT*(R2**2-RFR**2)/(R2**2+RFR**2)
      RDCFR = RFR*(FT-PR_C*SIG_FR)/EC
C
      SK6 = R1*((1.D0-PR_P)/EPR+LOG(RFR/R1)/EC)
C
      SIG_IR = (DPFP_R+SK1-RDCFR-DCFCZ-DCSH)/SK6    ! SIG_I = SIG_IR
C
      IF(SIG_IR.GT.FT_L) SIG_IR = FT_L
C
      RETURN
      END
C
C     =================== SUBROUTINE FRSTRESS ==========================
C     FRACTURE CONTACT PRESSURE INTERFACE
C
      SUBROUTINE FRSTRESS(R1,R2,PR_C,DPFP,FFCZ,EC,EPS_SH,PR_P,EPR,FT,
     &FT_L,RFR,RCR,WA,WO,SIG_IR,DPFP_R,SK2,SK3,SK4)
      IMPLICIT REAL*8 (A-H,O-Z)
C
      DPFP_R = DPFP*R1
      DCFCZ = FFCZ*RFR    !RFR       ! R1  (FFCZ*(PR_C/EC)*RFR)
      DCSH = EPS_SH*R1
C     CONSTANTS K2, K3, & K4
      SK2 = -(2.D0*WA/WO)*FT/(RFR-R1)
      SK3 = (WA/WO)**2*(FT/(RFR-R1)**2)
C
      SK41 = SK3*R1*(RFR**2-RFR*R1+R1**2/3.D0)
      SK4 = FT*R1+SK2*R1*(RFR-0.50D0*R1)+SK41
C     CONSTANT K5
      SK51 = (FT/EC)*(RFR-R1)*(1.D0-PR_C)
      SK52 = RFR*(RFR-R1)*(1.D0-PR_C)
      SK53 = 0.25D0*(RFR**2-R1**2)*(1.D0-2.D0*PR_C)
      SK54 = (RFR**2)*(RFR-R1)*(1.D0-PR_C)
      SK55 = 0.50D0*RFR*(RFR**2-R1**2)*(1.D0-2.D0*PR_C)
      SK56 = (RFR**3-R1**3)*(1.D0-3.D0*PR_C)/9.D0
      SK57 = (SK4/EC)*LOG(RFR/R1)
C
      SK5 = SK51+(SK2/EC)*(SK52-SK53)+(SK3/EC)*(SK54-SK55+SK56)-SK57
C      SK5 = SK57-SK51-(SK2/EC)*(SK52-SK53)-(SK3/EC)*(SK54-SK55+SK56)
C     RADIAL DISPLACEMENT RDCFR
      SIG_FR = (-1.D0)*FT*(R2**2-RFR**2)/(R2**2+RFR**2)
      RDCFR = RFR*(FT-PR_C*SIG_FR)/EC
```

155

```fortran
C     CONSTANT K7
C      SK7 = R1*((1.D0-PR_P)/EPR+LOG(RFR/R1)/EC)
      FRL = RCR*RFR/(R1**2)
      SK7 = R1*((1.D0-PR_P)/EPR+LOG(FRL)/EC)
C
      SIG_IR = (DPFP_R+SK5-RDCFR-DCFCZ-DCSH)/SK7
C
      IF(SIG_IR.GT.FT_L) SIG_IR = FT_L
C
      RETURN
      END
C
C     =================== SUBROUTINE RCRSTRESS ==========================
C     RADIAL CRACKED STRESS
C
      SUBROUTINE RCRSTRESS(R1,R2,DR,NR,SIG_I,RCR_I,RFR,FT,I,XL,XC,FINP1)
      IMPLICIT REAL*8 (A-H,O-Z)
      DIMENSION XC(1),XL(1)
      CHARACTER *80,FILENAME,FINP1
C
      ID = I
      WRITE(FILENAME,'("_RCR",I4.4,".PLT")')ID
      FILENAME = TRIM(FINP1)//TRIM(FILENAME)
      OPEN(8,FILE = FILENAME)
C
      N = NR+1
      DO 35 J = 1,N    !N
      R = R1+DR*(J-1)              ! DR = 0.01D0*(R2-R1)
      IF(R.GE.RCR_I) GO TO 10
      SIG_R = -SIG_I*R1/R
      SIG_T = 0.D0
      GO TO 30
  10  IF(R.GE.RFR) GO TO 20
      SKT = FT/((RFR-RCR_I)**2)
      SRI = -SIG_I*R1/R
      SIG_R = SRI+SKT*(R**2/3.D0-RCR_I*R+RCR_I**2-RCR_I**3/(3.D0*R))
      SIG_T = SKT*(R-RCR_I)**2      !  SKT*(R**2-2*R*RCR_I+RCR_I**2)
      GO TO 30
  20  IF(RFR.GE.R2) RFR = 0.9995*R2
      SIG_FR = FT*(R2**2-RFR**2)/(RFR**2+R2**2)      ! SHOULD BE +
C
      SIG_R = -SIG_FR*((R2/R)**2-1.D0)/((R2/RFR)**2-1.D0)
      SIG_T = SIG_FR*((R2/R)**2+1.D0)/((R2/RFR)**2-1.D0)
C      DIS_U = C1*RR/EC*((1.D0-PR_C)+(1.D0+PR_C)*(R2/RR)**2)-C4
C
C 30  WRITE(4,100)R,SIG_R,SIG_T,XL(I),XC(I)
  30  WRITE(8,100)R,SIG_R,SIG_T,XL(I),XC(I)
      WRITE(3,200)I,R,SIG_R,SIG_T,XL(I),XC(I)
  35  CONTINUE
C 30  WRITE(3,200)I,R,SIG_R,SIG_T,XL(I),XC(I)
 100  FORMAT(5F12.4)
 200  FORMAT(I5,5F12.4)
C
      RETURN
      END
C
C
```

156

```
C       =================== SUBROUTINE RFRSTRESS ==========================
C       RADIAL FRACTURE STRESS
C
        SUBROUTINE RFRSTRESS(R1,R2,DR,NR,SIG_IR,RFR,FT,SK2,SK3,SK4,
       &I,XL,XC,FINP1)
        IMPLICIT REAL*8 (A-H,O-Z)
        DIMENSION XC(1),XL(1)
        CHARACTER *80,FILENAME,FINP1
C
        ID = I
        WRITE(FILENAME,'("_RFR",I4.4,".PLT")')ID
        FILENAME = TRIM(FINP1)//TRIM(FILENAME)
        OPEN(8,FILE = FILENAME)
C
        N = NR+1
        DO 35 J = 1,N     ! N = 101
        R = R1+DR*(J-1)        ! DR = (0.01D0*(R2-R1))
        IF(R.GE.RFR) GO TO 10    !!!
C
        CK1 = -(R1*SIG_IR+SK4)/R
        SIG_R = CK1+(FT+SK2*(RFR-0.5D0*R)+SK3*(RFR**2-RFR*R+R**2/3.D0))
        SIG_T = FT+SK2*(RFR-R)+SK3*(RFR-R)**2   !(RFR**2-2.D0*RFR*R+R**2)
        GO TO 30
  10    SIG_FR = FT*(R2**2-RFR**2)/(RFR**2+R2**2)      ! SHOULD BE +
        IF(RFR.GE.R2) GO TO 30
C
        SIG_R = -SIG_FR*((R2/R)**2-1.D0)/((R2/RFR)**2-1.D0)
        SIG_T = SIG_FR*((R2/R)**2+1.D0)/((R2/RFR)**2-1.D0)
C       DIS_U = C1*RR/EC*((1.D0-PR_C)+(1.D0+PR_C)*(R2/RR)**2)-C4
C  30   WRITE(4,100)R,SIG_R,SIG_T,XL(I),XC(I)
  30    WRITE(8,100)R,SIG_R,SIG_T,XL(I),XC(I)
        WRITE(3,200)I,R,SIG_R,SIG_T,XL(I),XC(I)
  35    CONTINUE
C  30   WRITE(3,200)I,R,SIG_R,SIG_T,XL(I),XC(I)
 100    FORMAT(5F12.4)
 200    FORMAT(I5,5F12.4)
C
        RETURN
        END
C
C
C       =================== SUBROUTINE RELSTRESS ==========================
C       RADIAL ELASTIC STRESS
C
        SUBROUTINE RELSTRESS(R1,R2,DR,NR,SIG_I,I,XL,XC,FT,FT_L,FINP1,NTP)
        IMPLICIT REAL*8 (A-H,O-Z)
        DIMENSION XC(1),XL(1)
        CHARACTER *80,FILENAME,FINP1
C
        ID = I
        WRITE(FILENAME,'("_REL",I4.4,".PLT")')ID
        FILENAME = TRIM(FINP1)//TRIM(FILENAME)
        OPEN(8,FILE = FILENAME)
C
        FT_L = -FT_L
        N = NR+1
C
```

157

```fortran
C       WHEN THE SIG_I IS EQUAL TO FT
        IF(SIG_I.GT.FT.AND.NTP.EQ.1) THEN
        SIG_I = FT
        WRITE(3,*)'WHEN THE SIG_I IS EQUAL TO FT'
C
        DO 30 J = 1,N     !N
        R = R1+DR*(J-1)    !  DR = (0.01D0*(R2-R1))
C
        SIG_R = -SIG_I*((R2/R)**2-1.D0)/((R2/R1)**2-1.D0)
        SIG_T = SIG_I*((R2/R)**2+1.D0)/((R2/R1)**2-1.D0)
C  DIS_U = C1*RR/EC*((1.D0-PR_C)+(1.D0+PR_C)*(R2/RR)**2)-C4
C
C    WRITE(4,100)R,SIG_R,SIG_T,FT,FT_L,XL(I),XC(I)
        WRITE(8,100)R,SIG_R,SIG_T,FT,FT_L,XL(I),XC(I)
        WRITE(3,200)I,R,SIG_R,SIG_T,FT,FT_L,XL(I),XC(I)
C  30  WRITE(3,200)I,R,SIG_R,SIG_T,XL(I),XC(I)
   30   CONTINUE
        ELSE
        DO 20 J = 1,N    !N
        R = R1+DR*(J-1)    !  DR = (0.01D0*(R2-R1))
C
        SIG_R = -SIG_I*((R2/R)**2-1.D0)/((R2/R1)**2-1.D0)
        SIG_T = SIG_I*((R2/R)**2+1.D0)/((R2/R1)**2-1.D0)
C  DIS_U = C1*RR/EC*((1.D0-PR_C)+(1.D0+PR_C)*(R2/RR)**2)-C4
C
C    WRITE(4,100)R,SIG_R,SIG_T,FT,FT_L,XL(I),XC(I)
        WRITE(8,100)R,SIG_R,SIG_T,FT,FT_L,XL(I),XC(I)
        WRITE(3,200)I,R,SIG_R,SIG_T,FT,FT_L,XL(I),XC(I)
C  20  WRITE(3,200)I,R,SIG_R,SIG_T,FT,FT_L,XL(I),XC(I)
   20   CONTINUE
        END IF
C
 100    FORMAT(7F12.4)
 200    FORMAT(I5,7F12.4)
C
        RETURN
        END
C
C
C    CUBIC ASSUMPTION
C    ================== SUBROUTINE CRSTRESS3 =========================
C    CRACKED CONTACT PRESSURE INTERFACE
C
        SUBROUTINE CRSTRESS3(R1,R2,PR_C,DPFP,FFCZ,EC,EPS_SH,PR_P,EPR,FT,
       &FT_L,RFR,RCR,SIG_IR,DPFP_R,SKT)
        IMPLICIT REAL*8 (A-H,O-Z)
C
        DPFP_R = DPFP*R1
        DCFCZ = FFCZ*RFR     !RFR      !R1  (FCZ*(PR_C/EC)*RFR)
        DCSH = EPS_SH*R1
C
        SKT = FT/(RFR-RCR)**3
C    CONSTANT K1
        SK11 = (RFR**4-RCR**4)*(1.D0-4.D0*PR_C)/16.D0
        SK12 = RCR*(RFR**3-RCR**3)*(1.D0-3.D0*PR_C)/3.D0
        SK13 = 3.D0*RCR**2*(RFR**2-RCR**2)*(1.D0-2.D0*PR_C)/4.D0
        SK14 = (RCR**3)*(RFR-RCR)*(1.D0-PR_C)
```

158

```
      SK15 = (RCR**4)*(LOG(RFR/RCR))/4.D0
C
      SK1 = (SKT/EC)*(SK11-SK12+SK13-SK14+SK15)
C     RADIAL DISPLACEMENT FRACTURE : RDCFR
      SIG_FR = FT*(RFR**2-R2**2)/(RFR**2+R2**2)
      RDCFR = RFR*(FT-PR_C*SIG_FR)/EC
C
      SK6 = R1*((1.D0-PR_P)/EPR+LOG(RFR/R1)/EC)
C
      SIG_IR = (DPFP_R+SK1-RDCFR-DCFCZ-DCSH)/SK6      ! SIG_I = SIG_IR
C
      IF(SIG_IR.GT.FT_L) SIG_IR = FT_L
C
      RETURN
      END
C
C     =================== SUBROUTINE FRSTRESS3 =========================
C     FRACTURE CONTACT PRESSURE INTERFACE
C
      SUBROUTINE FRSTRESS3(R1,R2,PR_C,DPFP,FFCZ,EC,EPS_SH,PR_P,EPR,FT,
     &FT_L,RFR,RCR,WA,WO,SIG_IR,DPFP_R,SK2,SK3,SK23,SK4)
      IMPLICIT REAL*8 (A-H,O-Z)
C
      DPFP_R = DPFP*R1
      DCFCZ = FFCZ*RFR    !RFR      ! R1   (FFCZ*(PR_C/EC)*RFR)
      DCSH = EPS_SH*R1
C     CONSTANTS K2, K3, & K4
      SK2 = -(3.D0*WA/WO)*FT/(RFR-R1)
      SK3 = 3.D0*(WA/WO)**2*(FT/(RFR-R1)**2)
      SK23 = -(WA/WO)**3*(FT/(RFR-R1)**3)
C
      SK41 = SK3*R1*(RFR**2-RFR*R1+R1**2/3.D0)
      SK42 = SK23*R1*(RFR**3-1.5D0*RFR**2*R1+RFR*R1**2-0.25D0*R1**3)
      SK4 = FT*R1+SK2*R1*(RFR-0.50D0*R1)+SK41+SK42
C     CONSTANT K5
      SK51 = (FT/EC)*(RFR-R1)*(1.D0-PR_C)
      SK52 = RFR*(RFR-R1)*(1.D0-PR_C)
      SK53 = 0.25D0*(RFR**2-R1**2)*(1.D0-2.D0*PR_C)
      SK54 = (RFR**2)*(RFR-R1)*(1.D0-PR_C)
      SK55 = 0.50D0*RFR*(RFR**2-R1**2)*(1.D0-2.D0*PR_C)
      SK56 = (RFR**3-R1**3)*(1.D0-3.D0*PR_C)/9.D0
      SK57 = RFR**3*(RFR-R1)*(1.D0-PR_C)
      SK58 = 0.75D0*(RFR**2)*(RFR**2-R1**2)*(1.D0-2.D0*PR_C)
      SK59 = RFR*(RFR**3-R1**3)*(1.D0-3.D0*PR_C)/3.D0
      SK510 = (RFR**4-R1**4)*(1.D0-4.D0*PR_C)/16.D0
      SK511 = (SK4/EC)*LOG(RFR/R1)
C
      SK5 = SK51+(SK2/EC)*(SK52-SK53)+(SK3/EC)*(SK54-SK55+SK56)+
     &      (SK23/EC)*(SK57-SK58+SK59-SK510)-SK511
C      SK5 = SK57-SK51-(SK2/EC)*(SK52-SK53)-(SK3/EC)*(SK54-SK55+SK56)
C     RADIAL DISPLACEMENT RDCFR
      SIG_FR = FT*(RFR**2-R2**2)/(RFR**2+R2**2)
      RDCFR = RFR*(FT-PR_C*SIG_FR)/EC
C     CONSTANT K7
C      SK7 = R1*((1.D0-PR_P)/EPR+LOG(RFR/R1)/EC)
      FRL = RCR*RFR/(R1**2)
      SK7 = R1*((1.D0-PR_P)/EPR+LOG(FRL)/EC)
```

159

```fortran
C
      SIG_IR = (DPFP_R+SK5-RDCFR-DCFCZ-DCSH)/SK7
C
      IF(SIG_IR.GT.FT_L) SIG_IR = FT_L
C
      RETURN
      END
C
C     =================== SUBROUTINE RCRSTRESS3 =======================
C     RADIAL CRACKED STRESS
C
      SUBROUTINE RCRSTRESS3(R1,R2,DR,NR,SIG_I,RCR_I,RFR,FT,I,XL,XC,
     &FINP1)
      IMPLICIT REAL*8 (A-H,O-Z)
      DIMENSION XC(1),XL(1)
      CHARACTER *80,FILENAME,FINP1
C
      ID = I
      WRITE(FILENAME,'("_RCR",I4.4,".PLT")')ID
      FILENAME = TRIM(FINP1)//TRIM(FILENAME)
      OPEN(8,FILE = FILENAME)
C
      N = NR+1
      DO 35 J = 1,N      !N
      R = R1+DR*(J-1)               ! DR = 0.01D0*(R2-R1)
      IF(R.GE.RCR_I) GO TO 10
      SIG_R = -SIG_I*R1/R
      SIG_T = 0.D0
      GO TO 30
  10  IF(R.GE.RFR) GO TO 20
      SKT = FT/((RFR-RCR_I)**3)
      SRI = -SIG_I*R1/R
      SIG1 = R**3/4.D0-RCR_I*R**2
      SIG2 = 1.5D0*R*RCR_I**2-RCR_I**3+RCR_I**4/(4.D0*R)
      SIG_R = SRI+SKT*(SIG1+SIG2)
      SIG_T = SKT*(R-RCR_I)**3
C     SIG_T = SKT*(R**3-3*R**2*RCR_I+2*R*RCR_I**2-RCR_I**3)
      GO TO 30
  20  IF(RFR.GE.R2) RFR = 0.9995*R2
      SIG_FR = FT*(R2**2-RFR**2)/(RFR**2+R2**2)      ! SHOULD BE +
C
      SIG_R = -SIG_FR*((R2/R)**2-1.D0)/((R2/RFR)**2-1.D0)
      SIG_T = SIG_FR*((R2/R)**2+1.D0)/((R2/RFR)**2-1.D0)
C      DIS_U = C1*RR/EC*((1.D0-PR_C)+(1.D0+PR_C)*(R2/RR)**2)-C4
C
C 30  WRITE(4,100)R,SIG_R,SIG_T,XL(I),XC(I)
  30  WRITE(8,100)R,SIG_R,SIG_T,XL(I),XC(I)
      WRITE(3,200)I,R,SIG_R,SIG_T,XL(I),XC(I)
C 30  WRITE(3,200)I,R,SIG_R,SIG_T,XL(I),XC(I)
  35  CONTINUE
 100  FORMAT(5F12.4)
 200  FORMAT(I5,5F12.4)
C
      RETURN
      END
C
C
```

160

```
C       =================== SUBROUTINE RFRSTRESS3 ========================
C       RADIAL FRACTURE STRESS
C
        SUBROUTINE RFRSTRESS3(R1,R2,DR,NR,SIG_IR,RFR,FT,SK2,SK3,SK23,SK4,
     &I,XL,XC,FINP1)
        IMPLICIT REAL*8 (A-H,O-Z)
        DIMENSION XC(1),XL(1)
        CHARACTER *80,FILENAME,FINP1
C
        ID = I
        WRITE(FILENAME,'("_RCR",I4.4,".PLT")')ID
        FILENAME = TRIM(FINP1)//TRIM(FILENAME)
        OPEN(8,FILE = FILENAME)
C
        N = NR+1
        DO 35 J = 1,N    ! N = 101
        R = R1+DR*(J-1)        ! DR = (0.01D0*(R2-R1))
        IF(R.GE.RFR) GO TO 10    !!!
C
        CK1 = -(R1*SIG_IR+SK4)/R
        SIG_R = CK1+(FT+SK2*(RFR-0.5D0*R)+SK3*(RFR**2-RFR*R+R**2/3.D0)+
     &        SK23*(RFR**3-1.5D0*RFR**2*R+RFR*R**2-R**3/4.D0))
        SIG_T = FT+SK2*(RFR-R)+SK3*(RFR-R)**2+SK23*(RFR-R)**3
        GO TO 30
  10    SIG_FR = FT*(R2**2-RFR**2)/(RFR**2+R2**2)      ! SHOULD BE +
        IF(RFR.GE.R2) GO TO 30
C
        SIG_R = -SIG_FR*((R2/R)**2-1.D0)/((R2/RFR)**2-1.D0)
        SIG_T = SIG_FR*((R2/R)**2+1.D0)/((R2/RFR)**2-1.D0)
C       DIS_U = C1*RR/EC*((1.D0-PR_C)+(1.D0+PR_C)*(R2/RR)**2)-C4
C 30    WRITE(4,100)R,SIG_R,SIG_T,XL(I),XC(I)
  30    WRITE(8,100)R,SIG_R,SIG_T,XL(I),XC(I)
        WRITE(3,200)I,R,SIG_R,SIG_T,XL(I),XC(I)
C 30    WRITE(3,200)I,R,SIG_R,SIG_T,XL(I),XC(I)
  35    CONTINUE
 100    FORMAT(5F12.4)
 200    FORMAT(I5,5F12.4)
C
        RETURN
        END
C
C
C       =================== SUBROUTINE SHRINKAGE ========================
C
        SUBROUTINE SHRINKAGE(FVS,FFCI,VS,FCI,HR,TM,EPS_SH)
        IMPLICIT REAL*8 (A-H,O-Z)
C
C       STRAIN  DUE TO SHRINKAGE, ESH, AT TIME T (AASHTO LRFD 5.4.2.3.3-1)
C
C       EPS_SH = 0.D0              ! FOR TIME TM = 0.D0
        VS = VS/FVS
        FCI = FCI*FFCI   ! FROM PSI TO KSI
        HR = HR/100.D0
C       PRINT*,HR
C       FACTORS
        FKHS = 2.D0-0.014D0*HR    ! HR: RELATIVE HUMINITY IN PERCENT
        FKS = 1.45D0-0.13D0*VS    ! >= 1    ! VS = VOL/SUP
```

161

```fortran
      IF(FKS.LT.1.D0) FKS = 1.D0
      FKF = 5.D0/(1.D0+FCI)
      FKTD = TM/(61.D0-4.D0*FCI+TM)
C
      SHRG = FKS*FKHS*FKF*FKTD
C      PRINT*,'VS,FKHS,FKS,FKF,FKTD'
C      PRINT*,VS,FKHS,FKS,FKF,FKTD
C      WRITE(6,*)FKS,FKHS,FKF,FKTD
      EPS_SH = -FKS*FKHS*FKF*FKTD*(0.00048D0)
      FSTR_SH = -FKS*FKHS*FKF*FKTD*(0.00048D0)
C      EPS_SH = -KS*KH*(T/(T+35))*0.51*10**(-3)
C      PRINT*,FSTR_SH,EPS_SH,SHRG
C
      RETURN
      END
C
C
C
C      ===============SUBROUTINE INTERPOLATION =========================
      SUBROUTINE INTERP(X1,X,X2,Y1,Y,Y2)
      IMPLICIT REAL*8 (A-H,O-Z)
      FAC = (X2-X1)/(Y2-Y1)
      X = X1+(Y-Y1)*FAC
C      B = A+(C-A)*(X2-X1)/(X3-X1)
      RETURN
      END
C
C      =================== SUBROUTINE PINFLECTION =====================
C      GET THE FIRST MAXIMUN INFLECTION POINT
      SUBROUTINE PINFL(NNS,FSEL,NJD,DATAR,FSE95,DINTP)
      IMPLICIT REAL*8 (A-H,O-Z)
      DIMENSION DATAR(NNS,NNS),FSEL(NNS,3),DINTP(2,2)
C      SET UP TO ZERO
      DO I = 1,6
      FSEL(I,1) = 0; FSEL(I,2) = 0.D0; FSEL(I,3) = 0.D0
      END DO
C
      J = 0  ; J1 = 0
      DO I = 1,NJD-1
         A1 = DATAR(I,3); B1 = DATAR(I+1,3)
         IF(B1.GT.FSE95.AND.FSE95.GT.A1) THEN
            J = 1+J
            FSEL(J,1) = DATAR(I+1,1); FSEL(J,2) = DATAR(I+1,2)
            FSEL(J,3) = B1
            X1 = DATAR(I,2); X2 = DATAR(I+1,2)
            Y1 = A1; Y2 = B1
         END IF
      END DO
C
      DO I = 1,NJD-1
         A1 = DATAR(I,3); B1 = DATAR(I+1,3)
         IF(B1.GT.FSE95.AND.FSE95.GT.A1) THEN
            DINTP(1,1) = DATAR(I,2); DINTP(1,2) = DATAR(I+1,2)
            DINTP(2,1) = A1; DINTP(2,2) = B1
         END IF
      END DO
C
```

162

```fortran
      RETURN
      END
C
C
C     ================== SUBROUTINE PLOT LT LINE ======================
C
      SUBROUTINE PSLOP(NNS,NJD,DATAR,PLINE,X,Y)
      IMPLICIT REAL*8 (A-H,O-Z)
      DIMENSION DATAR(NNS,NNS),PLINE(NNS,4)
C     SET UP TO ZERO
      DO I = 1,6
      PLINE(I,1) = 0.D0; PLINE(I,2) = 0.D0
      PLINE(I,3) = 0.D0; PLINE(I,4) = 0.D0
      END DO
C
      DO I = 1,NJD
         XLT = DATAR(I,2)
         PLINE(I,1) = XLT
         SLOP = Y/X
         PLINE(I,2) = SLOP*XLT
         PLINE(I,3) = X
         PLINE(I,4) = Y
      END DO
C
      RETURN
      END
C
```

163

B.2   Input Data File

See Table 1, Chapter 04, for the input data

Name of the input file: DNSCII12

2, 15.2, 1396.6, 199900.0, 0.30, 1

48.8, 0.15

57.0, 51.0, 51.0

165.0, 305.0, 5500.0

0.50, 0.05, 1000

70.0, 1.0

B.3   Output Data File

ANALYSIS OF TRANSFER LENGTH IN PRESTRESSED CONCRETE
        DEPARTMENT OF CIVIL ENGINEERING
          UNIVERSITY OF ARKANSAS

Written by: Alberto Ramirez
Email: axr031@uark.edu
Professor: Dr. Micah Hale
Email: micah@uark.edu

 CUSTOMARY S.I. UNITS

   STRAND PROPERTIES
   =========================

STRAND NUMBER(S).............. =   2
DIAMETER................................ =   15.20
AREA.. =   140.00
INTIAL JACKING STRESS........ =   1396.60
ELASTIC MODULUS…............. = 199900.00
POISSONS RATIO……............... =   0.30

164

CONCRETE PROPERTIES

=========================

COMPRESSIVE STRENGTH AT RELEASE..... =   48.80
ELASTIC MODULUS.. = 31435.65
POISSONS RATIO .... =   0.15
CONCRETE COVER .... =   44.63
LIMIT TENSILE STRENGTH............................ =   4.33
LIMIT COMPRESSION STRENGTH................ =   29.28

THICK-WALLED CYLINDER

==============================

INNER RADIUS............................... = 7.60
OUTER RADIUS .... = 44.63
NUMBER OF RADIAL PARTS .… = 1000
INCREMENT OF RADIUS .... = 0.03703

PRESTRESSED CONCRETE BEAM

==================================

WIDTH OF THE BEAM .... =   165.00
HIGHT OF THE BEAM .... =   305.00
AREA....................................... = 50325.00
INERTIA.................................. =   0.390E+09
ECCENTRICITY .... =   101.50

VALUES ASSUMED

=================================

NUMBER OF RADIAL CRACK .... =   6
COEFFICIENT OF FRICTION .... = 0.50
WIDTH OF THE CRACK...................... = 0.05
NUMBER OF ITERATIONS .... = 1000

COMPLETE CRACK AND FRACTURE ZONE ANALYSIS
ANALYSIS TYPE: THIRD ORDER
STRAIN DUE TO SHRINKAGE: -2.06413039939869836E-005

RESULTS FROM THE ANALYSIS

165

```
=========================
INITIAL PRESSTRESS ............................. = 1396.6
PRESTRESS AT 95% AMS METHOD…..... = 1326.8
CONCRETE STRENGHT AT RELEASE ... =    48.8
CALCULATED TRANSFER LENGTH....... =   612.2
NUMBER OF RADIAL CRACKS............... =    6
```